Virasoro Blocks and the Black Hole Information Paradox

A Thesis

submitted to
Indian Institute of Science Education and Research Pune
in partial fulfilment of the requirements for the
BS-MS Dual Degree Programme

by

Aaditya Jitendra Datar

Indian Institute of Science Education and Research Pune
Dr. Homi Bhabha Road,
Pashan, Pune 411008, INDIA.

April, 2025

Supervisor: Dr. Chethan Krishnan

Certificate

This is to certify that this dissertation entitled "Virasoro Blocks and the Black Hole Information Paradox" towards the partial fulfilment of the BS-MS dual degree programme at the Indian Institute of Science Education and Research, Pune represents study/work carried out by Aaditya Jitendra Datar at the Indian Institute of Science Education and Research, Pune under the supervision of Dr. Chethan Krishnan, Professor, Center of High Energy Physics (IISc) during the academic year 2024-2025.

Dr. Chethan Krishnan

Committee:

Dr. Chethan Krishnan

Dr. Sachin Jain

This thesis is dedicated to my parents Jitendra and Mukta, and my sister Maitreyee.

Declaration

I hereby declare that the matter embodied in the report entitled "Virasoro Blocks and the Black Hole Information Paradox" are the results of the work carried out by me at the Center of High Energy Physics (IISc) and Indian Institute of Science Education and Research, Pune under the supervision of Dr. Chethan Krishnan and the same has not been submitted elsewhere for any other degree.

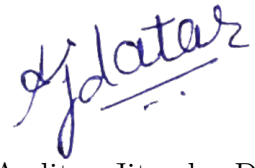

Aaditya Jitendra Datar

Acknowledgments

I would like to express my heartfelt gratitude to my supervisor, Prof. Chethan Krishnan, for his invaluable support and guidance throughout my MS thesis project. His mentorship has been instrumental in helping me gain valuable insights in the project work that we undertook, as well as in navigating the non-academic aspects of a life in research.

I am deeply indebted to the professors in the Department of Physics at IISER Pune for their significant influence on my academic journey. Whether as course instructors or semester project mentors, their guidance has shaped my understanding of physics and fostered my growth as a student.

Finally, I would like to extend my thanks to my friends and peers for their unwavering support in academic as well as non-academic issues. It has been a source of great strength and encouragement throughout this endeavour and its their presence that kept me going and made college years a lot more fun!

Abstract

This thesis explores the black hole information paradox within the context of AdS_3/CFT_2, focusing on BTZ black holes and the role of Virasoro conformal blocks in encoding quantum gravitational effects. The main object of study is the four-point CFT correlator, which manifests key signatures of information loss: the presence of "forbidden singularities" in Euclidean correlators and the late-time exponential decay of Lorentzian correlators. These effects signal a breakdown of the semi-classical approximation $G_N \to 0$, and suggest the presence of non-perturbative corrections in unitarity and information restoration.

To understand these corrections, this thesis investigates the structure of Virasoro conformal blocks, particularly in the large central charge $c \to \infty$ limit. The vacuum block, in particular, serves as a universal probe of information loss, encoding the effects of multi-graviton exchanges between probe scalars in AdS_3. We review work done on degenerate Virasoro blocks and their analytic continuation to understand semi-classical Virasoro blocks in the heavy-light limit and investigate the so-called Master Equation that includes non-perturbative finite c effects. Different scaling regimes near the forbidden singularities are tested and verified to match with perturbative $1/c$ corrections to the block which are known via field-theoretic methods previously.

The thesis further explores the connection between Virasoro blocks and geodesic Witten diagrams, which provide a holographic prescription for computing these blocks in the bulk. A novel prescription for constructing the bulk dual of Virasoro blocks specifically for the case of BTZ black holes is proposed. We hope that this refines the existing approaches and offers insights into how the bulk-bulk propagator (AdS Green's function) is intimately connect to Virasoro blocks.

By reviewing non-perturbative corrections and finding novel bulk interpretations, this thesis extends the understanding of the black hole information paradox in AdS_3/CFT_2, providing new perspectives on unitarity restoration and the role of the black hole horizon in quantum gravity.

Contents

Abstract **xi**

I Preliminaries 9

1 Why Conformal Field Theories and Anti-De Sitter spaces 11

2 Conformal Field Theory (CFT) 13

2.1 Conformal Invariance 13

2.2 Conformal Invariance in Two Dimensions 19

2.3 The Operator Formalism in Two Dimensional CFTs 27

3 Black Holes in Anti-de Sitter space (AdS) 33

3.1 Anti-de Sitter space 33

3.2 Three-dimensional black holes Anti-De Sitter space (AdS_3) 34

3.3 BTZ black holes 36

3.4 Black holes in Euclidean AdS_3 39

II Virasoro Blocks and Information Loss I: Degenerate blocks

and non-perturbative corrections **45**

4 Setting up the stage **47**

4.1 Forbidden Singularities: A hallmark of information loss in AdS/CFT 47

5 Minimal models and degenerate Virasoro blocks **53**

5.1 Degenerate Virasoro blocks 54

5.2 Consistency of unitarity requirements and analytic continuation 56

5.3 Analysis of the BPZ equation for heavy degenerate states at order $1/c$ 57

5.4 Analysis of the Master Equation 61

6 Analysis of "physical" Virasoro blocks **65**

6.1 The master equation after analytic continuation 65

6.2 Analysis of the analytically continued Master Equation 67

7 Analysis of the non-perturbative information restoration effects due to the master equation **73**

7.1 Borel resummation 73

7.2 Analysis of the non-perturbative corrections in Virasoro blocks 75

III Virasoro blocks and Information Loss II: A prescription to construct the holographic dual for the conformal Virasoro block in the bulk **79**

8 Why conformal Virasoro blocks and geodesic Witten diagrams **81**

8.1 Witten diagrams 82

8.2 Geodesic Witten Diagrams 83

9 The geodesic Witten diagram in the semi-classical heavy-light limit 87

9.1 Review of the "Kraus" prescription 87

9.2 A new prescription for calculating the geodesic Witten diagram in the heavy-light limit 89

9.3 Geodesic Witten diagram using an explicit wave equation solution 99

9.4 Geodesics in the bulk prescription 103

IV Conclusion 105

10 Concluding remarks and future directions of research 107

10.1 Summary and conclusion 107

10.2 Directions for future research 108

V Appendix 109

A Miscellaneous calculations 111

A.1 Action of the differential operators on correlation functions 111

A.2 Coefficients of $\tilde{\mathcal{V}}$ and $\tilde{\mathcal{V}}''$ in the Master Equation 113

A.3 Calculations of the analytically continued Master Equation 117

List of Figures

1 A cartoon representation of the heavy-light four-point CFT correlator 6

2.1 Global conformal mappings 14

2.2 The radial quantization mapping 27

3.1 A d-dimensional AdS hyperboloid embedded in $d+1$-dimensional flat space . 34

3.2 The AdS_3 cylinder 35

3.3 BTZ coordinate patches embedded in the global AdS cylinder (Lorentzian signature) 38

3.4 The cigar representation of a Euclidean BTZ black hole 41

3.5 BTZ coordinate patches embedded in the global AdS cylinder (Euclidean signature) I 43

3.6 BTZ coordinate patches embedded in the global AdS cylinder (Euclidean signature) II 44

4.1 A cartoon representation of Virasoso descendants as scalar and graviton exchanges 51

6.1 Comparison between exact and semi-classical Virasoro blocks 71

6.2 Comparison of the numerical solution and semi-classical analytical Virasoro block 72

8.1 Tree-level Witten diagrams 83

8.2 Tree-level geodesic Witten diagram 84

9.1 Modified bulk prescription for geodesic Witten diagrams in the semi-classical heavy-light limit 90

9.2 Geodesics in the new bulk prescription I 102

9.3 Geodesics in the new bulk prescription II 103

List of Tables

2.1 Conformal mappings and generators 14

2.2 A Verma module 32

4.1 The AdS/CFT extrapolate dictionary 48

Introduction

The black hole information paradox [1, 2] remains one of the deepest puzzles in modern science, pitting two established pillars of theoretical physics: quantum mechanics and general relativity, against each other. In its most well-known form, it appears when one considers the evaporation of a black hole due to quantum effects at its horizon, known to us as Hawking radiation. A key feature of this radiation is that only the information of the black hole's mass, charge and angular momentum in its initial state is retained. However, if one considers this in the context of a physical black hole that is formed due to different astrophysical processes and yet has the same three parameters, it implies that much of the information of the initial state of collapsing matter is lost irretrievably due to the black hole's thermal behaviour. This is in direct conflict with a core tenet of quantum mechanics: the evolution of a physical system must be unitary and must conserve information. More broadly, the information loss problem is captured in the inconsistency of the equivalence principle in gravity with the unitarity of quantum mechanical evolution. Unsurprisingly, any effort at resolving or even ameliorating the information loss problem will lead us to a more complete quantum theory of gravity, and thus, the study of quantum black holes has been a topic of immense scrutiny and deliberation ever since.

The AdS/CFT correspondence [3, 4, 5] which postulates a duality between a quantum theory of gravity in $d+1$-dimensional anti-de Sitter (AdS) space and a d-dimensional conformal quantum field theory (CFT) that resides at the boundary of this space has turned out to be a natural framework to resolve the black hole information paradox. It declares that the unitarity derived from the CFT wins the fight: black holes should evolve in a manner consistent with quantum mechanics. This is because black holes in the context of AdS/CFT correspond to a sliver of heavy states on the boundary CFT and since these states obey the usual rules of quantum mechanics (that is, they evolve unitarily), the black hole must also evolve in a unitary fashion, respecting the principles of quantum mechanics. Thus, if this duality is to be believed, we know that information is not lost irreversibly around black holes; but unfortunately we only know the result, and not the bulk mechanism by which this is enforced!

The general problem of understanding the exact mechanism by which unitarity is enforced in the bulk via a theory of gravity is quite difficult: that would invariably mean knowing a

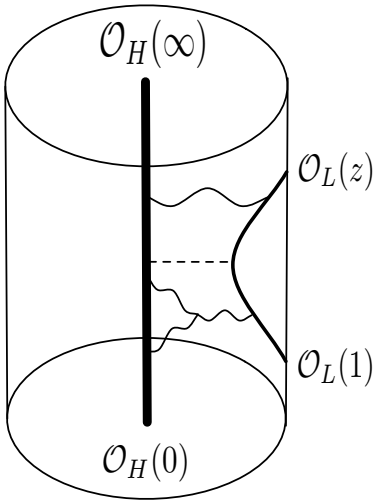

Figure 1: The AdS interpretation for the heavy-light CFT correlator; a light probe object ($\mathcal{O}_L$) interacting with a BTZ black hole background (due to $\mathcal{O}_H$). The black hole is sitting static somewhere in AdS space (denoted by the cylinder) and a light probe is interacting with it from the boundary. Reprinted from [15]

complete quantum theory of gravity! However, one can ask more tractable questions that can help tackle the bigger problem incrementally. One such "easy" information loss question can be formulated in terms of correlation functions in CFT [6]. The broad goal of this thesis is to understand information loss in $\text{AdS}_3/\text{CFT}_2$ by studying the structure of such correlation functions.

One of the motivations behind this project is to understand the intimate connection between the horizon and information loss, motivated by work that goes back many decades. A selected set of references in this direction include [7, 8, 9, 10, 11, 12, 13, 14].

CFT correlation functions and information loss

The AdS/CFT resolution to the black hole information paradox posits that the Hawking radiation is not exactly thermal. Instead, it receives quantum corrections at the horizon which leads to information being conserved in the black hole. Put another way, the reason information is lost is because the semi-classical treatment of quantum black holes is "too thermal", there are (presumably, non-perturbative) corrections that will take care of the excessive thermal behaviour and restore the unitarity in the exact (finite c) theory. Finding these corrections will possibly inform us on the precise manner in which unitarity is preserved in the exact theory and how taking the semi-classical limit (the gravitational coupling constant $G_N \to 0$) leads to the perfect thermal behaviour exhibited by black holes.

Consider the two-point correlator of a light probe (given by $\mathcal{O}_L$) present in the background geometry of a heavy object (given by $\mathcal{O}_H$) which in our case, is a black hole microstate (refer

to Fig. 1). Such a correlator can be written as a four-point correlator

$$\langle \mathcal{O}_L(t)\mathcal{O}_L(0)\rangle_{T_H} \sim \langle \mathcal{O}_H(\infty)\mathcal{O}_L(0)\mathcal{O}_L(z)\mathcal{O}_H(0)\rangle \tag{1}$$

using the state−operator correspondence in CFT_2. The thermality of the L.H.S correlator implies that it is periodic in Euclidean time $t_E = -it_L$ on the boundary of the global AdS cylinder. However, such a periodic behaviour is forbidden for pure-state correlation functions like $\langle \mathcal{O}_H(\infty)\mathcal{O}_L(0)\mathcal{O}_L(1)\mathcal{O}_H(0)\rangle$ of local CFT operators, and this is a very clear indication of unitarity violation. A crude way in which one can appreciate this is as follows: the periodic behaviour $\sim e^{it_E}$ in Euclidean time leads to a decaying behaviour $\sim e^{-t_L}$ of the thermal correlator $\langle \mathcal{O}_L(t)\mathcal{O}_L(0)\rangle_{T_H}$ in Lorentzian time t_L; and this decaying behaviour is already known to be a signature of the information paradox and unitarity violation [6].

Virasoro blocks and information loss

The four-point correlator in CFT_2 can be written in terms of Virasoro conformal blocks ($\mathcal{V}_h$,$V_{\bar{h}}$) as

$$\langle \mathcal{O}_H(\infty)\mathcal{O}_L(0)\mathcal{O}_L(1)\mathcal{O}_H(0)\rangle = \sum_{h,\bar{h}} P_{h,\bar{h}}\mathcal{V}_h(z)\mathcal{V}_{\bar{h}}(\bar{z}) \tag{2}$$

where the sum is over a theory-dependent spectrum of some parameters $h, \bar{h}$. The block decomposition of the four-point correlator is very useful for a couple of reasons. First, it divides the contribution of the correlator into irreducible representations of the symmetry group (here, the Virasoro conformal group). This is precisely what we do when we consider partial waves when we study scattering amplitudes. Second, it also helps in identifying theory-independent signatures of information loss. Different CFTs have different spectra for $h, \bar{h}$; but the contribution of the vacuum Virasoro block (which is given by $h, \bar{h} = 0$, or alternatively, due to the insertion of the $|0\rangle\langle 0|$ projector) exists in all theories. Thus, it is known to be a universal contribution that manifests information loss in the semi-classical ($G_N \to 0$) limit [16]. Furthermore, when interpreted in the AdS language, it turns out that the vacuum Virasoro block is associated with the effects of the exchange of multi-graviton states between the light probe and black hole; it contains an incredible amount of information about quantum gravity!

Knowing the analytic structure of these blocks would have been extremely useful, but unfortunately, no such closed-form expression for the general Virasoro block is known. Fortunately, one can explicitly calculate them for various special limits which turn out to be physically relevant too; and in fact the vacuum semi-classical Virasoro block can be shown to be of the form [15, 17]

$$\mathcal{V}_0(t_E) \sim \left[\frac{1}{\sin\left(\pi T_H t_E\right)}\right]^{2h_L} \tag{3}$$

for a certain semi-classical limit called the "heavy-light" limit which corresponds exactly to the AdS interpretation of a light probe in the geometry of a heavy object (black hole) as

shown in Fig. 1. Clearly, the vacuum Virasoro block (and presumably, ALL the Virasoro blocks) know about black hole physics in AdS_3; the forbidden periodic behaviour (as well as the decay in Lorentzian time $t_L = it_E$) is reproduced by just the vacuum block alone. Understanding this as a signature of information loss and trying to understand possible unitarity restoration mechanisms will be a major theme of this thesis, and we will discuss this in detail later. Furthermore, we will also investigate its status as a non-perturbative correction using methods of Borel resummation [18].

The holographic dual of the Virasoro block

The analysis of correlators and Virasoro blocks as a proxy to understanding information loss is done on the boundary CFT, and while we have an AdS interpretation, we do not have a concrete AdS construction. That is to say, we do not know what AdS "observable" corresponds to the Virasoro block in the bulk. While the relation between correlators in CFT and Witten diagrams in AdS has been known for a long time [19, 20, 21, 22, 23, 24, 25, 26], how the Witten diagram decomposes into conformal blocks was not, until recently.

In a series of papers [27, 28, 29], the construction of the holographic dual of the Virasoro block via geodesic Witten diagrams was done leading to an exact prescription for comparing an analytical structure in the boundary theory with an "observable" in the bulk. While this has been computed in only semi-classical regimes, extending the calculation to include unitarity restoration schemes that are known on the boundary might be useful in understanding the unitarity restoration mechanism in the bulk. In this thesis, we will describe a new prescription to calculate the semi-classical heavy-light Virasoro block which is very suggestive of the significance of the horizon in the departures between the exact block and a semi-classical approximation.

Structure of the thesis

This thesis is divided into different parts. While thematically diverse, they all have an obvious underlying relationship that connects them intimately.

Part I contains all the preliminary theory that is required to read this thesis. It is presented in a self-contained manner, but owing to the nature of the subject, it is impractical for it to be completely self-contained. The reader is encouraged to go through the references that are mentioned wherever required. **Part** II reviews the degenerate Virasoro block formalism, and how it can be connected to non-perturbative e^{-c} corrections. This part is heavily based on [18], with a few numerical and analytic checks done independently. **Part** III deals with a procedure to find the holographic dual to the Virasoro block. An original prescription that gives a cleaner way of understanding the nature of the block in the bulk is introduced (inspired from [28]). We conclude the thesis in **Part** IV with a short summary and a few comments. We also add some remarks about future research directions that are being worked on at the time of writing.

Part I

Preliminaries

Chapter 1

Why Conformal Field Theories and Anti-De Sitter spaces

Studying quantum field theories (QFTs) that accommodate scale invariance in addition to the usual Poincaré invariance has proved to be a fruitful exercise; such QFTs that exhibit conformal invariance are called conformal field theories (CFTs). They provide a powerful framework for understanding phenomena such as phase transitions and critical exponents; as also applications spanning string theory, statistical mechanics and condensed matter physics. In fact, the proposition of scale invariance means that there are no "cutoff" length (or alternatively, energy) scales associated with a CFT; this makes it the ideal prototypical QFT to study, and one can heuristically think of most studied QFTs as perturbations of some CFT. Consequently, studying CFTs has emerged as an active area of research across multiple domains of theoretical physics.

The foundational work on two-dimensional CFTs was laid out in a landmark paper by Belavin, Polyakov, and Zamolodchikov [30] which demonstrated the extraordinary power of conformal symmetry in two dimensions. The local conformal group in two-dimensional spacetime becomes infinite-dimensional; it is governed by the Virasoro algebra which significantly increases the analytic capabilities of two-dimensional CFTs. This enhanced symmetry enables exact calculations of correlation functions and critical exponents, making two-dimensional CFTs an essential tool for exploring statistical mechanics, string theory and aspects of quantum gravity. In particular, two-dimensional CFTs play a central role in the AdS/CFT correspondence, where they describe the dynamics of the boundary of three-dimensional anti-de Sitter (AdS) spaces.

The connection to AdS geometry is especially useful in three dimensions, as it provides a simple yet rich and non-trivial framework for exploring aspects of quantum gravity and holography. One particularly significant solution in AdS_3 geometry is the Bañados-Teitelboim-Zanelli (BTZ) black hole [31], a three-dimensional black hole solution for a negative cosmo-

logical constant. The BTZ black hole serves as a powerful model for studying the interface of gravity, thermodynamics, and quantum information: it is to quantum gravity what the hydrogen atom is to quantum mechanics; accessible for study and yet complex enough to give significant results. Remarkably, the dynamics of the BTZ black hole can often be encoded in two-dimensional CFTs, with the Virasoro algebra providing a natural structure for analysing entropy, Hawking radiation, and other thermodynamic properties. Furthermore, conformal Virasoro blocks, a decomposition of correlation functions into contributions from primary operators and their descendants, offer crucial analytic tools for probing the mathematical structure of CFTs and their holographic duals. In recent years, the idea that the Virasoro blocks "know" about information loss in AdS_3 has led it to become a central object of study in understanding the information paradox in black holes.

To establish a foundation for this, we will begin by briefly reviewing the main features of (two-dimensional) CFTs and (three-dimensional) AdS space; this will grant us with the necessary vocabulary for more advanced discussions later.

Chapter 2

Conformal Field Theory (CFT)

Presenting an overview of two-dimensional CFT in just a single chapter is a difficult task; we will be pragmatic about it and exclude topics that are irrelevant to a basic understanding of the scope of CFTs or the main contents of this thesis. To that end, a certain level of familiarity with QFT and the notion of a path integral will be assumed.

The contents of this chapter are based on many excellent resources on the subject: primarily *Conformal Field Theory* by Di Francesco, Mathieu and Sénéchal [32] along with the introduction to CFT in David Tong's notes on *String Theory* [33] and Paul Ginsparg's extensive treatment in *Applied Conformal Field Theory* [34].

2.1 Conformal Invariance

While we will want to specialize to the specific case of two-dimensional CFTs, it is good to have an overview of the conformal group in $d \geq 3$ dimensions; what follows is a quick summary of the same.

2.1.1 The Conformal Group

Consider the metric tensor $g_{\mu\nu}(x)$ of a d dimensional Euclidean spacetime. A **conformal transformation** is an invertible coordinate mapping $x \to x'(x)$ that leaves the metric invariant up to a scale factor $\Lambda(x) > 0$, given by

$$\boxed{g_{\mu\nu}(x) \to g'_{\mu\nu}(x') = \Lambda(x) g_{\mu\nu}(x)} \tag{2.1}$$

One can easily check that the set of conformal transformations so defined follow the group axioms, and thus, they form the conformal group. Notice how the Poincaré group is a subgroup of the conformal group, it corresponds to transformations with $\Lambda = 1$.

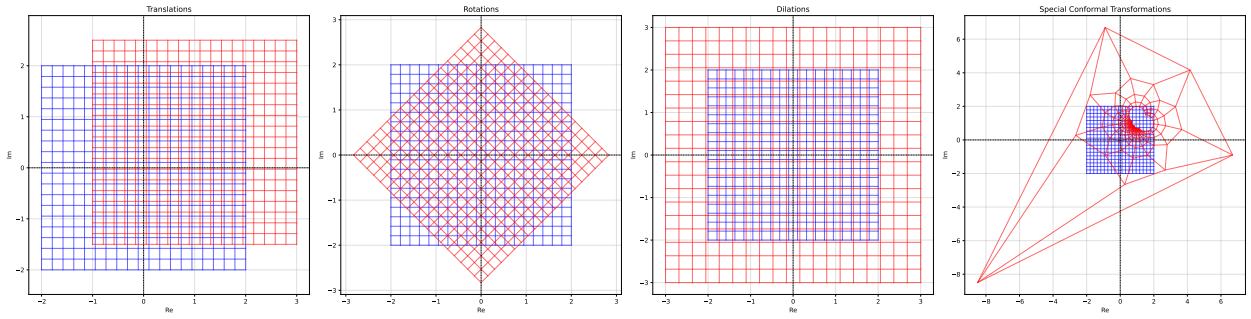

(a) Translations (b) Rotations (c) Dilations (d) SCT

Figure 2.1: Visualization of the action of the global conformal mappings (red grid) on a blue grid. It is clear that conformal mappings preserve angles but not distances.

Global Conformal Transformations

Eq. 2.1 constrains the possible independent global (that is, "exponentiated") coordinate transformations that respect conformal invariance to translations, rotations, dilatations and special conformal transformations (SCTs). They are summarized in Table 2.1 (and visualized in Fig. 2.1) along with the generators that effect them. The conformal group for d dimensional Euclidean space is isomorphic to $SO(d+1,1)$.

	Translation	Rotation	Dilatation	SCT
Mapping	$x'^{\mu} = x^{\mu} + a^{\mu}$	$x'^{\mu} = M^{\mu}{}_{\nu} x^{\nu}$	$x'^{\mu} = \alpha x^{\mu}$	$x'^{\mu} = \frac{x^{\mu} - b^{\mu} x^2}{1 - 2b\cdot x + b^2 x^2}$
Generator	$P_{\mu} = -i\partial_{\mu}$	$L_{\mu\nu} = i(x_{\mu}\partial_{\nu} - x_{\nu}\partial_{\mu})$	$D = -ix^{\mu}\partial_{\mu}$	$K_{\mu} = -i(2x_{\mu}x^{\nu}\partial_{\nu} - x^2\partial_{\mu})$

Table 2.1: Coordinate transformations and their generators for the conformal group in $d \geq 3$ dimensions. All parameters in the transformations are finite and constant, emphasizing their global nature.

2.1.2 Conformal Invariance in Classical Field Theory

A classical field theory is usually described with a set of local fields $\{\Phi(x)\}$, a Lagrangian density $\mathcal{L}(\Phi(x), \partial_{\mu}\Phi(x))$ and the associated action functional

$$S[\Phi(x)] = \int d^d x \mathcal{L}(\Phi(x), \partial_{\mu}\Phi(x)) \tag{2.2}$$

Consider a transformation

$$\begin{aligned} x &\to x'(x) \\ \Phi(x) &\to \Phi'(x') = \mathcal{F}(\Phi(x)) \end{aligned} \tag{2.3}$$

If the equations of motion remain invariant under the action of this transformation, it is called a **symmetry of the classical theory**. Thus, if the action remains invariant under conformal transformations (or more generally, if the Lagrangian density only differs by a total derivative), then we have a classical field theory with conformal symmetry.

Infinitesimal Transformations and Conserved Currents in Classical Field Theory

Consider an infinitesimal transformation with the parameters $\{\omega_a\}$ of the coordinates and fields

$$\begin{aligned} x^\mu \to x'^\mu(x) &= x^\mu + \omega_a \frac{\delta x^\mu}{\delta \omega_a} \\ \Phi(x) \to \Phi'(x') &= \Phi(x) + \omega_a \frac{\delta \mathcal{F}(x)}{\delta \omega_a} \end{aligned} \tag{2.4}$$

where

$$\Phi'(x') = \mathcal{F}(\Phi(x)) \tag{2.5}$$

encapsulates the change of the field due to the changes in spacetime coordinates ($x' \to x$) and "internal" field space effected via the representations of the symmetry (here, conformal) group. The use of Noether's theorem to calculate conserved currents for every symmetry that leaves the equation of motions invariant is well-known, and accordingly, we find the current

$$j_a^\mu = \left(\frac{\partial \mathcal{L}}{\partial(\partial_\mu \Phi)} \partial_\nu \Phi - \delta^\mu_\nu \right) \frac{\delta x^\nu}{\delta \omega_a} - \frac{\partial \mathcal{L}}{\partial(\partial_\mu \Phi)} \frac{\delta \mathcal{F}(x)}{\delta \omega_a} \tag{2.6}$$

which follows conservation law

$$\boxed{\partial_\mu j_a^\mu = 0} \tag{2.7}$$

for each type of conformal transformation: translations, rotations, dilatations and SCTs. A particular example of a well-known conserved current associated with spacetime translations is the energy-momentum tensor

$$T^{\mu\nu} = \frac{\partial \mathcal{L}}{\partial(\partial_\mu \Phi)} \partial^\nu \Phi - \eta^{\mu\nu} \mathcal{L} \tag{2.8}$$

which will play an important role in understanding OPEs later. Note that these results are for the classical theory, and we will have more to say about the realization of these symmetries in the quantum theory.

Representations of the Conformal Group in d dimensions

Under an infinitesimal conformal transformation parametrized by $\{\omega_a\}$, the field $\Phi(x)$ changes by an amount $\delta_\omega \Phi(x)$. The **generator G_a of a symmetry transformation** is defined by

$$\delta_\omega \Phi(x) \equiv \Phi'(x) - \Phi(x) \equiv -i\omega_a G_a \Phi(x) \tag{2.9}$$

and is given by

$$\boxed{iG_a\Phi(x) \equiv \frac{\delta x^\mu}{\delta\omega_a}\partial_\mu\Phi(x) + \frac{\delta\mathcal{F}(x)}{\delta\omega_a}} \tag{2.10}$$

The analysis to find the forms of the generators is non-trivial; we only highlight the salient points regarding the action of the complete generators on the fields:

1. Translations:

$$P_\mu\Phi(x) = -i\partial_\mu\Phi(x) \tag{2.11}$$

2. Rotations:

$$L_{\mu\nu}\Phi(x) = i(x_\mu\partial_\nu - x_\nu\partial_\mu)\Phi(x) + S_{\mu\nu}\Phi(x) \tag{2.12}$$

   where $S_{\mu\nu}$ is the appropriate spin operator associated with Φ.

3. Dilatations:

$$D\Phi(x) = -i(x^\mu\partial_\mu + \Delta)\Phi(x) \tag{2.13}$$

   where Δ is the usual scaling dimension of the field ($\Phi(x) \to \lambda^{-\Delta}\Phi(x)$) under scaling transformations ($x \to \lambda x$); the field part of the generator is indeed proportional to identity.

4. Special Conformal Transformations (SCTs):

$$K_\mu\Phi(x) = -(2ix_\mu\Delta + x^\nu S_{\mu\nu} + 2ix_\mu x^\nu\partial_\nu - ix^2\partial_\mu)\Phi(x) \tag{2.14}$$

Quasi-primary Fields

For a scalar field $\phi(x)$, the spin operator vanishes and if we consider this field at the origin, we observe that under a conformal transformation $x \to x'$, it transforms as

$$\phi(x) \to \phi'(x') = \left|\frac{\partial x'}{\partial x}\right|^{-\frac{\Delta}{d}}\phi(x) \tag{2.15}$$

where the Jacobian of the conformal transformation is related to the scale factor of the transformation by

$$\left|\frac{\partial x'}{\partial x}\right| = \Lambda^{-\frac{d}{2}} \tag{2.16}$$

and d is the number of spacetime dimensions. A field transforming this way is called **quasi-primary**.

2.1.3 Conformal Invariance in Quantum Field Theory

We now transition to the study of conformal invariance in QFTs where we deal with (projective) unitary representations of symmetry groups, field operators, and correlation functions. In this setting, the way to understand symmetries is through the **Ward Identities** which give a "quantum" interpretation of conserved currents.

Correlation Functions

An n-point correlation function of a theory involving the fields $\Phi(x)$ with an action $S[\Phi]$ is given by the path integral as

$$\boxed{\langle \Phi(x_1) \dots \Phi(x_n) \rangle = \frac{1}{Z} \int \mathcal{D}\Phi \; \Phi(x_1) \dots \Phi(x_n) e^{-S[\Phi]}} \tag{2.17}$$

where Z is the path integral without insertions (note that this is in the Euclidean time prescription)

$$Z = \int \mathcal{D}\Phi \; e^{-S[\Phi]} \tag{2.18}$$

A symmetry transformation that keeps the action invariant implies that

$$\boxed{\langle \Phi(x_1') \dots \Phi(x_n') \rangle = \langle \mathcal{F}(\Phi(x_1)) \dots \mathcal{F}(\Phi(x_n)) \rangle} \tag{2.19}$$

Here, we assume that the path integral measure ($\mathcal{D}\Phi$) remains unchanged under a change of variables; it is worth pointing out that non-trivial changes in the measure are the source of anomalies in QFTs.

Ward Identities

The action of a symmetry transformation on a correlation function is usually expressed in the form of Ward identities. Consider the n-point correlation function

$$\langle \Phi(x_1) \dots \Phi(x_n) \rangle = \frac{1}{Z} \int \mathcal{D}\Phi \; \Phi(x_1) \dots \Phi(x_n) e^{-S[\Phi]} \tag{2.20}$$

Under a symmetry transformation, we have (Eq. 2.7)

$$\delta S = \int d^d x \; \partial_\mu j_a^\mu \omega_a(x) \tag{2.21}$$

while $\langle X \equiv \Phi(x_1) \dots \Phi(x_n) \rangle$ in terms of the new fields $\Phi'(x)$ will be

$$\langle X \rangle = \frac{1}{Z} \int \mathcal{D}\Phi' \; (X + \delta X) e^{-S[\Phi]} e^{-\int d^d x \; \partial_\mu j_a^\mu \omega_a(x)} \tag{2.22}$$

Assuming that the path integral measure remains invariant under this local transformation, to first order in ω, we have

$$\langle \delta X \rangle = \int d^d x \, \partial_\mu \langle j_a^\mu(x) \Phi(x_1) \dots \Phi(x_n) \rangle \omega_a(x) \tag{2.23}$$

Using Eq. 2.9, we find out the first order variation in X

$$\begin{aligned} \delta X &= -i \sum_{i=1}^{n} \Phi(x_1) \dots \omega_a(x_i) G_a \Phi(x_i) \dots \Phi(x_n) \\ &= -i \int d^d x \, \omega_a(x) \delta(x - x_i) \sum_{i=1}^{n} \Phi(x_1) \dots G_a \Phi(x_i) \dots \Phi(x_n) \end{aligned} \tag{2.24}$$

which leads us to the Ward identity for the current $j_a^\mu(x)$

$$\boxed{\partial_\mu \langle j_a^\mu(x) \Phi(x_1) \dots \Phi(x_n) \rangle = -i \sum_{i=1}^{n} \delta(x - x_i) \langle \Phi(x_1) \dots G_a \Phi(x_i) \dots \Phi(x_n) \rangle} \tag{2.25}$$

Observe that when we have no field insertions, the Ward identity reduces to

$$\boxed{\partial_\mu \langle j_a^\mu(x) \rangle = 0} \tag{2.26}$$

which is consistent with our expectations regarding the correspondence between classical dynamical equations and expectation values of quantum operators.

Ward Identities of Conformal Invariance

We can now enumerate the Ward identities implied by conformal invariance using our knowledge of conformal group generators. The three main Ward identities associated with conformal invariance are:

1. Translations:
   The generator is $-i\partial_\mu$, while the current is given by the energy-momentum tensor (each index gives one conserved current)

$$\boxed{\partial_\mu \langle T^\mu_{\ \nu}(x) \Phi(x_1) \dots \Phi(x_n) \rangle = -\sum_i \delta(x - x_i) \langle \Phi(x_1) \dots \frac{\partial}{\partial x_i^\nu} \Phi(x_i) \dots \Phi(x_n) \rangle} \tag{2.27}$$

2. Lorentz Transformations/Rotations:
   The symmetrized conserved current is given $j^{\mu\nu\rho} = T^{\mu\nu} x^\rho - T^{\mu\rho} x^\nu$ while the generator

is given by $L^{\mu\nu} = i(x^\mu \partial^\nu - x^\nu \partial^\mu) + S^{\mu\nu}$

$$\boxed{\langle (T^{\mu\nu} - T^{\mu\rho})(x)\Phi(x_1)\dots\Phi(x_n)\rangle = -i\sum_i \delta(x - x_i)\langle \Phi(x_1)\dots S_i^{\mu\nu}\Phi(x_i)\dots\Phi(x_n)\rangle} \tag{2.28}$$

3. Dilatations:
   The dilatation current is given by $j_D^\mu = T^\mu_\nu x^\nu$ and the energy-momentum tensor is assumed to be in a traceless form. The generator is given by $D = -ix^\nu\partial_\nu - i\Delta$ for a field of scaling dimension Δ

$$\boxed{\langle T^\mu_{\ \mu}(x)\Phi(x_1)\dots\Phi(x_n)\rangle = -\sum_i \delta(x - x_i)\langle \Phi(x_1)\dots\Delta_i\Phi(x_i)\dots\Phi(x_n)\rangle} \tag{2.29}$$

2.2 Conformal Invariance in Two Dimensions

2.2.1 The Conformal Group in Two Dimensions

Conformal Mappings

Consider a two-dimensional Euclidean manifold mapped by the coordinates $x \equiv (x, y)$. Under a coordinate transformation $x \to x'$, the metric will transform as

$$g^{\mu\nu} \to \frac{\partial x'^\mu}{\partial x^\alpha}\frac{\partial x'^\nu}{\partial x^\beta} g^{\alpha\beta} \tag{2.30}$$

The conformal condition

$$\frac{\partial x'^\mu}{\partial x^\alpha}\frac{\partial x'^\nu}{\partial x^\beta} g^{\alpha\beta} \propto g^{\mu\nu} \tag{2.31}$$

implies

$$\begin{aligned} \left(\frac{\partial x'}{\partial x}\right)^2 + \left(\frac{\partial x'}{\partial y}\right)^2 &= \left(\frac{\partial y'}{\partial x}\right)^2 + \left(\frac{\partial y'}{\partial y}\right)^2 \\ \frac{\partial x'}{\partial x}\frac{\partial y'}{\partial x} + \frac{\partial x'}{\partial y}\frac{\partial y'}{\partial y} &= 0 \end{aligned} \tag{2.32}$$

or equivalently

$$\boxed{\begin{array}{ll} \dfrac{\partial y'}{\partial x} = \dfrac{\partial x'}{\partial y} & \dfrac{\partial x'}{\partial x} = -\dfrac{\partial y'}{\partial y} \\ \dfrac{\partial y'}{\partial x} = -\dfrac{\partial x'}{\partial y} & \dfrac{\partial x'}{\partial x} = \dfrac{\partial y'}{\partial y} \end{array}} \tag{2.33}$$

We recognize these as the Cauchy-Riemann conditions for holomorphic and antiholomorphic functions. For the analogy to be clear, consider the following redefinitions

$$\begin{gathered} x' \to u(x,y) \quad y' \to v(x,y) \\ \text{for} \\ f(z = x + iy) = u(x,y) + iv(x,y) \end{gathered} \tag{2.34}$$

and we recognize Eq. 2.33 to be the criterion for analyticity of the complex function $f(z)$. This immediately warrants the usage of the complex variables $\{z, \bar{z}\}$ instead of $\{x, y\}$; with changes in the form of the coordinates

$$\begin{aligned} z &= x + iy \quad & x &= \frac{1}{2}(z + \bar{z}) \\ \bar{z} &= x - iy \quad & y &= \frac{1}{2i}(z - \bar{z}) \end{aligned} \tag{2.35}$$

derivatives

$$\begin{aligned} \partial_z &= \frac{1}{2}(\partial_x - i\partial_y) \quad & \partial_x &= (\partial_z + \partial_{\bar{z}}) \\ \partial_{\bar{z}} &= \frac{1}{2}(\partial_x + i\partial_y) \quad & \partial_y &= i(\partial_z - \partial_{\bar{z}}) \end{aligned} \tag{2.36}$$

and the metric

$$g_{\mu\nu} = \frac{1}{2}\begin{pmatrix} 0 & 1 \\ 1 & 0 \end{pmatrix} \qquad g^{\mu\nu} = 2\begin{pmatrix} 0 & 1 \\ 1 & 0 \end{pmatrix} \tag{2.37}$$

It is important to note that $\{z, \bar{z}\}$ are independent variables; we have simply extended the range of the Cartesian coordinates into the complex plane. The physical space is the submanifold $\bar{z} = z^*$.

The introduction of complex variables considerably simplifies the constraint equation on conformal mappings in two dimensions. The holomorphic Cauchy-Riemann equations can be written in the simple form

$$\boxed{\partial_{\bar{z}} w(z, \bar{z}) = 0} \tag{2.38}$$

which has a trivial solution: any function $w(z, \bar{z})$ that has no $\bar{z}$ dependence. In short, we observe that the conformal group in two dimensions is just the set of all analytic maps (on the complex plane) with function composition as the product rule. This is manifestly infinite-dimensional.

Global Conformal Transformations

If one is interested in global two-dimensional conformal transformations, that is, transformations that are non-singular, invertible and those that map the Riemann sphere (extended complex plane) onto itself, it turns out that they are form a finite group. The set of global

conformal transformations form the **special conformal group**, which comprises of all the mappings of the form

$$f(z) = \frac{az+b}{cz+d} \qquad (ad-bc=1) \tag{2.39}$$

We can associate with them a matrix of the form

$$A = \begin{pmatrix} a & b \\ c & d \end{pmatrix} \tag{2.40}$$

and noting that functional composition $f_1 \circ f_2$ is equivalent to the matrix multiplication of the associated matrices $A_2 \cdot A_1$, we see that the global conformal group in two dimensions is actually isomorphic to $SL(2,\mathbb{C})$, which itself is isomorphic to the Lorentz group in four dimensions, $SO(3,1)$.

In a sense, the enhanced (infinite) degrees of symmetry obtained from the analytic properties of local conformal transformations are lost when we exponentiate them to global transformations. Global conformal invariance in two dimensions does not differ from global d-dimensional conformal invariance; it is the increase in local conformal degrees of symmetry that makes the two-dimensional case special.

Local Conformal Transformations and Generators

It is convenient to study infinitesimal or local conformal transformations; this is the set of all (anti) holomorphic mappings which may not be invertible or defined globally. The obvious way to proceed is to go from the language of the conformal group to that of the conformal algebra and generators. Since the mapping is analytic, we can express the infinitesimal transformations

$$z \to z' = z + \epsilon(z) \qquad \bar{z} \to \bar{z}' = \bar{z} + \bar{\epsilon}(\bar{z}) \tag{2.41}$$

in terms of the Laurent series

$$\epsilon(z) = \sum_{n=-\infty}^{\infty} c_n z^{n+1} \qquad \bar{\epsilon}(\bar{z}) = \sum_{n=-\infty}^{\infty} \bar{c}_n \bar{z}^{n+1} \tag{2.42}$$

We introduce the generators

$$\boxed{l_n = -z^{n+1}\partial_z \qquad \bar{l}_n = -\bar{z}^{n+1}\partial_{\bar{z}}} \tag{2.43}$$

which effect these local conformal transformations, each associated with one of the basis element $\epsilon_n, \bar{\epsilon}_n$ in the Laurent series of the infinitesimal conformal transformations. The

algebra of the generators is given by

$$\boxed{\begin{aligned}[l_n, l_m] &= (n-m)\, l_{n+m} \\ [\bar{l}_n, \bar{l}_m] &= (n-m)\, \bar{l}_{n+m} \\ [l_n, \bar{l}_m] &= 0\end{aligned}} \tag{2.44}$$

Observe that the two-dimensional conformal algebra is the direct sum of two isomorphic algebras; the total algebra is sometimes called the Witt algebra ($\mathcal{W} = \mathcal{A} \oplus \bar{\mathcal{A}}$).

Furthermore, we observe that these two infinite-dimensional algebras contain a finite subalgebra generated by $l_{-1} = -\partial$, $l_0 = -z\partial$ and $l_1 = -z^2\partial$ (and their $\bar{z}$ counterparts). These are associated with the global conformal group; l_{-1} generates the translations, l_0 the scale transformations and rotations while l_1 generates the special conformal transformations.

Primary Fields

It is useful to extend (analytically continue to the extended complex plane) the notion of a quasi-primary field when in two dimensions. A field with scaling dimension Δ and spin s has a **holomorphic dimension** h and **antiholomorphic dimension** $\bar{h}$ given by

$$\boxed{h = \frac{1}{2}(\Delta + s) \qquad \bar{h} = \frac{1}{2}(\Delta - s)} \tag{2.45}$$

The transformation rule for the mapping $z \to w(z)$ is given by

$$\phi'(w, \bar{w}) = \left(\frac{dw}{dz}\right)^{-h} \left(\frac{d\bar{w}}{d\bar{z}}\right)^{-h} \phi(z, \bar{z}) \tag{2.46}$$

One can also view this in the form of an infinitesimal mapping $w(z) = z + \epsilon(z)$ as

$$\begin{aligned}\delta\phi &= \phi'(z, \bar{z}) - \phi(z, \bar{z}) \\ &= -(h\phi\, \partial\epsilon + \bar{h}\phi\, \partial_{\bar{z}}\bar{\epsilon}) - (\epsilon\, \partial\phi + \bar{\epsilon}\, \partial_{\bar{z}}\phi)\end{aligned} \tag{2.47}$$

A field that transforms according to this rule under local conformal transformations (in two dimensions) is called a **primary field with conformal dimensions** $(h, \bar{h})$. Note that all primary fields are also quasi-primary, but the converse is not true: a field may transform in this manner under an element of the global conformal group $SL(2, \mathbb{C})$ but not under local conformal transformations.

2.2.2 Ward Identities

Holomorphic Form of the Conformal Ward Identities

We can now study the holomorphic Ward identities using the known forms of the conserved currents and generators in addition to a useful identity, namely,

$$\delta(x) = \frac{1}{\pi}\partial_{\bar{z}}\frac{1}{z} = \frac{1}{\pi}\partial\frac{1}{\bar{z}} \tag{2.48}$$

The Ward identities can be expressed as (note that X is used to denote the string of n primary fields $\Phi(x_1)\dots\Phi(x_n)$)

1. Translations:

$$\partial_\mu\langle T^\mu_{\ \nu}(x)X\rangle = -\sum_i \delta(x-x_i)\frac{\partial}{\partial x_i^\nu}\langle X\rangle \tag{2.49}$$

which leads to

$$\boxed{\begin{aligned} 2\pi\partial_z\langle T_{\bar{z}z}X\rangle + 2\pi\partial_{\bar{z}}\langle T_{zz}X\rangle &= -\sum_{i=0}^{n}\partial_{\bar{z}}\frac{1}{z-w_i}\partial_{w_i}\langle X\rangle \\ 2\pi\partial_z\langle T_{\bar{z}\bar{z}}X\rangle + 2\pi\partial_{\bar{z}}\langle T_{z\bar{z}}X\rangle &= -\sum_{i=0}^{n}\partial_{z}\frac{1}{\bar{z}-\bar{w}_i}\partial_{\bar{w}_i}\langle X\rangle \end{aligned}} \tag{2.50}$$

2. Lorentz Transformations/Rotations:

$$\epsilon_{\mu\nu}\langle T^{\mu\nu}(x)X\rangle = -i\sum_{i=0}^{n}\delta(x-x_i)s_i\langle X\rangle \tag{2.51}$$

with the two-dimensional spin generators $S^i_{\mu\nu} = s_i\epsilon_{\mu\nu}$ (s_i is the spin of the field ϕ_i and $\epsilon_{\mu\nu}$ is the two dimensional antisymmetric tensor).

$$\boxed{-2\langle T_{z\bar{z}}X\rangle + 2\langle T_{\bar{z}z}X\rangle = -\sum_{i=0}^{n}\delta(x-x_i)s_i\langle X\rangle} \tag{2.52}$$

3. Scale Transformations:

$$\langle T^\mu_{\ \mu}(x)X\rangle = -i\sum_{i=0}^{n}\delta(x-x_i)\Delta_i\langle X\rangle \tag{2.53}$$

which becomes

$$\boxed{2\langle T_{z\bar{z}}X\rangle + 2\langle T_{\bar{z}z}X\rangle = -\sum_{i=0}^{n}\delta(x-x_i)\Delta_i\langle X\rangle} \tag{2.54}$$

The Conformal Ward Identity

For an arbitrary infinitesimal conformal transformation by $\epsilon^\nu(x)$, we have

$$\begin{aligned}\partial_\mu(\epsilon_\nu T^{\mu\nu}) &= \epsilon_\nu\partial_\mu T^{\mu\nu} + \partial_\mu\epsilon_\nu T^{\mu\nu} \\ &= \epsilon_\nu\partial_\mu T^{\mu\nu} + \frac{1}{2}(\partial_\rho\epsilon^\rho)\eta_{\mu\nu}T^{\mu\nu} + \frac{1}{2}\epsilon^{\alpha\beta}\partial_\alpha\epsilon_\beta\epsilon_{\mu\nu}T^{\mu\nu}\end{aligned} \tag{2.55}$$

where we use tensor identities involving the metric $\eta^{\mu\nu}$ and the antisymmetric tensor $\epsilon^{\mu\nu}$. Multiplying by $X = \Phi(x_1)\dots\Phi(x_n)$ and integrating both sides, we have (for a region M containing all the spacetime positions of the fields in X)

$$\delta_\epsilon\langle X\rangle = \int_M d^2x\ \partial\langle T^{\mu\nu}(x)\epsilon_\nu(x)X\rangle \tag{2.56}$$

where $\delta_\epsilon\langle X\rangle$ is the variation of X under a local conformal transformation. Using the Gauss theorem, we have the **conformal Ward identity**

$$\boxed{\delta_{\epsilon,\bar{\epsilon}}\langle X\rangle = -\frac{1}{2\pi i}\oint_C dz\ \epsilon(z)\langle T(z)X\rangle + \frac{1}{2\pi i}\oint_C d\bar{z}\ \bar{\epsilon}(\bar{z})\langle\bar{T}(\bar{z})X\rangle} \tag{2.57}$$

where we can now choose any contour C as long as it encloses all the positions of the fields in X.

2.2.3 The Operator Product Expansion (OPE)

It is known that correlation functions in QFTs have singularities when the positions of two or more fields coincide. For instance, the two-point function of a scalar field theory has an ultraviolet divergence originating from the Feynman propagator $D_F(x-y)$ as $x \to y$. This is indicative of the infinite fluctuations of a quantum field when calculated for two spacetime points which are infinitesimally close.

A way to deal with this analytically in two-dimensional CFTs is to represent divergent quantities such as product of operators (at positions, say z and w) by a sum of fields or any well-defined local operators. This representation is called the **Operator Product Expansion** (OPE). In general, we write the OPE of two fields $A(z)$ and $B(w)$ as

$$A(z)B(w) = \sum_{n=-\infty}^{N}\frac{(AB)_n(w)}{(z-w)^n} \tag{2.58}$$

where the composite field $(AB)_n(w)$ is regular at $z = w$ and the singular nature of the product as $z \to w$ is contained in the denominators. It is understood that this expression really makes sense only within $\langle \ldots \rangle$ which is usually dropped and kept implicit. We will present the specific example of scalar fields to get acquainted with the concept of an OPE.

The Free Massless Boson

Consider the theory of a free massless boson ϕ in two dimensions, given by the action

$$S[\phi] = \frac{1}{2} g \int d^2x \partial_\mu \phi \partial^\mu \phi \tag{2.59}$$

where g is some unspecified normalization parameter. Solving the equation for the Green's function, we get

$$\langle \phi(x)\phi(y) \rangle = -\frac{1}{4\pi g} \ln (x-y)^2 + \text{const.} \tag{2.60}$$

which becomes

$$\langle \phi(z,\bar{z})\phi(w,\bar{w}) \rangle = -\frac{1}{4\pi g} \{ \ln (z-w) + \ln (\bar{z}-\bar{w}) \} + \text{const.} \tag{2.61}$$

in terms of complex coordinates. Taking the correct derivative and then finding the expectation value of the time-ordered product, we get the OPE of $\partial\phi$ as

$$\boxed{\partial_z \phi(z) \partial_w \phi(w) \sim -\frac{1}{4\pi g} \frac{1}{(z-w)^2}} \tag{2.62}$$

Observe how the OPE also inherits the bosonic character of the field; it remains symmetric under the exchange of the fields. Next, consider the energy-momentum tensor for the free massless boson given by

$$T_{\mu\nu} = g \left(\partial_\mu \phi \partial_\nu \phi - \frac{1}{2} \eta_{\mu\nu} \partial_\rho \phi \partial^\rho \phi \right) \tag{2.63}$$

Finding the expectation value of the time-ordered product of $T(z) = T_{zz}$ and $\partial\phi$, we have

$$T(z)\partial\phi(w) \sim \frac{\partial_w \phi(w)}{(z-w)^2} + \frac{\partial_w^2 \phi(w)}{(z-w)} \tag{2.64}$$

which is a special case of a more general result: the OPE of the energy-momentum tensor $T(z)$ with a primary field $\phi_i(w,\bar{w})$ of conformal dimensions $(h,\bar{h})$ is

$$\boxed{T(z)\phi(w,\bar{w}) \sim \frac{h}{(z-w)^2} \phi_i(w,\bar{w}) + \frac{1}{z-w} \partial_w \phi_i(w,\bar{w})} \tag{2.65}$$

We can also find out the OPE for the energy-momentum tensor with itself

$$\boxed{T(z)T(w) \sim \frac{1}{2}\frac{1}{(z-w)^4} + \frac{2T(w)}{(z-w)^2} + \frac{\partial_w T(w)}{(z-w)}} \tag{2.66}$$

We observe that due to the anomalous $(z-w)^{-4}$ term, the energy-momentum tensor is not a primary field.

2.2.4 The Central Charge

The general form of the OPE of the energy-momentum tensor is given by

$$\boxed{T(z)T(w) \sim \frac{c}{2}\frac{1}{(z-w)^4} + \frac{2T(w)}{(z-w)^2} + \frac{\partial T(w)}{(z-w)}} \tag{2.67}$$

where the constant c is a model dependent quantity. For instance, a free boson has $c = 1$, a free fermion has $c = 1/2$ and so on. This model dependent constant is called the **central charge**. Notice that without the central charge term, T would have been a quasi-primary field with conformal dimension $h = 2$. (Note that there is an analogous antiholomorphic central charge $\bar{c}$ which we do not describe explicitly)

Physical Meaning of the Central Charge c

The **central charge** c, also known as the **conformal anomaly**, quantifies the anomaly in the conservation of the energy-momentum tensor to capture the breakdown of classical conformal invariance in the quantum theory. It is determined by the short-distance behaviour of the theory.

For decoupled systems, say two free fields with no interaction terms, the energy-momentum tensors add up and so the central charge of the combined system will simply be the sum of the central charges of each system. In this sense, the central charge also acts like an extensive measure of the effective number of degrees of freedom of the theory.

For us, it is more useful to cast it in the context of the AdS/CFT correspondence. Here, it serves as a dual to the gravitational coupling constant G_N

$$c \sim \frac{1}{G_N} \tag{2.68}$$

and we will be interested in it as a parameter that controls the regime of various (semi-classical) limits. We will sharpen these remarks in a later section as required.

2.3 The Operator Formalism in Two Dimensional CFTs

Thus far, we understood the consequences of conformal invariance on two-dimensional QFTs through the path integral formalism. It is, however, instructive to use the language of Hilbert spaces and operators in CFT because of the powerful algebraic and group-theoretic structures present, and that is the goal of this section.

2.3.1 The Operator Formalism of Conformal Field Theory

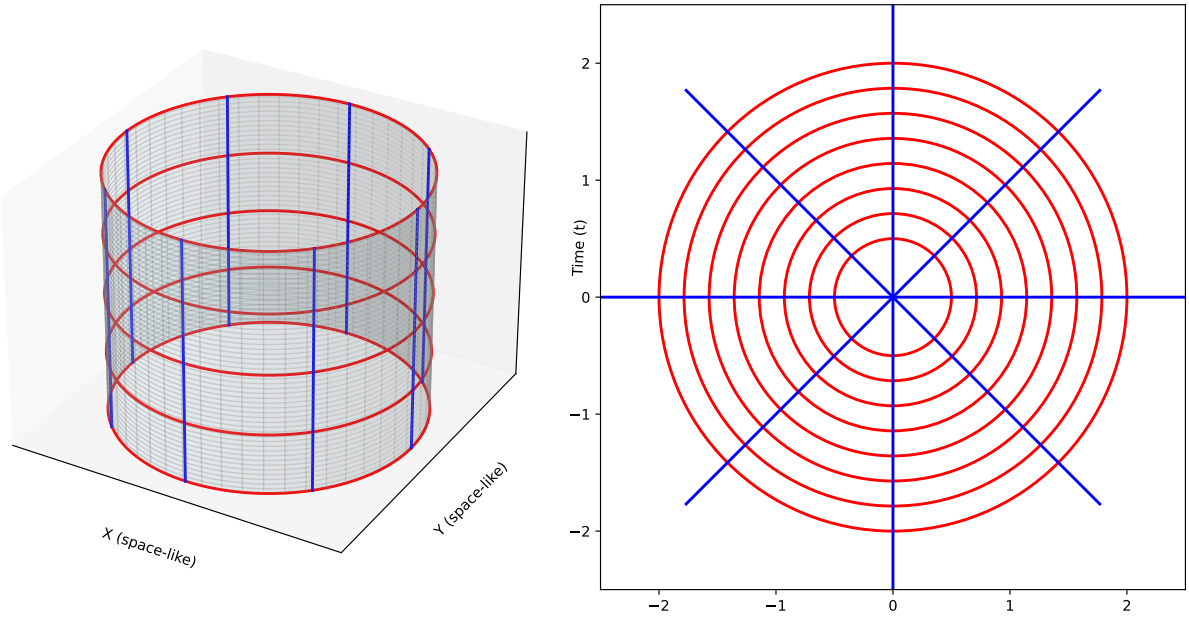

Figure 2.2: Radial Quantization: A cylinder in Euclidean spacetime is mapped to the complex plane. The concentric circles with radius $e^{\frac{2\pi t}{L}}$ are constant time curves, while constant space curves are straight lines emanating radially from the origin.

Radial Quantization

We define our theory on an infinite spacetime cylinder, with time t going from $-\infty$ to $+\infty$ along the axial direction of the cylinder and space is compactified with a coordinate x going from 0 to L. Analytically continuing the coordinates in the Euclidean space, the cylinder is described by the complex coordinate $\xi = t + ix$ (and its complex conjugate) and is mapped to the extended complex plane by

$$z = e^{\frac{2\pi\xi}{L}} = e^{\frac{2\pi t}{L}} e^{\frac{2\pi i x}{L}} \tag{2.69}$$

The complex plane is spanned by a radial time direction and an angular space direction (refer to Fig 2.2). The remote past ($t \to -\infty$) is mapped to the origin $z = 0$, while the remote future ($t \to +\infty$) is mapped to the point at infinity. This choice of space and time

directions leads to **radial quantization** of two-dimensional CFTs. To construct such a theory, we assume the existence of a vacuum state $|0\rangle$ from which the Hilbert space can be constructed (presumably by the application of creation operators). For free field theories, we define the vacuum as the state that is annihilated by the positive frequency (annihilation operator) component of the field.

Radial Ordering

The radial quantization mapping causes time-ordering in correlation functions on the cylinder to become **radial-ordering** on the complex plane

$$\boxed{\mathcal{R}\Phi(z)\Phi(w) = \begin{cases} \Phi(z)\Phi(w) & \text{if } |z| > |w| \\ \Phi(w)\Phi(z) & \text{if } |z| < |w| \end{cases}} \tag{2.70}$$

If the fields are fermions, then we need to put an extra negative sign when we exchange the two fields. Note that this means that all the OPEs we have written previously have an operator meaning only when $|z| > |w|$, it only makes sense if it is radial-ordered.

Contour Integrals as Commutation Relations

Consider the integral of two holomorphic fields $a(z)$ and $b(z)$

$$\oint_w dz\, a(z)b(z) \tag{2.71}$$

where the subscript w denotes the contour that circles around w in a counter-clockwise manner. This expression will have an operator meaning within a correlation function if we consider its radial-ordered product. Accordingly, operators described by the contour integral of holomorphic fields

$$A = \oint dz\, a(z) \qquad B = \oint dz\, b(z) \tag{2.72}$$

have the commutator

$$\boxed{[A, B] = \oint_0 dw \oint_w dz\, a(z)b(w)} \tag{2.73}$$

where integral over z is taken around w, and the integral over w is taken around the origin. In practice, we compute such integrals by substituting the OPE of $a(z)$ with $b(w)$ in the integral and using the residue theorem. This also means that we only need to know the $1/(z-w)$ term, as only the simple pole contributes via the residue theorem. Thus, we can now relate OPEs to commutation relations, and this allows us to translate dynamical or symmetry statements (like the Ward identities) contained in the OPE into the operator language.

2.3.2 The Virasoro Algebra

Conformal Generators

Recall the conformal Ward identity

$$\delta_{\epsilon,\bar{\epsilon}}\langle X\rangle = -\frac{1}{2\pi i}\oint_C dz\ \epsilon(z)\langle T(z)X\rangle + \frac{1}{2\pi i}\oint_C d\bar{z}\ \bar{\epsilon}(\bar{z})\langle \bar{T}(\bar{z})X\rangle \tag{2.74}$$

We define the conformal charge for the holomorphic part $\epsilon(z)$ of an infinitesimal conformal transformation to be

$$Q_\epsilon = \frac{1}{2\pi i}\oint dz\ \epsilon(z)T(z) \tag{2.75}$$

which can be written as

$$\begin{aligned}\delta_\epsilon\Phi(w) &= -\frac{1}{2\pi i}\oint_C dz\ \epsilon(z)T(z)\Phi(w)\\ &= -[Q_\epsilon, \Phi(w)]\end{aligned} \tag{2.76}$$

using the integral form of the commutator. The expression implies that the operator Q_ϵ is the generator of conformal transformations (as expected). Next, we find the mode expansion of the energy-momentum tensor

$$\begin{aligned}T(z) &= \sum_{n\in\mathbb{Z}} z^{-n-2}L_n \qquad L_n = \frac{1}{2\pi i}\oint dz\ z^{n+1}T(z)\\ \bar{T}(\bar{z}) &= \sum_{n\in\mathbb{Z}} \bar{z}^{-n-2}\bar{L}_n \qquad \bar{L}_n = \frac{1}{2\pi i}\oint dz\ \bar{z}^{n+1}\bar{T}(z)\end{aligned} \tag{2.77}$$

If we also expand the conformal change $\epsilon(z)$ in terms of modes

$$\epsilon(z) = \sum_{n\in\mathbb{Z}} z^{n+1}\epsilon_n \tag{2.78}$$

then, we can plug it into the definition of Q_ϵ to get

$$\begin{aligned}Q_\epsilon &= \frac{1}{2\pi i}\oint dz\ \epsilon(z)T(z)\\ &= \sum_{n\in\mathbb{Z}} \epsilon_n L_n\end{aligned} \tag{2.79}$$

These mode operators $\{L_n, \bar{L}_n\}$ are exactly the same as the generators $\{l_n, \bar{l}_n\}$ that we found previously; those were the generators of local conformal transformation on the space of functions, whereas these are the generators of local conformal transformations on the corresponding Hilbert space! In fact, we can use this equivalence even further to deduce that

the generators of $SL(2,\mathbb{C})$ in the Hilbert space are L_{-1}, L_1 and L_0 (and their antiholomorphic components). In particular, the operator $L_0 + \bar{L}_0$ generates the dilatations $(z, \bar{z}) \to (\lambda z, \lambda \bar{z})$, which are correspond to time translations according to the radial quantization convention. This implies that $L_0 + \bar{L}_0 \propto H$, the Hamiltonian of the system!

We can now derive the celebrated **Virasoro Algebra** by using Eqs. 2.67, 2.73 and 2.77 to get

$$\begin{aligned}[L_m, L_n] &= \frac{1}{2\pi i}\oint_0 dz\ z^{n+1}T(z)\frac{1}{2\pi i}\oint_z dw\ w^{m+1}T(w) \\ &= \frac{c}{12}(m^2-1)m\delta_{n+m,0} + (m-n)L_{n+m}\end{aligned} \tag{2.80}$$

followed by the antiholomorphic commutation relation using the exact same calculations. The trivial OPE $T(z)\bar{T}(w) \sim 0$ leads to

$$[L_m, \bar{L}_n] = 0 \tag{2.81}$$

which completes the set of commutation relations.

$$\boxed{\begin{aligned}&[L_n, L_m] = (n-m)L_{n+m} + \frac{c}{12}n(n^2-1)\delta_{n+m,0} \\ &[L_m, \bar{L}_n] = 0 \\ &[\bar{L}_n, \bar{L}_m] = (n-m)\bar{L}_{n+m} + \frac{c}{12}n(n^2-1)m\delta_{n+m,0}\end{aligned}} \tag{2.82}$$

The Hilbert Space

We start with the vacuum state. This ought to be invariant under global conformal transformations, which implies that it is annihilated by L_{-1}, L_1 and L_0 and their antiholomorphic components. Further, consider the modes of the energy-momentum tensor, specifically the relation

$$L_n = \frac{1}{2\pi i}\oint dz\ z^{n+1}T(z) \tag{2.83}$$

Since $T(z)$ is well-defined as $z \to 0$, we should have

$$L_n|0\rangle = \frac{1}{2\pi i}\oint dz\ z^{n+1}T(z)|0\rangle = 0 \quad \text{for} \quad n \geq -1 \tag{2.84}$$

This leads us to the conditions

$$\boxed{\begin{aligned}&L_n|0\rangle = 0 \\ &\bar{L}_n|0\rangle = 0\end{aligned} \qquad (n \geq -1)} \tag{2.85}$$

which also subsumes the invariance of the vacuum under the global conformal group. It also implies the vanishing of the vacuum expectation of the energy-momentum tensor

$$\boxed{\langle 0|T(z)|0\rangle = \langle 0|\bar{T}(\bar{z})|0\rangle = 0} \tag{2.86}$$

Primary fields when acting on the vacuum create asymptotic states, which are eigenstates of the Hamiltonian. Consider the OPE of $T(z)$ and a primary field $\phi(z,\bar{z})$ of conformal dimensions $(h,\bar{h})$, which we can translate into the operator formalism using the commutation relation identity as follows

$$\begin{aligned}
[L_n, \phi(w,\bar{w})] &= \frac{1}{2\pi i}\oint_w dz\; z^{n+1} T(z)\phi(w,\bar{w}) \\
&= \frac{1}{2\pi i}\oint_w dz\; z^{n+1}\left[\frac{h\phi(w,\bar{w})}{(z-w)^2} + \frac{1}{z-w}\partial\phi(w,\bar{w}) + \text{regular terms}\right] \\
&= h(n+1)w^n\phi(w,\bar{w}) + w^{n+1}\partial\phi(w,\bar{w}) \qquad (n \geq -1)
\end{aligned} \tag{2.87}$$

and the equivalent antiholomorphic expression. We can then apply these relations to the asymptotic state defined by this primary operator $\phi_h(z,\bar{z})$ at the origin $z,\bar{z} = 0$ acting on the vacuum state as

$$\boxed{|h,\bar{h}\rangle \equiv \phi_h(0,0)|0\rangle} \tag{2.88}$$

to get

$$\boxed{L_0|h,\bar{h}\rangle = h|h,\bar{h}\rangle \qquad \bar{L}_0|h,\bar{h}\rangle = \bar{h}|h,\bar{h}\rangle} \tag{2.89}$$

which also implies that $|h,\bar{h}\rangle$ is an eigenstate of the Hamiltonian $H \propto L_0 + \bar{L}_0$, with an eignevalue proportional to $h + \bar{h}$. In general, for $n > 0$, we have

$$\boxed{\begin{aligned} L_n|h,\bar{h}\rangle &= 0 \\ \bar{L}_n|h,\bar{h}\rangle &= 0 \end{aligned} \qquad (n>0)} \tag{2.90}$$

We now know one eigenstate of the Hamiltonian. We can then obtain the other states by applying ladder operators to $|h,\bar{h}\rangle$. For that, first, we need to expand the field $\phi(w)$ into its modes and then find the commutation relation

$$\begin{aligned}
[L_n, \phi_m] &= \left(\frac{1}{2\pi i}\right)^2 \oint_0 dw \oint_w dz\; z^{n+1} T(z) w^{m+h-1}\phi(w) \\
&= [n(h-1) - m]\phi_{n+m}
\end{aligned} \tag{2.91}$$

of which, we have the special case,

$$[L_0, \phi_m] = -m\phi_m \tag{2.92}$$

Note again that there is an antiholomorphic field, which acts as a spectator because it is decoupled from the holomorphic part. Evidently, the application of the $\phi_{\pm m}$ results in a change of the conformal dimension by $\mp m$. We also observe that by virtue of the Virasoro algebra, we have the commutation relation (for $m > 0$)

$$[L_0, L_{-m}] = mL_{-m} \tag{2.93}$$

which implies that the generators also change the conformal dimension in the same way. This means that excited states may be obtained by successive applications of these operators on the asymptotic state $|h, \bar{h}\rangle \equiv |h\rangle$ (dropping the decoupled antiholomorphic component). Thus, we have

$$|\text{descendant}\rangle = L_{-k_1} L_{-k_2} \dots L_{-k_n} |h\rangle \qquad (1 \leq k_1 \leq k_2 \leq \dots \leq k_n) \tag{2.94}$$

The increasing order of the k_i's is just to have a straightforward ordering convention of the excited states, one can always have a different ordering by taking linear combinations of the aforementioned states and then applying the commutation rules of the Virasoro algebra as required. The state described above is an eigenstate of L_0 with eigenvalue $h' = h + k_1 + k_2 + \dots + k_n \equiv h + N$. Such states are called **descendants** of the asymptotic state $|h\rangle$; and N is called the **level of the descendant**. The number of distinct, linearly independent states at level N is simply the **partition number** of the integer N, given by $p(N)$.

Level	Descendant
0	$\|h\rangle$
1	$L_{-1}\|h\rangle$
2	$L_{-2}\|h\rangle, \quad L_{-1}^2\|h\rangle$
3	$L_{-3}\|h\rangle, \quad L_{-2}L_{-1}\|h\rangle, \quad L_{-1}^3\|h\rangle$
...	...
N	$p(N)$

Table 2.2: A Verma module for conformal dimension h. Note that this represents only the holomorphic component.

The effect of a conformal transformation on a descendent state is obtained when some appropriate function of the generators L_m acts on it. The subset of the full Hilbert space generated by the state $|h\rangle$ and its descendants is closed under the action of the Virasoro generators, which forms a representation of the Virasoro algebra. This subspace is called a **Verma module** and we will return to this topic when we discuss minimal models and degenerate Virasoro blocks later.

We close our discussion on CFTs here, and move on to understanding AdS spaces and black holes in them.

Chapter 3

Black Holes in Anti-de Sitter space (AdS)

After concluding our discussion on (two-dimensional) CFTs, we will now briefly review three-dimensional anti-de Sitter space (AdS_3) which sets the stage to study theories in the bulk as postulated by the duality presented by the AdS/CFT correspondence. More importantly, we will focus on understanding the construction of the Bañados-Teitelboim-Zanelli (BTZ) black hole [31], a three-dimensional black hole that will serve as the main system of interest for the majority of this thesis.

No definite resource can be quoted for this mini-review, but there is undeniable inspiration regarding structure and exposition from various notes and review papers including *Anti-De Sitter Space* by Bengtsson [35], *The (2+1)-Dimensional Black Hole* by Carlip [36] and Satoh [37, 38].

3.1 Anti-de Sitter space

Anti-de Sitter (AdS) space is an exact solution to Einstein's equations

$$G_{\mu\nu} + \Lambda g_{\mu\nu} = \frac{8\pi G}{c^4} T_{\mu\nu} \tag{3.1}$$

with a **negative cosmological constant** ($\Lambda < 0$). Mathematically, one usually describes it as a maximally symmetric Lorentzian manifold with a constant negative curvature. Unlike flat or positively curved spaces, AdS possesses a boundary at infinity and exhibits a high degree of symmetry governed by the $SO(2, d-1)$ isometry group in d-dimensional AdS.

While a general analysis of AdS spaces is interesting in its own right, we will begin our study on AdS exclusively in three dimensions: we do not aim at exploring the entire scope

of AdS spaces, and this specific case teaches us enough about AdS that can be generalized in a straightforward manner.

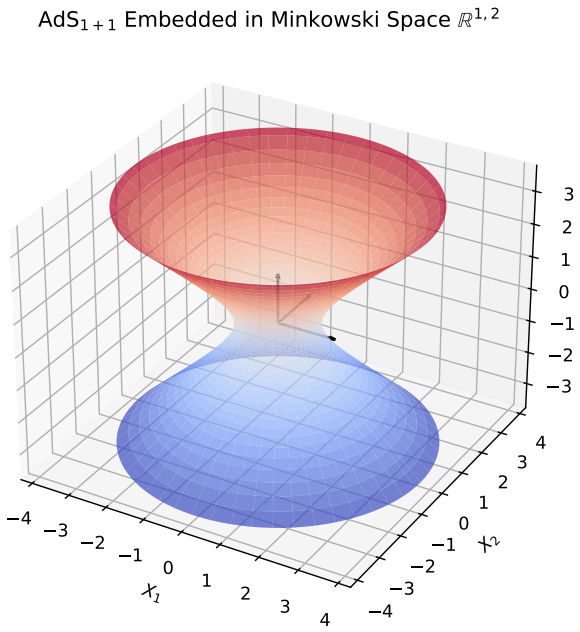

Figure 3.1: A visualization of (1+1)-dimensional anti-de Sitter space embedded in flat (1+2)-dimensional space.

3.2 Three-dimensional black holes Anti-De Sitter space ($\mathbf{AdS_3}$)

AdS_3 can be defined as the hyperboloid

$$-u^2 - v^2 + x^2 + y^2 = -l^2 \tag{3.2}$$

embedded in $\mathbb{R}^{2,2}$, which is a pseudo-Riemmanian manifold given by the metric

$$ds^2 = -du^2 - dv^2 + dx^2 + dy^2 \tag{3.3}$$

Here, l denotes the so-called **AdS length scale** and is related to the cosmological constant

$$\Lambda = -\frac{1}{l^2} \tag{3.4}$$

The most useful thing we can do next is to parametrize the embedding in the so-called **global coordinates** $\{\tau, \rho, \theta\}$

$$\begin{aligned} u &= l \sin\tau \sec\rho \qquad v = l \cos\tau \sec\rho \\ x &= l \sin\theta \tan\rho \qquad y = l \cos\theta \tan\rho \end{aligned} \tag{3.5}$$

which trivially solve the constraint Eq. 3.2 using simple trigonometric identities. Plugging them into Eq. 3.3, we get the induced AdS_3 metric in terms of global coordinates

$$\boxed{ds^2 = \frac{l^2}{\cos^2\rho}\left(-d\tau^2 + d\rho^2 + \sin^2\rho\, d\theta^2\right)} \tag{3.6}$$

where the ranges of the coordinates are given by

$$0 \leq \rho < \frac{\pi}{2}, \qquad 0 \leq \theta < 2\pi, \qquad -\infty < \tau < +\infty \tag{3.7}$$

Note that the parametrization makes τ a periodic variable much like θ. However, we are usually interested in the decompactfied **universal covering space** of AdS_3, and so we let τ range over $(-\infty, +\infty)$. Henceforth, we will also use the term AdS_3 to mean the universal cover unless otherwise stated.

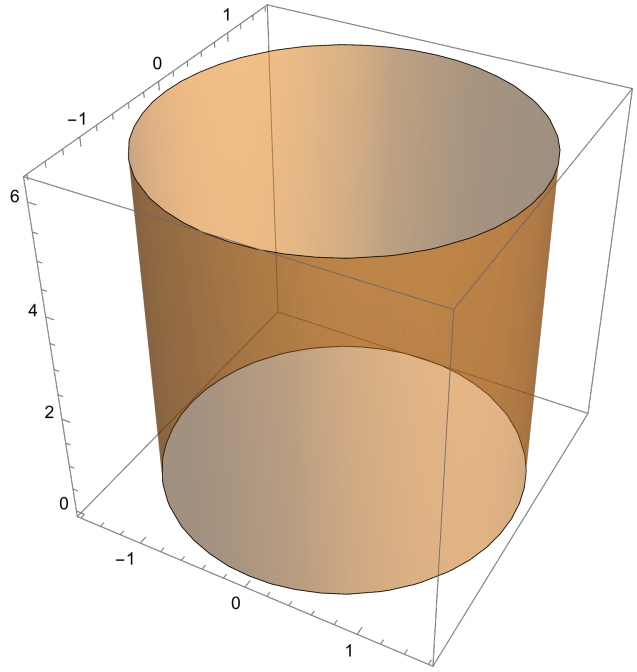

Figure 3.2: The AdS_3 cylinder

Conventionally, a pictorial representation of the global AdS_3 geometry is given using a cylinder which is the span of three global coordinates: ρ as the radial, θ as the angular and

τ as the axial span of the cylinder. This representation is referred to as the **global $\mathbf{AdS_3}$ cylinder**, as given in Fig. 3.2).

One can also parametrize the embedding coordinates using the following coordinate patches

$$\begin{aligned}
&\underline{\text{Region I: } r_+ < r < \infty} \\
&u = \sqrt{\tilde{r}^2}\cosh\tilde{\phi} \qquad v = \sqrt{\tilde{r}^2 - l^2}\sinh\tilde{t} \\
&x = \sqrt{\tilde{r}^2}\sinh\tilde{\phi} \qquad y = \sqrt{\tilde{r}^2 - l^2}\cosh\tilde{t} \\
&\underline{\text{Region II: } r_- < r < r_+} \\
&u = \sqrt{\tilde{r}^2}\cosh\tilde{\phi} \qquad v = \sqrt{l^2 - \tilde{r}^2}\cosh\tilde{t} \\
&x = \sqrt{\tilde{r}^2}\sinh\tilde{\phi} \qquad y = \sqrt{l^2 - \tilde{r}^2}\sinh\tilde{t} \\
&\underline{\text{Region III: } 0 < r < r_-} \\
&u = \sqrt{-\tilde{r}^2}\cosh\tilde{\phi} \qquad v = \sqrt{l^2 - \tilde{r}^2}\cosh\tilde{t} \\
&x = \sqrt{-\tilde{r}^2}\sinh\tilde{\phi} \qquad y = \sqrt{l^2 - \tilde{r}^2}\sinh\tilde{t}
\end{aligned} \tag{3.8}$$

where

$$\tilde{r}^2 = l^2\left(\frac{r^2 - r_-^2}{r_+^2 - r_-^2}\right) \qquad \begin{pmatrix}\tilde{t}\\ \tilde{\phi}\end{pmatrix} = \frac{1}{l}\begin{pmatrix} r_+ & -r_- \\ -r_- & r_+\end{pmatrix}\begin{pmatrix} t/l \\ \phi\end{pmatrix} \tag{3.9}$$

Plugging these into Eq. 3.3, we get

$$\boxed{ds^2 = -\left(\frac{r^2}{l^2} - M\right)dt^2 - Jdtd\phi + \left(\frac{r^2}{l^2} - M + \frac{J^2}{4r^2}\right)^{-1}dr^2 + r^2 d\phi^2} \tag{3.10}$$

for

$$\boxed{M = \frac{r_+^2 + r_-^2}{l^2} \qquad J = \frac{2r_+r_-}{l}} \tag{3.11}$$

with the coordinate ranges

$$0 \le r < \infty, \qquad -\infty < \phi, t < \infty \tag{3.12}$$

3.3 BTZ black holes

In the $\{t, r, \phi\}$ coordinates, the metric looks very suggestive of some relation to black holes. If we think of M as a mass term, and J as the angular momentum term, we observe a resemblance with the usual black hole metrics (but for three dimensions). In fact, this is the motivation for the construction of the BTZ metric.

We note that the metric has a **Killing vector** ∂_ϕ, and thus, there is a symmetry in the

manifold. One can then identify

$$\phi \sim \phi + 2\pi n \qquad n \in \mathbb{Z} \tag{3.13}$$

under the discrete subgroup generated by the aforementioned Killing vector; and this results in the BTZ black hole metric, which we now express completely as

$$\boxed{ds^2 = -\left(\frac{r^2}{l^2} - M\right) dt^2 - J dt d\phi + \left(\frac{r^2}{l^2} - M + \frac{J^2}{4r^2}\right)^{-1} dr^2 + r^2 d\phi^2} \tag{3.14}$$

where

$$0 \leq r < \infty, \qquad -\infty < t < \infty, \qquad 0 \leq \phi < 2\pi \tag{3.15}$$

and r_+ is called the **outer horizon** and r_- is called the **inner horizon**. The BTZ metric results from a quotienting of the AdS_3 space.

It is clear that since this metric has been derived from the AdS_3 metric, it shares the local properties of AdS. This means that it is a solution of Einstein gravity; and it provides a very simple system that has a constant negative curvature and no curvature singularities. In addition to this, it also has two characteristic horizons ($r = r_-, r_+$) along with the notion of a mass M and angular momentum J, making it a ubiquitous system for understanding various features of quantum gravity in a simplified setting. In this thesis, we are primarily concerned with the static, or non-rotating black hole. Setting $J, r_- = 0$, we get the static black hole metric which we will encounter frequently

$$\boxed{ds^2 = -\left(\frac{r^2 - r_+^2}{l^2}\right) dt^2 + \left(\frac{r^2 - r_+^2}{l^2}\right)^{-1} dr^2 + r^2 d\phi^2} \tag{3.16}$$

3.3.1 Mapping the black hole inside the AdS cylinder

One of the things that will turn out to be helpful in later calculations is to have an understanding of how the BTZ black hole "sits" inside the AdS cylider. In other words we want to know how the BTZ coordinates map into the AdS cylinder which is in terms of the global coordinates. To understand the different "Regions" specified in Eq. 3.8, we need to equate the various embedding coordinates; that will give us the BTZ coordinates as some functions $f(\tau, \rho, \theta)$. These can then be plotted inside the cylinder to visualize how the BTZ coordinate patches look like in global coordinates, refer to Fig. 3.3. Note that there is no Region III for a static ($r_- = 0$) black hole.

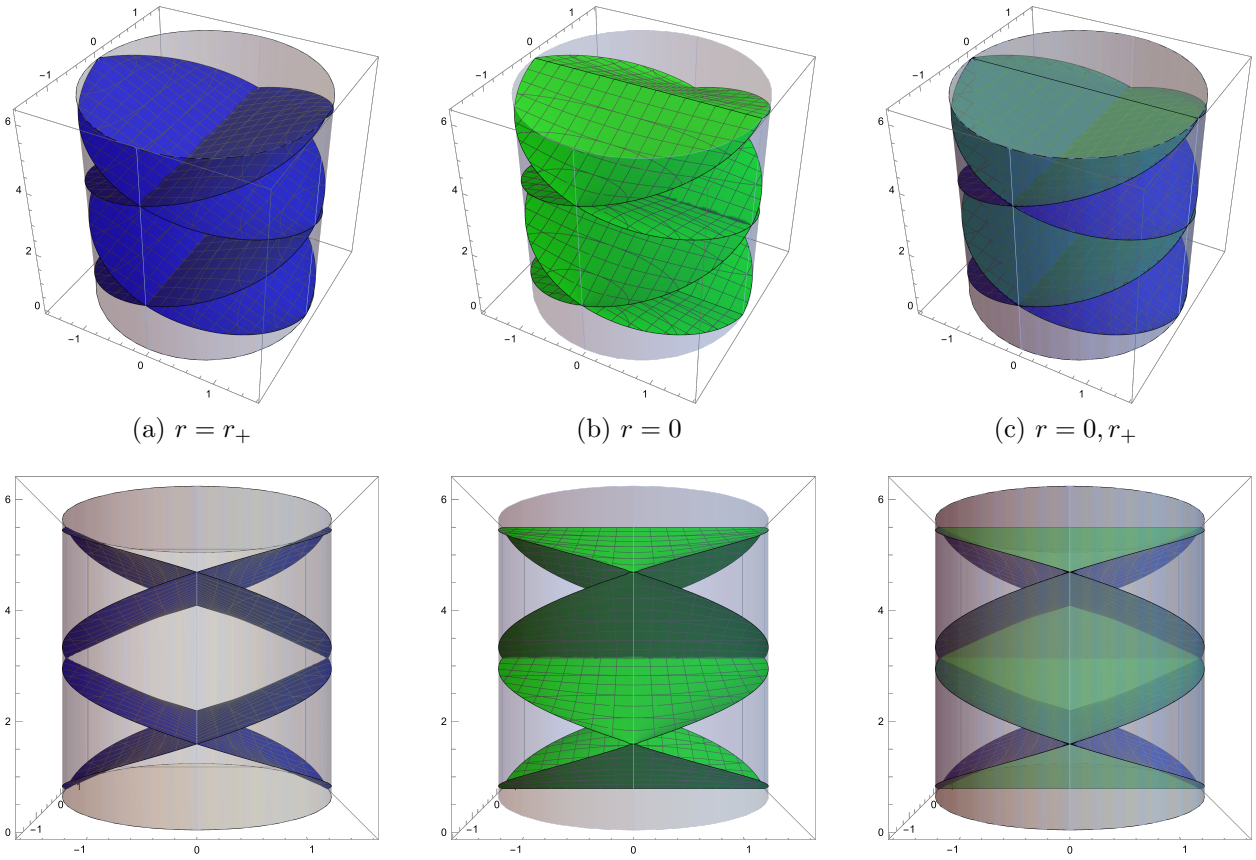

(a) $r = r_+$ (b) $r = 0$ (c) $r = 0, r_+$

(d) $r = r_+$ (e) $r = 0$ (f) $r = 0, r_+$

Figure 3.3: Fig. 3.3a and 3.3d correspond to the horizon $r = r_+$; and it is a periodic set of curves given by "planes" at 45°.
Fig. 3.3b and 3.3e correspond to $r = 0$; again, it is given by a periodic set of "planes" at 45° which look very similar to the ones in Fig. 3.3a and 3.3d. Indeed, these two are really the same, just rotated by 90° and shifted along the axis.
Fig. 3.3c and 3.3e show how the various regions exist in the cylinder: Region I is the one bounded by the blue curves and the surface of the cylinder, Region II is the one bounded by the blue and green curves; as we can see, BTZ coordinates do not cover the entirety of the cylinder.

Region I

When we match the various embedding equations, we get

$$\begin{aligned}\left(\frac{r}{r_+}\right)^2 &= \frac{\sin^2\tau - \sin^2\theta\sin^2\rho}{\cos^2\rho} \\ \tanh\frac{r_+}{l}\phi &= \frac{\sin\theta\tan\rho}{\sin\tau\sec\rho} = \frac{\sin\theta\sin\rho}{\sin\tau} \\ \tan\frac{r_+}{l^2}t &= \frac{\cos\tau\sec\rho}{\cos\theta\tan\rho} = \frac{\cos\tau}{\cos\theta\sin\rho}\end{aligned} \tag{3.17}$$

Region II

We can do the same for Region II to get

$$\begin{aligned}\left(\frac{r}{r_+}\right)^2 &= \frac{\sin^2\tau - \sin^2\theta\sin^2\rho}{\cos^2\rho} \\ \tanh\frac{r_+}{l}\phi &= \frac{\sin\theta\tan\rho}{\sin\tau\sec\rho} = \frac{\sin\theta\sin\rho}{\sin\tau} \\ \tan\frac{r_+}{l^2}t &= \frac{\cos\theta\tan\rho}{\cos\tau\sec\rho} = \frac{\cos\theta\sin\rho}{\cos\tau}\end{aligned} \tag{3.18}$$

3.4 Black holes in Euclidean AdS_3

To get the Euclidean version of AdS_3, we flip one negative sign in the embedding space hyperboloid

$$-u^2 + v^2 + x^2 + y^2 = -l^2 \tag{3.19}$$

as well as the metric

$$ds^2 = -du^2 + dv^2 + dx^2 + dy^2 \tag{3.20}$$

Next, we can again parametrize the embedding in terms of Euclidean global coordinates $\{\rho_E, \theta_E, \tau_E\}$ (henceforth, we will drop the subscript "E" used to denote Euclidean variables)

$$\begin{aligned}u &= l\cosh\tau\sec\rho \quad v = l\sinh\tau\sec\rho \\ x &= l\sin\theta\tan\rho \qquad y = l\cos\theta\tan\rho\end{aligned} \tag{3.21}$$

which trivially solve the constraint Eq. 3.19 using simple trigonometric and hyperbolic function identities. Plugging them into Eq. 3.20, we get the Euclidean AdS_3 metric in terms of

Euclidean global coordinates

$$\boxed{ds^2 = \frac{l^2}{\cos^2\rho}\left(d\tau^2 + d\rho^2 + \sin^2\rho\, d\theta^2\right)} \tag{3.22}$$

where the ranges of the coordinates are given by

$$0 \leq \rho < \frac{\pi}{2}, \qquad 0 \leq \theta < 2\pi, \qquad -\infty \leq \tau < +\infty \tag{3.23}$$

Note that here, we do not have to make any statement about this being the universal cover or otherwise, the range of τ is naturally over $(-\infty, +\infty)$. Also, it worth keeping in mind that in practice, one usually does not work their way through the embedding coordinates; a simple Wick rotation $\tau \to -i\tau$ suffices.

Similar to the Lorentzian case, we can solve for the Euclidean BTZ coordinates $\{t_E, r_E, \phi_E\}$ (again, we will be dropping the subscript "E" henceforth) just the way we did for Euclidean global coordinates. We will consider the static ($r_- = 0$) case. One of the first things we notice is that we cannot replicate an appropriate, consistent Region II for the Euclidean case, and so, we just have a mapping for Region I, namely

$$\begin{aligned} &\underline{\text{Region I: } r_+ < r < \infty} \\ &u = \sqrt{\tilde{r}^2}\cosh\tilde{\phi} \qquad v = \sqrt{\tilde{r}^2 - l^2}\sin\tilde{t} \\ &x = \sqrt{\tilde{r}^2}\sinh\tilde{\phi} \qquad y = \sqrt{\tilde{r}^2 - l^2}\cos\tilde{t} \end{aligned} \tag{3.24}$$

where

$$\tilde{r} = r\frac{l}{r_+} \qquad \tilde{\phi} = \phi\frac{r_+}{l} \qquad \tilde{t} = t\frac{r_+}{l^2} \tag{3.25}$$

Plugging these into Eq. 3.3, we get

$$\boxed{ds^2 = \left(\frac{r^2 - r_+^2}{l^2}\right)dt^2 + \left(\frac{r^2 - r_+^2}{l^2}\right)^{-1} dr^2 + r^2 d\phi^2} \tag{3.26}$$

with the coordinate ranges

$$r_+ \leq r < \infty, \qquad -\infty < \phi < \infty \qquad 0 \leq t < \frac{2\pi l^2}{r_+} \tag{3.27}$$

Again, recall that this discussion is for the static black hole. The general Lorentzian black hole has 3 regions, while the general Euclidean black hole has 2 regions. Meanwhile the static Lorentzian black hole has 2 regions and the static Euclidean black hole has 1 region (which is what we discussed above.)

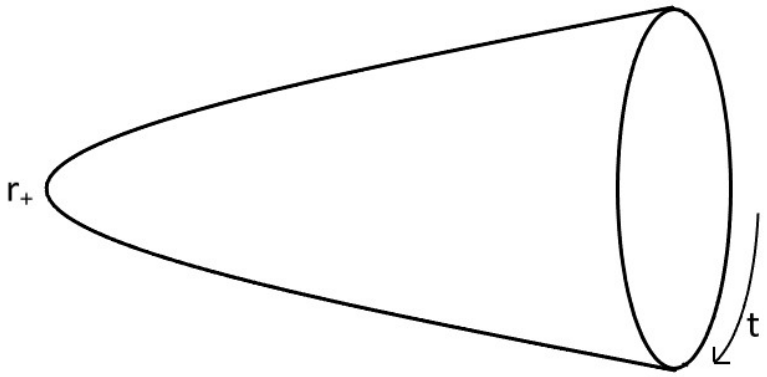

Figure 3.4: The Euclidean BTZ cigar geometry. The smooth tip corresponds to the horizon, while the circular cross sections extends to infinity as $r \to \infty$. The periodicity in the time coordinate t is β and the ϕ coordinate is suppressed.

3.4.1 Caveats about the Euclidean BTZ black hole

We can see that the coordinate range of t has been confined to one period, although, in principle, we have no reason to compactify the range of t. However, it turns out to be a necessary feature of the Euclidean metric. As $r \to r_+$, that is, as we go closer to the horizon, it turns out that for the manifold to be smooth around this point, the t coordinate must "close" properly. In other words, one has to make an identification

$$t \sim t + \beta \tag{3.28}$$

to avoid a conic defect or a conic singularity arising at $r = r_+$. A defect here would mean that the spacetime is locally AdS everywhere except the horizon and that it cannot be smoothly continued to include it. Because this is unphysical, we identify the t coordinate using

$$\beta = \frac{2\pi l^2}{r_+} \tag{3.29}$$

which is quite interesting, as that is exactly the inverse of the temperature that one usually gets due to the imaginary time prescription in path integrals. What we find is that smoothing the geometry is consistent with the fact that the black hole is a thermal system given by a

Hawking temperature of

$$T_H = \frac{r_+}{2\pi l^2} \tag{3.30}$$

This confirms the thermodynamic properties of BTZ black holes and also is the origin of the popular **cigar with a smooth tip representation** of the Euclidean BTZ black hole as depicted in Fig. 3.4.

3.4.2 Mapping the Euclidean black hole inside the Euclidean AdS cylinder

To map the various regions covered by the Euclidean BTZ coordinates patches in the Euclidean global cylinder, we apply the same algorithm as before; match the embedding coordinates. This leads us to the set of equations

$$\begin{aligned} \left(\frac{r}{r_+}\right)^2 &= \frac{\cosh^2\tau - \sin^2\theta\sin^2\rho}{\cos^2\rho} \\ \tanh\frac{r_+}{l}\phi &= \frac{\sin\theta\tan\rho}{\cosh\tau\sec\rho} = \frac{\sin\theta\sin\rho}{\cosh\tau} \\ \tan\frac{r_+}{l^2}t &= \frac{\sinh\tau\sec\rho}{\cos\theta\tan\rho} = \frac{\sinh\tau}{\cos\theta\sin\rho} \end{aligned} \tag{3.31}$$

We can now set t, r, ϕ to some constant values and see how they map inside the AdS_3 cylinder, that will help us determine how the exterior of the Euclidean black hole looks like.

Radial Dependence

The "allowed region" is given by the inequality

$$1 \leq \frac{\cosh^2\tau - \sin^2\theta\sin^2\rho}{\cos^2\rho} < \infty \tag{3.32}$$

τ Dependence

The "allowed region" is given by the inequality

$$-\infty < \frac{\sinh\tau}{\cos\theta\sin\rho} < +\infty \tag{3.33}$$

Angular Dependence

Here, we need to be careful; when we periodically identify ϕ, the domain becomes $[0, 2\pi)$, and so, the region available to the BTZ exterior is restricted owing to this "range cut-off".

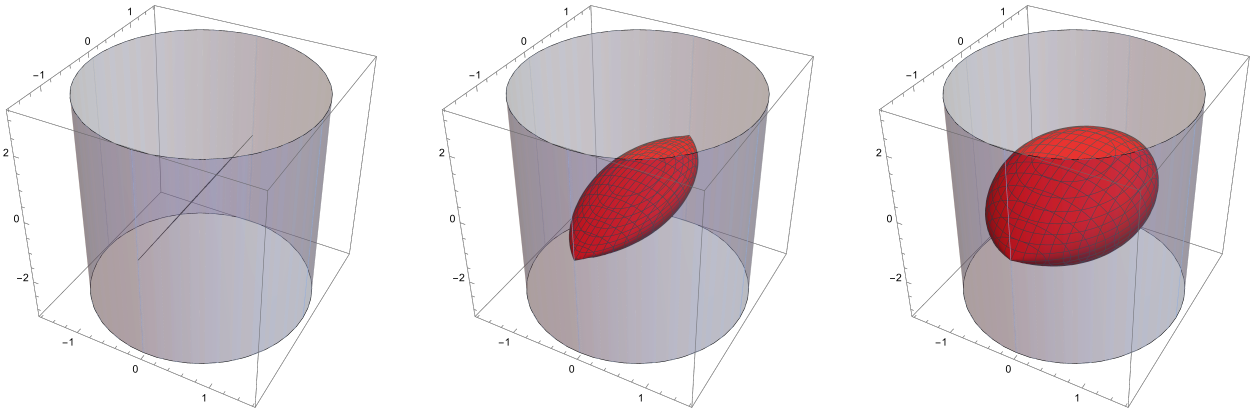

(a) $r = r_+$ (b) $r = 2r_+$ (c) $r = 3r_+$

Figure 3.5: Fig. 3.5a corresponds to the horizon $r = r_+$; and it is a line given by $(0 < \rho < \pi/2,\ \theta = \pi/2, 3\pi/2,\ \tau = 0)$. Fig. 3.5b and 3.5c correspond to constant values of r in units of r_+. As the value of the constant increases, the thickness of this surface increases, and in the limit $r \to \infty$, we find that the surface asymptotically becomes the surface of the cylinder $(\rho = \pi/2,\ \tau \to \pm\infty)$

In particular, we need

$$0 \leq \frac{\sin\theta \sin\rho}{\cosh\tau} < \tanh 2\pi \tag{3.34}$$

as opposed to the full range of ϕ which would have otherwise made the upper limit unity.

3.4.3 Discussion

We see that the Euclidean BTZ coordinates and Euclidean global coordinates cover the entirety of AdS_3, which is different than what we saw for the Lorentzian case. However, this is not true once we make the periodic identification of the BTZ angular coordinate ϕ, as now the range of the angular coordinate is $[0, 2\pi)$. Note that any periodic interval of 2π will suffice, our choice is the most obvious interval to pick for a harmonic function! Thus, the BTZ black hole does not cover the entirety of the AdS cylider, as is expected given its status as a quotient of AdS under identification.

As depicted in Fig. 3.6b and 3.6d one sees that the BTZ black hole exterior (not to be confused with AdS_3 space in terms of BTZ coordinates) covers only a region corresponding to half the cylinder, in particular, the region bounded by $0 \leq \theta \leq \pi$. That is not all; the upper bound of $\tanh 2\pi$ implies that only the region between the plane (the plane that divides the cylinder into two halves as mentioned above) and the curve that defines that $\phi = 2\pi$ curve is an "allowed" region. As one can see in Fig. 3.6a and 3.6c, this essentially means that an extremely small "pocket" of the cylinder is taken out.

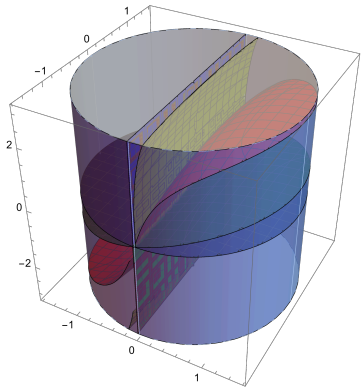

(a) Constant Euclidean BTZ time curves in global Euclidean AdS_3

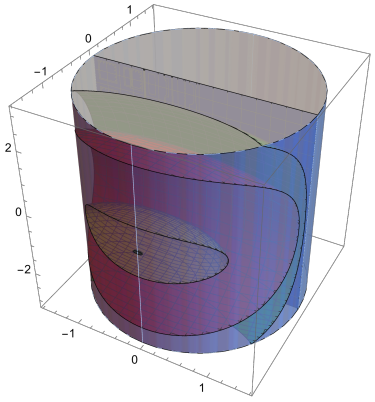

(b) Constant Euclidean BTZ ϕ curves in global Euclidean AdS_3

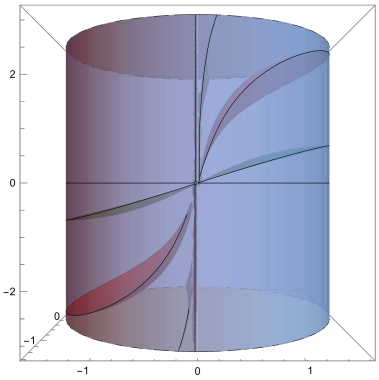

(c) Constant Euclidean BTZ time curves in global Euclidean AdS_3

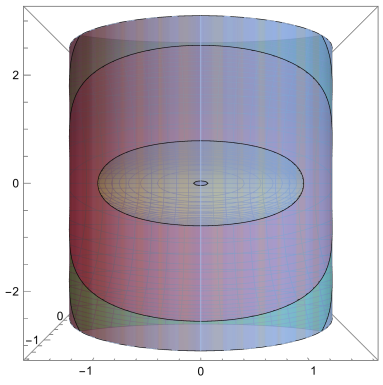

(d) Constant Euclidean BTZ ϕ curves in global Euclidean AdS_3

Figure 3.6: Fig. 3.6a and 3.6c give surfaces with constant values of Euclidean BTZ time t plotted in global Euclidean AdS_3 coordinates; while Fig. 3.6b and 3.6d give surfaces with constant values of Euclidean BTZ ϕ coordinate plotted in global Euclidean AdS_3 coordinates

We have thus identified the span of the BTZ exterior inside the AdS cylinder; while a simple exercise, it is worth doing once as it helps understand the geometry of the BTZ black hole. This, in turn, will motivate the set-up of various geometric prescriptions in the latter parts of this thesis. We close our discussion regarding AdS spaces and BTZ black holes with this.

Part II

Virasoro Blocks and Information Loss I: Degenerate blocks and non-perturbative corrections

Chapter 4

Setting up the stage

4.1 Forbidden Singularities: A hallmark of information loss in AdS/CFT

4.1.1 Thermal correlators in AdS black hole backgrounds

It is known that if one computes d-dimensional CFT correlation functions perturbatively for the gravitational coupling constant G_N in the corresponding thermal $d+1$-dimensional AdS space, then they satisfy the **Kubo−Martin−Schwinger** (KMS) condition which enforces periodicity in Euclidean time t_E. Thus, a two-point correlation function

$$\langle \mathcal{O}_L(t)\mathcal{O}_L(0)\rangle_{T_H} \tag{4.1}$$

in a canonical ensemble at some fixed temperature T_H should be periodic in Euclidean time t_E with a period $\beta = 1/T_H$, as is standard from the thermal path integral. One can compute such a thermal two-point correlator for the simple case of scalar fields (represented by the field $\mathcal{O}_L$) probing scalar BTZ black holes (represented by the field $\mathcal{O}_H$) by considering the appropriate Euclidean metric

$$ds^2 = (r^2 - r_+^2)dt^2 + \frac{dr^2}{(r^2 - r_+^2)} + r^2 d\phi^2 \tag{4.2}$$

where the AdS length scale l has been set to unity. As we have seen previously, the horizon radius r_+ is related to the Hawking temperature by

$$T_H = \frac{r_+}{2\pi} \tag{4.3}$$

To interpret the black hole as a CFT state, one has to set the holomorphic dimension h_H of the corresponding operator $\mathcal{O}_H$ to

$$r_+ = \sqrt{\frac{24h_H}{c} - 1} \tag{4.4}$$

The c that shows up here is the central charge of the CFT_2 dual to the AdS_3 space that we are considering, and it is related to the gravitational coupling constant G_N as (refer to Table 4.1 for an operational AdS/CFT extrapolate dictionary)

$$G_N = \frac{3}{2c} \tag{4.5}$$

This calculation results in [18, 39]

$$\langle \mathcal{O}_L(z,\bar{z})\mathcal{O}_L(1)\rangle_{r_+} = \sum_{n=-\infty}^{+\infty} [V(z,n)]^{h_L}[V(\bar{z},-n)]^{\bar{h}_L} \tag{4.6}$$

with

$$V(z,n) = \frac{1-z}{(\sin\left(\frac{r_+}{2}(\log(1-z)+2\pi i n)\right))^2} \tag{4.7}$$

We note that this correlator has periodic singularities that are due to the $n = 0$ piece, and at

$$z = 1 - e^{\frac{2\pi m}{r_+}} \qquad m \in \mathbb{Z} \tag{4.8}$$

The key takeaway point is that **correlators in a (BTZ) black hole background show periodic singularities**.

AdS (Bulk Theory)	**CFT (Boundary Theory)**
3-dimensional AdS space	2-dimensional conformal field theory
Gravitational coupling constant G_N	Central charge c
Metric $g_{\mu\nu}$	Stress tensor $T_{\mu\nu}$
Bulk scalar field $\phi(\rho,\tau,\theta)$	Scalar operator $\mathcal{O}_h(z)$
Mass of bulk field $m^2_{\text{AdS}} = \Delta(\Delta-2)$	Scaling dimension Δ $\Delta = 2h$
Black hole in AdS space	Thermal state in CFT

Table 4.1: A dictionary for the dual elements in $\text{AdS}_3/\text{CFT}_2$. Clearly the semi-classical limit $G_N \to 0$ is equivalent to $c \to \infty$, and we will use this as we go ahead.

To leading order in $G_N \to 0, c \to \infty$, we expect that such a thermal correlator is identical to the correlator in the background of a heavy microstate; that is, we can interpret it as a

four-point correlator in CFT_2 using the state-operator correspondence

$$\langle \mathcal{O}_L(z)\mathcal{O}_L(1)\rangle_{\text{black hole}} \sim \langle \mathcal{O}_H(\infty)\mathcal{O}_L(1)\mathcal{O}_L(z)\mathcal{O}_H(0)\rangle \tag{4.9}$$

However, it is well known that such a vacuum correlation function of local operators **cannot have singularities other than the OPE singularities** at $z \to 0, 1$ and ∞. Clearly, the semi-classical calculation is missing something that is leading to this inconsistency. In fact, this has a very close relation to the information loss paradox: it is known that information loss is related to the exponential decay of the correlator for large Lorentzian times t_L [6]. A periodic singularity due to a harmonic function in t_E will result in a hyperbolic function when we analytically continue it to Euclidean time $t_E = -it_L$ (which showcases exponential decay at large t_L). Thus, these **forbidden singularities** (and the decay in the Lorentzian case) are a **distinctive signature of unitarity violation and information loss** in AdS black holes.

4.1.2 Understanding information loss through Virasoro blocks

Virasoro conformal blocks

Consider the four-point function of primary operators $\mathcal{O}_i(z_i, \bar{z}_i)$ with conformal dimensions $(h_i, \bar{h}_i)$.

$$\langle \mathcal{O}_1(z_1, \bar{z}_1)\mathcal{O}_2(z_2, \bar{z}_2)\mathcal{O}_3(z_3, \bar{z}_3)\mathcal{O}_4(z_4, \bar{z}_4)\rangle \tag{4.10}$$

These are usually represented in terms of the **anharmonic cross ratio**

$$z = \frac{(z_1 - z_2)(z_3 - z_4)}{(z_1 - z_3)(z_2 - z_4)} \tag{4.11}$$

and the corresponding antiholomorphic version $\bar{z}$ which remain invariant under global conformal transformations. Using global conformal invariance, one conventionally fixes three of the points at $0, 1$ and ∞, and we can then consider the standard form of the four-point correlator

$$\langle \mathcal{O}_1(\infty)\mathcal{O}_2(0)\mathcal{O}_3(z)\mathcal{O}_4(1)\rangle \tag{4.12}$$

Now, as we have seen before, the operators $\mathcal{O}_h$ act on the vacuum state $|0\rangle$ to give asymptotic states $|h, \bar{h}\rangle$ and they (along with their Virasoro descendants) form a Verma module (refer to Table 2.2). The union of these Verma modules serves as a basis for the Hilbert space of the CFT. This is the **set of irreducible highest weight representations of the Virasoro algebra** and their descendants. Consequently, they can be used to create a block

decomposition of the four-point function as

$$\begin{aligned}\langle \mathcal{O}_1(\infty)\mathcal{O}_2(0)\mathcal{O}_3(z,\bar{z})\mathcal{O}_4(1)\rangle &= \sum_{h,\bar{h}} \langle \mathcal{O}_1(\infty)\mathcal{O}_2(0)|h,\bar{h}\rangle\langle h,\bar{h}|\mathcal{O}_3(z,\bar{z})\mathcal{O}_4(1)\rangle \\ &= \sum_{h,\bar{h}} P_{h,\bar{h}}\mathcal{V}_h(z,h_i)\mathcal{V}_{\bar{h}}(\bar{z},\bar{h}_i)\end{aligned} \tag{4.13}$$

where the sum is over all possible conformal dimensions $h, \bar{h}$ in the spectrum of the CFT. The $P_{h,\bar{h}}$ term is related to the OPE coefficients of the particular channel that has been expanded (one can insert the projection operator between any two $\mathcal{O}_i\mathcal{O}_j$ which will change the OPE coefficients, this is what we mean when we say a change in channel). Because the holomorphic and anti-holomorphic Virasoro algebras commute, one can conveniently write the block structure in a factorized form; and henceforth we will mean the holomorphic component $\mathcal{V}_h(z,h_i)$ when we talk about the **Virasoro conformal block**.

For the reader familiar with scattering in spherically symmetric potentials, this is the exact analogue of using the spherical harmonics $Y_{l,m}(\theta,\phi)$ (which are the irreducible representations of the rotation symmetry group $SO(3)$) to decompose amplitudes into partial waves. Since we want to understand the particular case of the h_H, h_L dimensions which have a physical interpretation of a light object interacting with a heavy black hole, for us the expression becomes

$$\langle \mathcal{O}_H(\infty)\mathcal{O}_L(1)\mathcal{O}_L(z,\bar{z})\mathcal{O}_H(0)\rangle = \mathcal{V}_0(1-z,h_i)\mathcal{V}_0(1-\bar{z},\bar{h}_i) + \sum_{h,\bar{h}} P_{h,\bar{h}}\mathcal{V}_h(1-z,h_i)\mathcal{V}_{\bar{h}}(1-\bar{z},\bar{h}_i) \tag{4.14}$$

Note that exchange of positions 0 and 1 in the correlator means that we are actually expanding the correlator through a different channel, and so we have to take $z \to 1-z$.

These blocks contain a tremendous amount of information about quantum gravity in AdS_3. This is because, as we see in Table 4.1, the stress-energy tensor $T_{\mu\nu}$ in the CFT is dual to the $g_{\mu\nu}$ curvature tensor in AdS (which is responsible for gravitons in the bulk) and the L_n's are simply modes of it (refer to Eq. 2.77). Thus, all the primary states $|h\rangle$ and their descendant states (due to the action of the L_n's) are related to some sort of graviton exchange. In short, summing over all the various Virasoro blocks is equivalent to summing over all possible graviton exchange effects between the light probe and the black hole! A cartoon representation of the same is given in Fig. 4.1

We are particularly interested in the vacuum Virasoro block ($h = 0$) for a couple of reasons:

1. The vacuum Virasoro block is universal since $h = 0$ always exists in the spectrum of all CFTs. Alternatively, since the vacuum projector $|0\rangle\langle 0|$ exists in all CFTs it is a universal presence by construction of the vacuum state.

$$\left\langle \mathcal{O}_H \mathcal{O}_H \left(\sum_{\{m_i,k_i\}} \frac{L_{-m_1}^{k_1} \cdots L_{-m_n}^{k_n} |h\rangle\langle h| L_{m_n}^{k_n} \cdots L_{m_1}^{k_1}}{\mathcal{N}_{\{m_i,k_i\}}} \right) \mathcal{O}_L \mathcal{O}_L \right\rangle \approx$$

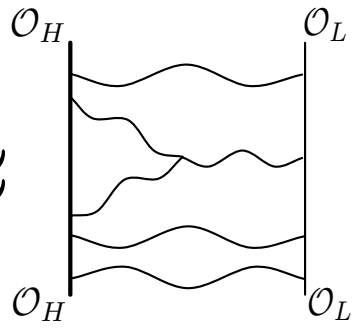

Figure 4.1: A figure that gives a suggestive representation of how the exchange of all Virasoro descendants of a state $|h\rangle$ corresponds to the exchange of $|h\rangle$ plus any number of gravitons in AdS_3. Reprinted from [15].

2. It corresponds exactly with the $n = 0$ piece $V(z, 0)$ in Eq. 4.6 in the semi-classical ($c \to \infty$) heavy-light ($h_L, h_H/c$ fixed) limit. This means that the claim that these blocks know about information loss is valid, as the forbidden singularities were due to the $V(z, n = 0)$ piece and were intimately connected to information loss.
3. We expect that the finite c (that is, the exact theory with no semi-classical limit) resolution should be within each Virasoro block itself, that is, it is a local corrective effect and not spread out over the entire sum of blocks. This is because it seems unlikely that the singularities are "cancelled" out when the entire series is summed over. In that case, understanding how the forbidden singularities get resolved in the vacuum block is tantamount to understanding how the information loss is resolved for the entire four-point function (at least in principle) and thus it offers a simple, yet non-trivial case study.

It is known that the vacuum Virasoro block for the heavy-light limit ($h_H/c, h_L, h$ fixed for $c \to \infty$) has the functional form [15]

$$\mathcal{V}_0(t) \sim \left[\frac{1}{\sin(\pi T_H t)} \right]^{2h_L} \tag{4.15}$$

Clearly, the **Virasoro blocks know about the black hole physics** in AdS_3; a clear indication of the same comes from the observation that the forbidden singularities occur at $t_* = n/T_H$, exactly where they ocur for the thermal correlator. We can see that clearly when we go from the boundary to the complex plane, using the relation $z = 1 - e^{-t}$ to get

$$z = 1 - e^{-\frac{n}{T_H}} = 1 - e^{-\frac{2\pi n}{r_+}} \qquad n \in \mathbb{Z} \tag{4.16}$$

Notice the congruence between this and Eq. 4.8, which further solidifies our motivation to study this block.

Chapter 5

Minimal models and degenerate Virasoro blocks

Based on our previous discussion, it is understandable that we would like to know some closed-form, analytic expression for the Virasoro block as that will help us in the analysis of the four-point function, and by extension, the two-point correlator in a black hole geometry. Unfortunately, as is known in the literature, **no analytic closed-form expressions exist for the general Virasoro block**.

However, all is not lost. As it turns out, one can solve for the Virisoro block exactly for certain special values of the external dimensions h_i, internal dimension h and the central charge c. This happens when one of the external operator $\mathcal{O}_i$ is degenerate, that is, it has a Virasoro descendant with zero norm [30]. This is studied under the framework of the theory of **minimal models** [32] in CFT_2, the most famous of which is the exact solution to the Ising model. We usually do not study these cases for QFTs as non-positive states decouple from the Hilbert space of a well-behaved quantum theory which respects unitarity.

Regardless, it seems that there is some merit in understanding these so-called **degenerate Virasoro blocks**, as we shall soon see. While we will not study the entire theory of minimal models, we will undertake a quick review of the most pertinent concepts relevant to our discussion.

5.1 Degenerate Virasoro blocks

5.1.1 Notation, conventions and definitions

First, we introduce a new parameter b implicitly defined by its relation with the central charge c as

$$\boxed{c \equiv 1 + 6\left(b + \frac{1}{b}\right)^2} \tag{5.1}$$

Note how $b \to 0$ or ∞ implies $c \to \infty$, and so both limits are valid for the semi-classical approximation. From here on, we will refer to the large c semi-classical limit in terms of $c \sim 6b^2$ as $b \to \infty$ implies $c \to \infty$.

A **degenerate state** is one which creates a null descendant; in other words, when a certain linear combination of Virasoro generators L_{-n} acting on it vanishes

$$\sum_n a_n L_{-n}|h\rangle = 0 \tag{5.2}$$

This basically means that the tower of states (Verma module) that one gets by applying the Virasoro generators to some highest weight state $|h\rangle$ will be finite, as one of the descendants will be a null state. The condition that one gets on the highest weight state conformal dimension h by demanding such a null descendant is described by the **Kac determinant**. Specifically, one finds out that the only possible holomorphic dimensions that degenerate states can have is given by the **Kac formula** [32]

$$\boxed{h_{r,s} = \frac{b^2}{4}(1-r^2) + \frac{1}{4b^2}(1-s^2) + \frac{1}{2}(1-rs)} \tag{5.3}$$

parametrized by two positive integral parameters $r, s \in \mathbb{Z}^+$. More generally, it has been shown [32, 40] that the null descendant of degenerate states with dimension $h_{r,1}$ can be expressed as

$$\sum_{n_i} \frac{[(r-1)!]^2 (b^2)^{r-k}}{\prod_{i=1}^{k-1}(n_1 + \ldots + n_i)(r - n_1 + \ldots + n_i)} L_{-n_1} \ldots L_{-n_k}|h_{2,1}\rangle = 0 \tag{5.4}$$

where the sum is over the partitions of r into k positive integers n_i. We are interested in precisely these states which have $s = 1$. Observe how these have a dimension that varies linearly in b^2 (which is the same as varying linearly with c in the large b limit). Thus, these are exactly the type of "heavy" states that we look for in the heavy-light semi-classical limit, as clearly

$$\frac{h_{r,1}}{c} \sim \frac{1-r^2}{24} \quad \text{as} \quad c \to \infty \tag{5.5}$$

remains a fixed constant when $c \to \infty$. Note that $h_{r,1} < 0$ since $r \in \mathbb{Z}^+$ which means that they fail the unitarity condition ($h \geq 0$). We will have more to say about this shortly.

The fundamental idea is to enforce the null condition of a Virasoro descendant to obtain a differential equation (which is usually solvable, and of the hypergeometric variety). To illustrate this, consider the case of the second-level null descendant

$$\left(L_{-1}^2 + b^2 L_{-2}\right) |h_{2,1}\rangle = 0 \tag{5.6}$$

of the degenerate state $|h_{2,1}\rangle$ which has dimensions

$$h_{2,1} = -\frac{1}{2} - \frac{3b^2}{4} \tag{5.7}$$

We can now plug this into a correlator to get

$$\langle \mathcal{O}_1(z_1)\mathcal{O}_2(z_2)\mathcal{O}_3(z_3) \left(L_{-1}^2 + b^2 L_{-2}\right) \mathcal{O}_{2,1}\rangle = 0 \tag{5.8}$$

and use the fact that L_{-n} acts as a differential operator

$$L_{-n} \to -\sum_{i, z_i \neq z} \left[\frac{(1-m)h_i}{(z_i - z)^m} + \frac{1}{(z_i - z)^{m-1}} \frac{\partial}{\partial z_i}\right] \tag{5.9}$$

to get a differential equation. Using global conformal invariance, one can send the various z_i's to the standard values of $0, 1, \infty$ and z (the corresponding conformal dimensions are $h_0, h_1, h_\infty, h_{2,1}$). Finally, the conformal Ward identities (refer to Sec. 2.2.2) simplify this further and we end up with the well-known **Belavin-Polyakov-Zamolodchikov (BPZ)** differential operator [30] for the degenerate operator $\mathcal{O}_{2,1}$, namely

$$\mathcal{D}_{BPZ} = \left[\frac{1}{b^2}\frac{\partial^2}{\partial z^2} - \left(\frac{1}{z} - \frac{1}{1-z}\right)\frac{\partial}{\partial z} + \frac{h_0}{z^2} + \frac{h_1}{(1-z)^2} - \frac{h_\infty - h_{(2,1)} - h_0 - h_1}{z(1-z)}\right] \tag{5.10}$$

which acts on the four-point function to give zero.

5.1.2 Motivation for the analysis of degenerate blocks

Before we rush into the various derivations of differential equations, let us look at a simple example that motivates the entire analysis. We consider the simplest possible BPZ equation, that of the state $|h_{2,1}\rangle$ (refer to Eq. 5.10). We can rewrite it as

$$\left[\frac{1}{b^2}\frac{\partial^2}{\partial z^2} + \frac{h_L}{(1-z)^2} + \left(\frac{2}{b^2 z} + \frac{2-z}{z(1-z)}\right)\frac{\partial}{\partial z}\right] \tilde{\mathcal{V}}_{2,1} = 0 \tag{5.11}$$

where we have taken $h_0 = h_{2,1}$ and $h_1 = h_\infty = h_L$. Also, we have written it in terms of the "normalized" block $\tilde{\mathcal{V}}_{2,1} = z^{2h_{2,1}}\tilde{\mathcal{V}}_{2,1}$ as that helps in taking various limits.

It turns out that the exact solution to this differential equation is known, and for $h_L = 1$, it takes on a particularly simple form given by

$$\tilde{\mathcal{V}}_{2,1} = (1-z)\ {}_2F_1(2, b^2+1, 2b^2+2; z) \tag{5.12}$$

So far, we do not see any singularities. But, when we take the $b \to \infty$ limit of the differential equation, we get

$$\left[\frac{h_L}{(1-z)} + \left(\frac{2-z}{z}\right)\frac{\partial}{\partial z}\right]\tilde{\mathcal{V}}_{2,1} = 0 \tag{5.13}$$

which has the solution (again, for $h_L = 1$)

$$\tilde{\mathcal{V}}_{2,1} = \frac{1-z}{(2-z)^2} \tag{5.14}$$

Here, we see the singularity at $z = 2$. Clearly, the solution of the finite b equation does not have singularities, while the semi-classical limit is manifestly singular. This is even more clear when we look at it in terms of the t coordinate, given by $z = 1 - e^t$. Basically, the singularity at $z = 2$ implies

$$1 + e^t = 0 \implies t = i\pi \tag{5.15}$$

which is a forbidden singularity as it is in addition to the $t = 0$ OPE singularity. The goal of the next few sections is to discuss the general treatment of this phenomenon in detail.

5.2 Consistency of unitarity requirements and analytic continuation

Previously, we mentioned that degenerate states are not studied in relation to QFTs because they have descendant states with non-positive norms. This is because any unitary quantum theory must have states with positive norms. For CFT_2, the equivalent statement is that the central charge of the theory $c > 0$ and all states must have conformal dimension $h \geq 0$.

Therefore, it is not immediately obvious why we do this analysis of degenerate states and Virasoro blocks as they are characteristically non-unitary. The first indication that there is something non-trivial here is revealed by the analysis done in Sec. 5.1.2. A more robust justification is due to [18]: we observe that Virasoro blocks are:

1. meromorphic functions of c, h_i with only simple poles
2. completely analytic functions of the parameters h_L, h_H
3. have no branch cuts or singularities in h_H when expanded out in the z or t coordinates

Basically, when one considers the behaviour of the blocks with respect to the external parameters like h_L, h_H, c, there are no misbehaving branch cuts or singularities more complex than

simple poles. Thus, one can consider the parameter h_H as something that can be controlled smoothly, or more precisely, a parameter that can be analytically continued. Recall that

$$h_{r,1} \sim \frac{b^2}{4}(1-r^2) \tag{5.16}$$

in the large b limit. So, while all the analysis is in terms of a negative $h_{r,1}$, one can leverage the existence of differential equations to understand the exact closed-form solutions for positive $r \in \mathbb{Z}^+$ (that is, for the case of degenerate operators) and then analytically continue to $r^2 < 0$.

Thus, heavy states $h_H \equiv h_{r,1}$ can be studied under this paradigm of degenerate blocks, and then can be analytically continued as mentioned above to understand the "physical" Virasoro blocks. We will also provide strong evidence later that the technique outlined above is a reasonable hypothesis, following the outline given in [18].

5.3 Analysis of the BPZ equation for heavy degenerate states at order $1/c$

5.3.1 Setting up the calculation

We will now analyze the Virasoro block where the heavy operator dimension is $h_{r,1}$ and the light operator dimension h_L is an independent parameter such that $h_L << b^2$. This is the semi-classical heavy-light limit. Using Eq. 5.4, we see that in the limit of large c, the states $\mathcal{O}_{r,1}$ with dimensions $h_{r,1}$ have the null descendant

$$0 \approx \left[L_{-r} + \frac{6}{c} \sum_{j=1}^{r-1} \frac{1}{j(r-j)} L_{-r+j} L_{-j} \right] |h_{r,1}\rangle = |\psi\rangle \tag{5.17}$$

at order $1/c \sim 1/b^2$. We can then write down the four-point correlator with this null descendant as

$$\langle \psi | \mathcal{O}_{r,1}(0)\mathcal{O}_L(x)\mathcal{O}_L(y)\rangle = \langle h_{r,1}| \left[L_r + \frac{6}{c} \sum_{j=1}^{r-1} \frac{1}{j(r-j)} L_j L_{r-j} \right] \mathcal{O}_{r,1}(0)\mathcal{O}_L(x)\mathcal{O}_L(y)\rangle \approx 0 \tag{5.18}$$

and we can keep commuting the L_r's to the right using the commutation relation

$$\boxed{[L_r, \mathcal{O}(z)] = \left[z^{r+1}\frac{d}{dz} + h(r+1)z^r \right] \mathcal{O}(z) = \mathcal{D}_{r,z}\mathcal{O}(z)} \tag{5.19}$$

for a primary operator $\mathcal{O}$ with dimensions h. Repeated use of the commutation relations will lead to these differential operators acting on the four-point correlator $\langle h_{r,1}|\mathcal{O}_{r,1}(0)\mathcal{O}_L(x)\mathcal{O}_L(y)\rangle$,

which is related to the vacuum Virasoro block $\mathcal{V}(z)$ as

$$\boxed{\langle h_{r,1}|\mathcal{O}_{r,1}(0)\mathcal{O}_L(x)\mathcal{O}_L(y)\rangle = \frac{1}{(x-y)^{2h_L}}\tilde{\mathcal{V}}\left(1-\frac{x}{y}\right)} \tag{5.20}$$

and thus, we will have a differential equation for the Virasoro block. An important thing to note about Eq. 5.20 is that it is written in terms of $\tilde{\mathcal{V}}$ instead of $\mathcal{V}$. The relation between the two is given by

$$\tilde{\mathcal{V}} = z^{2h_{2,1}}\mathcal{V} \tag{5.21}$$

and the reason is quite simple. When one calculates Virasoro blocks, we usually normalize them as

$$\mathcal{V}(h, h_i, z) = z^{-(h_3+h_4)}\tilde{\mathcal{V}}(h, h_i, z) \tag{5.22}$$

so that in the $c \to \infty$ they match exactly with the global conformal blocks (conformal blocks that arise due to the global conformal algebra and not the Virasoro conformal algebra, the former is a subset of the latter as we have seen earlier). In our case, $h_3 = h_4 = h_{2,1}$.

One might question why we have equated the four-point function directly to the vacuum Virasoro block in Eq. 5.20. We give the following justification for the same: The differential equation for the four-point function (the BPZ equation) can written informally as

$$\mathcal{D}_{BPZ}\langle\mathcal{O}_1\mathcal{O}_2\mathcal{O}_3\mathcal{O}_{r,1}\rangle = 0 \tag{5.23}$$

This implies the block decomposed form

$$\mathcal{D}_{BPZ}\sum_h P_h\mathcal{V}_h(h_i, z) = 0 \tag{5.24}$$

Now, since the OPE coefficients are sufficiently arbitrary to not cause a conspiratorial cancellation of the entire sum, and furthermore, since the Virasoro blocks are built using the linearly independent basis provided by the $|h\rangle$ (and descendant) states, it is reasonable that

$$\mathcal{D}_{BPZ}\mathcal{V}_h(h_i, 0) = 0 \tag{5.25}$$

is **true for each individual block** and thus, at the **level of the differential equation**, the vacuum Virasoro block and the four-point function have equivalent structures. A similar argument was put forth in Appendix D of [41].

5.3.2 Getting the differential equation

We will now derive the differential equation using the algorithm outlined beforehand. Note that the first commutation is trivial since $\mathcal{O}_{r,1}$ is at $z = 0$. Thus, we now have

$$0 \approx \langle h_{r,1}|\mathcal{O}_{r,1}(0)\left[L_r + \frac{6}{c}\sum_{j=1}^{r-1}\frac{1}{j(r-j)}L_jL_{r-j}\right]\mathcal{O}_L(x)\mathcal{O}_L(y)\rangle \tag{5.26}$$

We can now split this into the leading and the sub-leading terms and calculate them individually; putting them together will give us the complete differential equation.

5.3.3 Leading order contribution given by the L_r term

We want to calculate

$$\langle h_{2,1}|\mathcal{O}_{2,1}(0)L_r\mathcal{O}_L(x)\mathcal{O}_L(y)\rangle \tag{5.27}$$

We can use the commutation relation Eq. 5.19 to $\mathcal{O}_L(x)$ and $\mathcal{O}_L(y)$ sequentially (for detailed derivations, refer to Appendix A.1), and then by setting $x = 1 - z, y = 1$ and converting it in terms of the boundary Euclidean time coordinate t by substituting $1 - z = e^{-t}$, we get

$$\begin{aligned} &h_L\tilde{\mathcal{V}}(z)\left[(2-z)\{1-(1-z)^r\} - rz\{1-(1+z)^r\}\right] - z(1-z)\tilde{\mathcal{V}}'(z)\left[1-(1-z)^r\right] \\ \implies &h_L\tilde{\mathcal{V}}(t)\left[(1+e^{-t})(1-e^{-rt}) - r(1-e^{-t})(1+e^{-rt})\right] - (1-e^{-t})(1-e^{-rt})\tilde{\mathcal{V}}'(t) \end{aligned} \tag{5.28}$$

which gives us

$$\boxed{\begin{aligned}&\langle h_{2,1}|\mathcal{O}_{2,1}(0)L_r\mathcal{O}_L(x)\mathcal{O}_L(y)\rangle = \\ &\qquad h_L\tilde{\mathcal{V}}(t)\left[(1+e^{-t})(1-e^{-rt}) - r(1-e^{-t})(1+e^{-rt})\right] - (1-e^{-t})(1-e^{-rt})\tilde{\mathcal{V}}'(t)\end{aligned}} \tag{5.29}$$

This is the contribution of the leading order term. In fact, as we will see later, it also gives us the semi-classical Virasoro block.

5.3.4 Sub-leading order contributions given by the L_jL_{r-j} terms

Next, we want to calculate

$$\langle h_{2,1}|\mathcal{O}_{2,1}(0)\left[\frac{6}{c}\sum_{j=1}^{r-1}\frac{1}{j(r-j)}L_jL_{r-j}\right]\mathcal{O}_L(x)\mathcal{O}_L(y)\rangle \tag{5.30}$$

Again, we use the same algebra as before (refer to Appendix A.1) to get an expression in terms of x, y. Note that this contribution is suppressed by the $6/c \sim 1/b^2$ factor in front.

We get $1/c$ suppressed corrections to $\tilde{\mathcal{V}}, \tilde{\mathcal{V}}'$ terms and a new $\tilde{\mathcal{V}}''$ term. Now, we know

that while the subdominant $1/c$ corrections are present in both $\tilde{\mathcal{V}}, \tilde{\mathcal{V}}'$, they do not change the order of the differential equation and thus, we do not expect them to cause any changes to the nature of the solutions. Therefore, we omit them and only retain the order unity terms. However, introducing a second derivative term in the differential equation, even with its $1/c$ suppression, necessarily changes the order of the differential equation, and thus, the nature of the solutions themselves (the reader is encouraged to check this from the toy example in Sec. 5.1.2). We expect this to help in regulating the forbidden singularities. Thus, the only additional input that arises from this calculation is the second derivative

$$\begin{aligned} &\frac{\tilde{\mathcal{V}}''(z)}{b^2}\sum_{j=1}^{r-1}\frac{1}{j(r-j)}z(1-z)^2\left[\frac{[(1-z)^j-1][(1-z)^j-(1-z)^r]}{(1-z)^j}\right] \\ \implies &\frac{\tilde{\mathcal{V}}''(t)}{b^2}\sum_{j=1}^{r-1}\frac{1}{j(r-j)}(1-e^{-t})(1-e^{jt})(e^{-jt}-e^{-rt}) \end{aligned} \tag{5.31}$$

which gives us

$$\boxed{\frac{\tilde{\mathcal{V}}''(t)}{b^2}\sum_{j=1}^{r-1}\frac{1}{j(r-j)}(1-e^{-t})(1-e^{jt})(e^{-jt}-e^{-rt})} \tag{5.32}$$

5.3.5 Master Differential Equation

We can put these results together to get the differential equation

$$\begin{aligned} &\langle h_{r,1}|\mathcal{O}_{r,1}(0)\left[L_r+\frac{6}{c}\sum_{j=1}^{r-1}\frac{1}{j(r-j)}L_jL_{r-j}\right]\mathcal{O}_L(x)\mathcal{O}_L(y)\rangle \\ &= h_L\tilde{\mathcal{V}}(t)\left[(1+e^{-t})(1-e^{-rt})-r(1-e^{-t})(1+e^{-rt})\right]-(1-e^{-t})(1-e^{-rt})\tilde{\mathcal{V}}'(t) \\ &\quad+\frac{\tilde{\mathcal{V}}''(t)}{b^2}\sum_{j=1}^{r-1}\frac{1}{j(r-j)}(1-e^{-t})(1-e^{jt})(e^{-jt}-e^{-rt}) \end{aligned} \tag{5.33}$$

Setting it to zero, we get

$$-h_L\tilde{\mathcal{V}}(t)\left[\frac{(1+e^{-t})}{(1-e^{-t})}-r\frac{(1+e^{-rt})}{(1-e^{-rt})}\right]+\tilde{\mathcal{V}}'(t)+\frac{\tilde{\mathcal{V}}''(t)}{b^2}\sum_{j=1}^{r-1}\frac{1}{j(r-j)}\left[\frac{(1-e^{jt})(e^{-rt}-e^{-jt})}{(1-e^{-rt})}\right]=0 \tag{5.34}$$

This can be rewritten as

$$\boxed{-h_Lg_r(t)\tilde{\mathcal{V}}(t)+\tilde{\mathcal{V}}'(t)+\frac{\Sigma_r(t)}{b^2}\tilde{\mathcal{V}}''(t)=0} \tag{5.35}$$

with

$$\boxed{\begin{aligned} g_r(t) &= \coth\left(\frac{t}{2}\right) - r\coth\left(\frac{rt}{2}\right) \\ \Sigma_r(t) &= -\frac{1}{r\sinh\frac{rt}{2}}\left[e^{-\frac{rt}{2}}\tilde{B}_r(t) + e^{\frac{rt}{2}}\tilde{B}_r(-t) - 2\cosh\left(\frac{rt}{2}\right)\tilde{B}_r(0)\right] \end{aligned}} \tag{5.36}$$

for

$$\boxed{\tilde{B}_r(t) = \sum_{j=1}^{r-1}\frac{e^{jt}}{j}} \tag{5.37}$$

The coefficients of $\tilde{\mathcal{V}}(t)$ and $\tilde{\mathcal{V}}''(t)$ are computed in Appendix A.2. We have derived the so-called **perturbative second-order master equation** that is hypothesized to incorporate non-perturbative physics that resolves the forbidden singularities [18].

5.4 Analysis of the Master Equation

5.4.1 Behaviour in the semi-classical limit

The obvious limit that one can impose immediately is the semi-classical ($c \to \infty$) limit. In this case, we drop the $\tilde{\mathcal{V}}''(t)$ term to get

$$\boxed{-h_L g_r(t)\tilde{\mathcal{V}}(t) + \tilde{\mathcal{V}}'(t) = 0} \tag{5.38}$$

The solution to this is the semi-classical Virasoro block given by

$$\tilde{\mathcal{V}}(t) = \frac{e^{h_L t}(1-e^{-t})^{2h_L}}{\left[\sinh\left(\frac{rt}{2}\right)\right]^{2h_L}} \tag{5.39}$$

We can clearly see that this has singularities at $t = 2i\pi n/r$. The $n = 0$ case is not a forbidden singularity, in fact, it is the only allowed OPE singularity. The structure of the block gives us confidence that we are indeed only an analytic continuation away from getting the correct semi-classical heavy-light vacuum block.

5.4.2 Behaviour under a scaling near the forbidden singularities

To understand the behaviour of the blocks near the forbidden singularities, we consider the scaling limit given by

$$t = \frac{2\pi i n}{r} + \frac{x}{b} \tag{5.40}$$

But before that, we extract out a factor

$$\tilde{\mathcal{V}}(t) = (1-e^{-t})^{2h_L}\mathcal{V}(t) \tag{5.41}$$

This is because the answer that we get in Eq. 5.39 differs from the "expected" answer by exactly that factor (z^{2h_L}). Note that this is slightly confusing as we have used $\mathcal{V}$ for the unnormalized Virasoro block too. However, we will continue with this convention as it is clear from context what we mean by $\mathcal{V}$ here.

This redefinition does does not affect the second derivative term, as any $\mathcal{V}(t)$ or $\mathcal{V}'(t)$ terms that it will generate are suppressed by $1/b^2$, and we have always dropped such terms as they are subdominant. However, there will be a term created by the first derivative as follows

$$\begin{aligned}\tilde{\mathcal{V}}'(t) &= \partial_t[(1-e^{-t})^{2h_L}]\mathcal{V}(t) + (1-e^{-t})^{2h_L}\mathcal{V}'(t) \\ &= 2h_L e^{-t}(1-e^{-t})^{2h_L-1}\mathcal{V}(t) + (1-e^{-t})^{2h_L}\mathcal{V}'(t)\end{aligned} \tag{5.42}$$

Plugging this into the master equation, we have

$$\boxed{-h_L\tilde{g}_r(t)\mathcal{V}(t) + \mathcal{V}'(t) + \frac{\Sigma_r(t)}{b^2}\mathcal{V}''(t) = 0} \tag{5.43}$$

where

$$\boxed{\tilde{g}_r(t) = 1 - r\coth\left(\frac{rt}{2}\right)} \tag{5.44}$$

Next, we make the scaling limit substitution to get

$$\mathcal{V}'(t) \to b\mathcal{V}'(x), \qquad \mathcal{V}''(t) \to b^2\mathcal{V}''(x) \tag{5.45}$$

where the derivatives are signified by the arguments of the functions. This gives us

$$-h_L\tilde{g}_r(x)\mathcal{V}(x) + b\mathcal{V}'(x) + \Sigma_r(x)\mathcal{V}''(x) \tag{5.46}$$

The detailed calculations for the coefficients $\tilde{g}_r(x), \Sigma_r(x)$ are given in Appendix A.2. Using them, and taking the limit $b \to \infty$ gives us

$$\sinh\left(\frac{rx}{2b}\right) \approx \frac{rx}{2b} \qquad \cosh\left(\frac{rx}{2b}\right) \approx 1 \tag{5.47}$$

and so, the scaled differential equation becomes

$$2h_L\mathcal{V}(x) + x\mathcal{V}'(x) - \mathcal{V}''(x)\left[4\sum_{j=1}^{r-1}\frac{1}{rj(r-j)}\sinh^2\left(\frac{jt}{2}\right)\right] = 0 \tag{5.48}$$

Lastly, we will simplify the expression that is the coefficient of $\mathcal{V}''(x)$. Since it is to be taken in the limit of $b \to \infty$, we effectively have $t = \frac{2\pi i n}{r}$

$$\sinh^2\left(\frac{jt}{2}\right) = \left[i\sin\left(\frac{jn\pi}{r}\right)\right]^2 \tag{5.49}$$

and thus, we finally have

$$\boxed{2h_L\mathcal{V}(x) + x\mathcal{V}'(x) + \mathcal{V}''(x)\left[4\sum_{j=1}^{r-1}\frac{1}{rj(r-j)}\sin^2\left(\frac{jn\pi}{r}\right)\right] = 0} \tag{5.50}$$

The scaled limit of the differential equation has an important role to play when we analytically continue r.

5.4.3 Behaviour near fixed points of interest

More generally, we would like to consider the master equation around certain points of interest. Essentially, we would like to find the limit under

$$t = t_* + x \tag{5.51}$$

as $x \to 0$ for some particular fixed t_*. Note how this is an extension of the scaling limit case that we discussed in the previous section.

Forbidden singularities: $t_* = \frac{2\pi in}{r}$

This is identical to the scaling limit case discussed before, but the analysis is a bit more general and thus, instructive for our extension to the analytically continued case. We consider Eq. 5.43 for

$$t = \frac{2\pi in}{r} + x \tag{5.52}$$

to calculate the various coefficients and take the limit $x \to 0$ to find out the behaviour of the Virasoro blocks near the forbidden singularity. We can calculate the coefficients of the various terms in the differential equation (refer to Appendix A.2 for detailed calculations) and putting them altogether, we get

$$\boxed{2h_L\mathcal{V}(x) + x\mathcal{V}'(x) + \frac{\sigma^2(n,r)}{b^2}\mathcal{V}''(x) = 0} \tag{5.53}$$

where

$$\boxed{\sigma^2(n,r) = \frac{2}{r^2}\left[2\log\left(2\sinh\left(\frac{\pi in}{r}\right)\right) + B(e^{\frac{2\pi in}{r}};r,0) + B(e^{-\frac{2\pi in}{r}};r,0) + 2H_{r-1}\right]} \tag{5.54}$$

Notice how this is exactly the same as Eq. 5.50, but given in terms of functions that can be analytically continued suitably (this will be explained in detail in the next chapter). This is the approximate differential equation that holds true in the vicinity of the n^{th} forbidden singularity, and we present this as a **cleaner and more robust alternative** to analyse the differential equation near the singularities than the one done using the scaling limits in the

previous chapter (outlined in [18]).

Halfway between the the OPE singularity and the first forbidden singularity: $t_* = \frac{\pi i}{r}$

For reasons that will be made clear in the next chapter, one can also consider the behaviour of the Virasoro blocks around $t_* = \frac{\pi i}{r}$, and running the same algorithm as before, we get

$$\boxed{-h_L \mathcal{V}(t) + \mathcal{V}'(t) + \frac{1}{b^2}\mathcal{V}''(t)\frac{1}{r}\left[\frac{i\pi}{2} + B(e^{-\frac{i\pi}{2}}; r, 0) - B(e^{\frac{i\pi}{2}}; r, 0)\right] = 0} \tag{5.55}$$

The coefficients have been worked out in Appendix A.2.

Chapter 6

Analysis of "physical" Virasoro blocks

In the previous chapter, we looked at degenerate Virasoro blocks and found differential equations for various approximation regimes. The main idea, summarized in Sec. 5.2, is to analytically continue the integer parameter r and relate it to the horizon radius r_+, or equivalently, the black hole temperature T_H. As such, this entails a simple substitution of $r = \alpha$, where the relationship between all the aforementioned parameters is given by

$$\alpha = \sqrt{1 - \frac{24h_H}{c}} \approx 2\pi i T_H = i r_+ \tag{6.1}$$

but one has to tweak the expressions slightly so as to make the analytic continuation manifest.

6.1 The master equation after analytic continuation

Observe that there are two r-dependent functions, namely $g_r(t)$ and $\Sigma_r(t)$ as given in Eq. 5.36. The former has a simple hyperbolic function in it, and thus, the analytic continuation is straightforward: just plug in $r = ir_+$. However, analytically continuing the latter, given by

$$\Sigma_r(t) = -\frac{1}{r \sinh \frac{rt}{2}} \left[e^{-\frac{rt}{2}} \tilde{B}_r(t) + e^{\frac{rt}{2}} \tilde{B}_r(-t) - 2\cosh\left(\frac{rt}{2}\right) \tilde{B}_r(0) \right] \tag{6.2}$$

is not as simple because of the form

$$\tilde{B}_r(t) = \sum_{j=1}^{r-1} \frac{e^{jt}}{j} \tag{6.3}$$

as a sum over the discrete parameter $r \in \mathbb{Z}^+$. Fortunately, there is a way in which one can rewrite it to ensure a smooth analytic continuation. The $\tilde{B}_r(0)$ can be handled quite

trivially. We observe that

$$\tilde{B}_r(0) = \sum_{j=1}^{r-1} \frac{1}{j} = H_{r-1} \tag{6.4}$$

where H_n is just the **harmonic sum/number** in number theory. It has a well-defined analytic continuation in terms of its integral representation, and so, we are done here. For the more general $\tilde{B}_r(t)$, we break the finite sum into a difference of two infinite sums

$$\begin{aligned} \tilde{B}_r(t) &= \sum_{j=1}^{r-1} \frac{e^{jt}}{j} = \sum_{j=1}^{\infty} \frac{e^{jt}}{j} - \sum_{j=r}^{\infty} \frac{e^{jt}}{j} \\ &= -\log\left(1-e^t\right) - \sum_{k=0}^{\infty} \frac{e^{rt}e^{kt}}{k+r} \end{aligned} \tag{6.5}$$

We recognize that the last sum is related to the series expansion of the **hypergeometric function**

$${}_2F_1(a,b,c;z) = \sum_{n=0}^{\infty} \frac{(a)_n (b)_n}{(c)_n} \frac{z^n}{n!} \quad \text{for} \quad (q)_n = \frac{\Gamma(q+n)}{\Gamma(q)} \tag{6.6}$$

which is further related to the **incomplete beta function** $B(z;a,b)$ due to an identity

$$B(z;a,b) = \frac{z^a}{a}\, {}_2F_1(a, 1-b, a+1; z) \tag{6.7}$$

leading to

$$\tilde{B}_r(t) = \sum_{j=1}^{r-1} \frac{e^{jt}}{j} = -\log\left(1-e^t\right) - \frac{e_2^{rt} F_1(1, r, 1+r, e^t)}{r} = -\log\left(1-e^t\right) - B(e^t; r, 0) \tag{6.8}$$

Now this is a form in which one can do the analytic continuation $r = ir_+$, since all the special functions noted above have well-known analytic properties for complex parameters.

There is one last caveat about a potential sign ambiguity in $r = \pm ir_+$, and in order to circumvent it, we declare that we will consider the contribution of both roots. For instance, we consider the total contribution as $\Sigma_r + \Sigma_{-r}$ when $r \to ir_+$. Accordingly, the master equation generalizes to

$$\boxed{-h_L g_r(t)\tilde{\mathcal{V}}(t) + \tilde{\mathcal{V}}'(t) + \frac{\Sigma_r(t) + \Sigma_{-r}(t)}{b^2}\tilde{\mathcal{V}}''(t) = 0} \tag{6.9}$$

and the substitution $r = ir_+$ is made in all the appropriate places. Whether this is reasonable or not depends on how well the results are when compared to boundary CFT calculations that were done perturbatively in $1/c$. It turns out that this is indeed the correct way to go about (we will see the agreement with previous results soon).

Note that this equation is exact only for $r = 2$. For $r > 2$, this equation loses all contributions from order $1/c^2$ to order $1/c^{r-1}$, as can be seen easily from the derivation. However, this is still a good enough approximation as long as the order of the second derivative term becomes equal to that of the remaining two, which means that till

$$\Sigma_r(t) \sim c \implies \frac{t}{T_H} \sim c \tag{6.10}$$

we are can work with this approximate equation.

6.2 Analysis of the analytically continued Master Equation

6.2.1 Behavior in the semi-classical limit

In the semi-classical limit ($c \to \infty$) limit, we drop the $\tilde{\mathcal{V}}''(t)$ term to get

$$\boxed{-h_L g_{r_+}(t)\tilde{\mathcal{V}}(t) + \tilde{\mathcal{V}}'(t) = 0} \tag{6.11}$$

The solution to this is the semi-classical Virasoro block given by

$$\tilde{\mathcal{V}}(t) = \frac{e^{h_L t}(1 - e^{-t})^{2h_L}}{\left[\sin\left(\frac{r_+ t}{2}\right)\right]^{2h_L}} \tag{6.12}$$

When one takes care of Jacobian $e^{-h_L t}$ prefactor that arises due to the change of coordinates from $z \to t$, one see that the correct vacuum Virasoro block (modulo some constant factors at most) has been reproduced exactly using the analytic continuation of the degenerate Virasoro block master equation (compare it with 6.9). The forbidden singularities at $t = 2\pi n/r_+$ are obvious, and yet again, the $n = 0$ case is not a forbidden singularity but rather the only allowed (OPE) singularity.

The presence of the extra $z^{2h_L} = (1 - e^{-t})^{h_L}$ factor is also exactly why we absorbed it into a redefinition of $\mathcal{V}$ back in Eq. 5.41 when we calculated the differential equation in the various scaling limits, the difference between the exact answer to the semi-classical Virasoro block and the solution of the differential equation was precisely this.

The above calculation agrees perfectly with the expected form of the semi-classical heavy light Virasoro blocks, and thus, we are confident that we are onto something non-trivial when we consider this approach that involves analytic continuation of r.

6.2.2 Behaviour near fixed points of interest

Next, we would like to consider this r_+ modified master equation around certain points of interest. Essentially, we would like to find the limit under

$$t = t_* + x \tag{6.13}$$

again for $x \to 0$ for some particular fixed t_*.

Forbidden singularities: $t_* = \frac{2\pi n}{r_+}$

We want to understand Eq. 6.9 for

$$t = \frac{2\pi n}{r_+} + x \tag{6.14}$$

in the limit $x \to 0$ to find out the behaviour of the Virasoro blocks near the forbidden singularity. We can calculate the coefficients of the various terms in the differential equation (refer to Appendix A.3 for detailed calculations) and putting them altogether, we get

$$\boxed{2h_L\mathcal{V}(x) + x\mathcal{V}'(x) - \frac{\sigma^2}{b^2}\mathcal{V}''(x) = 0} \tag{6.15}$$

which is the approximate differential equation that holds true in the vicinity of the n^{th} forbidden singularity. Here,

$$\boxed{\begin{aligned}\sigma^2 = \frac{2}{r_+^2}\Big[&B(e^{\frac{2\pi n}{r_+}}; ir_+, 0) + B(e^{-\frac{2\pi n}{r_+}}; ir_+, 0) + B(e^{-\frac{2\pi n}{r_+}}; -ir_+, 0) + B(e^{\frac{2\pi n}{r_+}}; -ir_+, 0) \\ &+2H_{ir_+} + 2H_{-ir_+} + 4\log\left(2\sinh\left(\frac{\pi n}{r_+}\right)\right) + 2\pi i\Big]\end{aligned}} \tag{6.16}$$

We can solve this differential equation, and the normalizable solution to it is given by (modulo a constant related to an initial condition)

$$\boxed{\mathcal{V}(x) = {}_1F_1\left(h_L, \frac{1}{2}; \frac{x^2b^2}{2\sigma^2}\right)} \tag{6.17}$$

This can be related to the parabolic cylindrical function for $\mathrm{Re}[z] > 0$ as

$$D_{-\nu}(z) = 2^{-\frac{\nu}{2}}e^{-\frac{z^2}{4}}\ {}_1F_1\left(\frac{\nu}{2}, \frac{1}{2}; \frac{z^2}{4}\right) \tag{6.18}$$

which is useful, as the parabolic cylindrical function has an integral representation given by

$$D_{-\nu}\left(\frac{\gamma}{\sqrt{2\beta}}\right) = \frac{1}{\Gamma(\nu)}(2\beta)^{\frac{\nu}{2}}e^{-\frac{\gamma^2}{8\beta}}\int_0^\infty dy\ y^{\nu-1}e^{-\beta y^2-\gamma y} \tag{6.19}$$

for $\mathrm{Re}[\beta]$, $\mathrm{Re}[\nu] > 0$. Plugging in all the appropriate values, we find that

$$\mathcal{V}(x) = \left(\frac{2\sigma^2}{b^2}\right)^{h_L} \frac{1}{\Gamma(2h_L)} \int_0^\infty dp\, p^{2h_L-1} e^{-px-\frac{\sigma^2}{2b^2}p^2} \tag{6.20}$$

and thus, we see that the blocks are modulated by the function (again, modulo a constant prefactor that can be taken care of)

$$\boxed{S[x,c] = \frac{1}{\Gamma(2h_L)} \int_0^\infty dp\, p^{2h_L-1} e^{-px-\frac{\sigma^2}{2b^2}p^2}} \tag{6.21}$$

Comparison with perturbative $1/c$ calculations

Now why is this a useful way to present the solution? Previous perturbative CFT_2 calculations [16, 42] have given us the analytic expression for the order $1/c$ correction to the semi-classical vacuum block, and a comparison with those results will help us verify this new method of finding the vacuum Virasoro block. To do that, we expand $S[x,c]$ in powers of $1/b^2$ as

$$\begin{aligned} S[x,c] &= \frac{1}{\Gamma(2h_L)} \int_0^\infty dp\, p^{2h_L-1} e^{-px-\frac{\sigma^2}{2b^2}p^2} \\ &= \frac{1}{\Gamma(2h_L)} \int_0^\infty dp\, p^{2h_L-1} e^{-px} \left(1 - \frac{\sigma^2}{2b^2}p^2 + \dots\right) \\ &= \frac{1}{\Gamma(2h_L)} \int_0^\infty dp\, p^{2h_L-1} e^{-px} - \frac{1}{\Gamma(2h_L)} \frac{\sigma^2}{2b^2} \int_0^\infty dp\, p^{2h_L+1} e^{-px} + \dots \\ &= \frac{1}{x^{2h_L}} - \frac{\sigma^2 h_L(2h_L+1)}{b^2} \frac{1}{x^{2h_L+2}} + \dots \end{aligned} \tag{6.22}$$

We can now compare this to the general $1/c$ corrections to the heavy-light Virasoro block given in [16, 42], namely

$$\mathcal{V}(t) = e^{h_L t} \left(\frac{\pi T_H}{\sin \pi T_H t}\right) \left[1 + \frac{h_L}{c}\mathcal{V}^{(1)}_{h_L} + \frac{h_L^2}{c}\mathcal{V}^{(1)}_{h_L^2}\right] \tag{6.23}$$

where $\mathcal{V}^{(1)}_{h_L}, \mathcal{V}^{(1)}_{h_L^2}$ are some known analytic functions of the parameter α and time t (one can refer to Appendix B of [18]). We want to consider the equation around

$$t_* = \frac{2\pi i n}{\alpha} = \frac{n}{T_H} \quad \text{for} \quad \alpha = i r_+ \cong 2\pi i T_H \tag{6.24}$$

Plugging in $t = t_* + x$ and then taking the $x \to 0$ limit, we obtain

$$\mathcal{V}^{(1)}_{h_L^2} = 2\mathcal{V}^{(1)}_{h_L} = -\frac{1}{x^2}\xi \tag{6.25}$$

where

$$\boxed{\xi = \frac{1}{2\pi^2 T_H^2}\left[B(e^{\frac{n}{T_H}};\alpha,0) + B(e^{-\frac{n}{T_H}};\alpha,0) + B(e^{-\frac{n}{T_H}};-\alpha,0) + B(e^{\frac{n}{T_H}};-\alpha,0) + 2H_\alpha + 2H_{-\alpha} \right.}$$
$$\boxed{\left. +4\log\left(2\sinh\left(\frac{n}{2T_H}\right)\right) + 2\pi i\right]} \tag{6.26}$$

Plugging this back in Eq. 6.23, we have

$$\begin{aligned}\mathcal{V}(t) &\approx \left(\frac{1}{x}\right)^{2h_L}\left[1 + \frac{h_L}{c}\mathcal{V}^{(1)}_{h_L} + \frac{h_L^2}{c}\mathcal{V}^{(1)}_{h_L^2}\right] \\ &= \frac{1}{x^{2h_L}}\left[1 - \frac{h_L}{2c}\frac{\xi}{x^2} - \frac{h_L^2}{c}\frac{\xi}{x^2}\right] \\ &= \frac{1}{x^{2h_L}} - \frac{h_L(2h_L+1)\xi}{2c}\frac{1}{x^{2h_L+2}}\end{aligned} \tag{6.27}$$

and thus, all we are left to do is compare

$$\frac{\xi}{2c} \stackrel{?}{=} \frac{\sigma^2}{b^2} \tag{6.28}$$

One can easily read off this equality by looking at Eq. 6.26 and Eq. 6.16 and noting the relation between r_+ and T_H given by Eq. 6.24. We have thus verified a **perfect agreement** between a previously **known exact result using perturbative CFT calculations** and a **solution obtained by the analytic continuation of a degenerate Virasoro block differential equation**! This gives us confidence that understanding corrections to the semi-classical Virasoro blocks through degenerate representations is a concrete and fruitful direction. Observe that this also reinforces our belief in the $\Sigma_r(t) \to \Sigma_r(t) + \Sigma_{-r}(t)$ ansatz that we made earlier in this chapter.

Halfway between the the OPE singularity and the first forbidden singularity: $t_* = \frac{\pi}{r_+}$

Previous numerical calculations [43] (refer to Fig. 6.1) show that the deviations between the analytic semi-classical and the numerically computed exact Virasoro blocks start at $t = \beta/2$. We know the relation between β, T_H and r_+, indeed $\beta/2 = \pi/r_+$.

To that end, let us consider the behaviour of the differential equation around $t_* = \pi/r_+$.

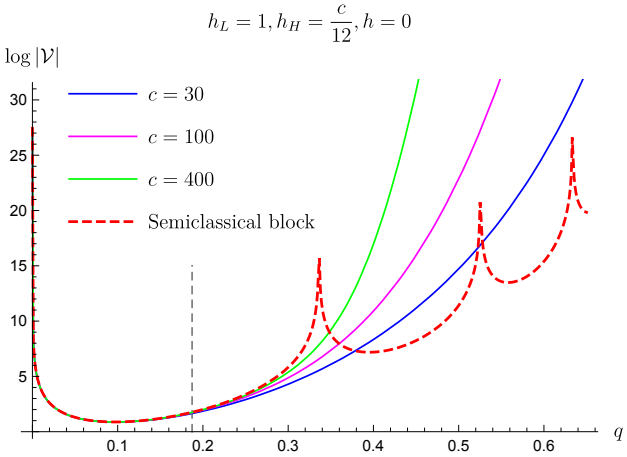

Figure 6.1: A comparison between the numerically computed (exact) finite c Virasoro block and the semi-classical heavy-light Virasoro block. The exact blocks approach the semi-classical block from the OPE singularity at the origin to the first forbidden singularity in the $c \to \infty$ limit, and they match quite well. However, after the first forbidden singularity, they deviate significantly. The grey dashed line marks the first instance of the deviation, at $\tau = \beta/2$. Reprinted from [43]

We can run the same algorithm again (details in Appendix A.3) to get

$$\boxed{-h_L \mathcal{V}(x) + \mathcal{V}'(x) + \frac{\epsilon}{b^2}\mathcal{V}''(x) = 0} \tag{6.29}$$

with

$$\boxed{\epsilon = \frac{i}{r_+}\left[-\frac{2\pi}{r_+} + B(e^{\frac{\pi}{r_+}}; ir_+, 0) + B(e^{\frac{\pi}{r_+}}; -ir_+, 0) - B(e^{\frac{-\pi}{r_+}}; ir_+, 0) - B(e^{\frac{-\pi}{r_+}}; -ir_+, 0)\right]} \tag{6.30}$$

Solving this equation, we obtain

$$\boxed{\mathcal{V}(x) = \exp\left[\frac{-b^2 \pm b\sqrt{b^2 + 4h_L\epsilon}}{2\epsilon}x\right]} \tag{6.31}$$

out of which, we consider only the solution that decays at $t \to \infty$ as dictated by the boundary conditions. A comparison was made of the normalized function given by Eq.6.31 and the normalized semi-classical block given by Eq. 6.12 near $t_* = \pi/r_+$ for $r_+ = 1/2$; the agreement is quite good. In fact, if we compare Fig. 6.2 with Fig. 6.1, we see that the qualitative features of the plots **after** $t = \pi/r_+$ are the same (the different graphs are for comparable c values too). This means that we can be confident about the nature of the solution for $t > \pi/r_+$ and $x \approx 0$. However, it seems like the solution does not agree quite as well for $t < \pi/r_+$ and $x \approx 0$, and that is something that is being worked on at the time of writing.

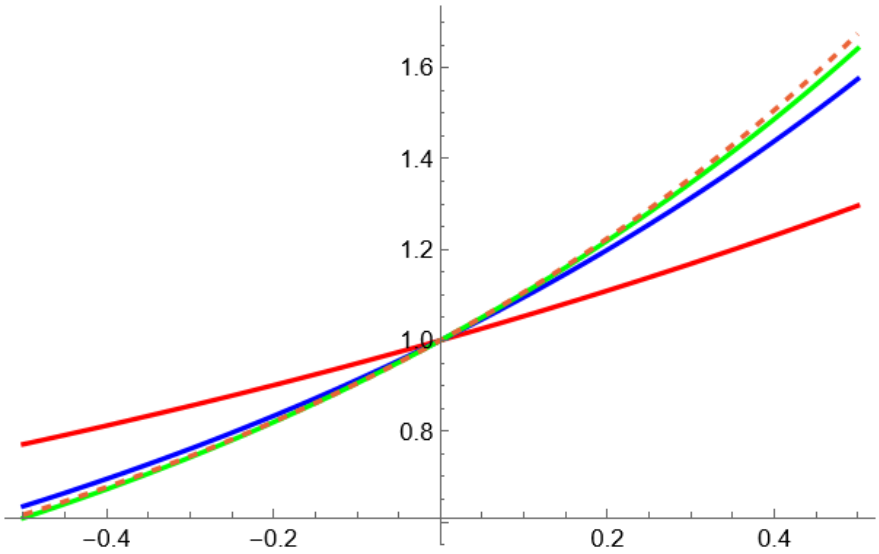

Figure 6.2: Comparison of the normalized semi-classical block (dashed) and solution to the differential equation Eq. 6.31 with $c = 10$ (red), 100 (blue) and 1000 (green). The x-axis origin corresponds to $t_* = \frac{\pi}{r_+}$, as we are checking for devations around it.

We will return to this idea in Sec. 9.4, and there, we will try to connect it with a more geometric interpretation in the bulk. For now, let us now move on to understand how we can relate these various unitary restoring features from the master equation with non-perturbative phenomenon.

Chapter 7

Analysis of the non-perturbative information restoration effects due to the master equation

While it is instructive to do calculations in the perturbative $G_N \sim 1/c$ limit, we also need to be aware of **non-perturbative effects** that cannot be encapsulated in a simple power series form. In general, we expect that the Virasoro block can be expanded as

$$\mathcal{V}(z) = \sum_{k=0}^{\infty} \frac{f_k(z)}{c^k} + e^{-cg(z)} \left[\sum_{k=0}^{\infty} \frac{h_k(z)}{c^k} \right] \tag{7.1}$$

with the identification $f_0(z) = \mathcal{V}_{c\to\infty}(z)$, that is, the semi-classical block. We can easily read off the perturbative and non-perturbative parts of the block, and based on our discussion in the previous sections, we expect that the non-perturbative part is the one that restores unitarity of the Virasoro block as a whole. One usually uses resummation techniques to understand non-perturbative phenomenon. Let us quickly review the basic ideas of Borel resummation.

7.1 Borel resummation

It is common to work in the perturbative limit amd express many quantities of interest in terms of a series expansion associated to a coupling constant, say g. However, we usually find that such series expansions are only well-defined when they have a vanishing radius of convergence, and so, it is difficult to extract any information from them for finite values away from the $g \to 0$ limit. The theory of Borel resummation deals with it in the following

manner: consider such a series given by

$$f(g) = \sum_n a_n g^n \tag{7.2}$$

Now this power series form may not be convergent for every value of g, but one can engineer it into one that has a finite radius of convergence by absorbing out an $n!$ factor to cancel out the divergent behaviour at large n. The series given by the **Borel transform** is

$$B[f(g)] = \sum_n \frac{a_n}{n!} g^n \tag{7.3}$$

and we can then define the function $f(g)$ via an integral representation

$$\boxed{f(g) = \int_0^\infty dt\ e^{-t} B[f(gt)]} \tag{7.4}$$

The original series representation of $f(g)$ can be reproduced from Eq. 7.2 after using Eq. 7.3. In fact, one can use this as the definition of the function $f(g)$ if the integral is convergent and non-singular on the real axis.

7.1.1 Relation to solutions in field theory and non-perturbative effects

Singularities on the real axis can cause ambiguities in the definition of $f(g)$ due to various problems such as selecting the "correct" contour to compute the aforementioned integral and so on. However, the presence of such singularities is quite helpful. It can be shown that they are associated with solutions of classical field theories due to an argument by t'Hooft [44]. In fact, the relation between these singularities and non-trivial classical solutions provides a heuristic explanation of the non-perturbative corrections to series expansions like Eq. 7.1.

We will give an informal illustration of the argument as follows: consider a correlator that is being computed for a coupling constant that does not satisfy the perturbative ansatz $g \to 0$. Such a correlator is best denoted by a Borel integral representation. Equating it to the path integral formulation of the correlator, we get

$$\int_0^\infty dy\ e^{-\frac{y}{g}} B[f(y)] \sim \int \mathcal{D}\phi\ e^{-\frac{-S[\phi]}{g}} \tag{7.5}$$

This implies that

$$\begin{aligned} B(y) &= \int \mathcal{D}\phi\ \delta(y - S[\phi]) \\ &= \left.\frac{\partial \phi}{\partial S}\right|_{S[\phi]=y} \end{aligned} \tag{7.6}$$

Thus, to get a singularity in the integral, a necessary condition is

$$\left.\frac{\partial S[\phi]}{\partial \phi}\right|_{S[\phi_{cl}]=y^*} = 0 \tag{7.7}$$

which is exactly the classical equation of motion for the system being described by the action $S[\phi]$. The solution ϕ_{cl} of this classical field theory corresponds to a singular point $y*$ on the real axis of the complex plane in which the Borel integral representation lives; the connection between the two is $y^* = S[\phi_{cl}]$.

Why is this important? Since there is a mapping between the singularities of the Borel integral in the complex plane and the solutions of the theory with action $S[\phi]$, we can think about the non-perturbative corrections to such divergent series as arising from expansions around solutions other than the free/vacuum solution. In other words, if we consider any formal series expansion of the type Eq. 7.1, the original perturbation series can be interpreted as an expansion around the perturbative vacuum; clearly, the e^{-c} part vanishes in the perturbative limit $c \to \infty$. However, for finite c, we observe that Borel integral singularities each correspond to other non-trivial solutions of the field theory, and one can thus qualitatively interpret the second (non-perturbative) term as an expansion around these other solutions. In our case, we expect the **singularities obtained from the CFT correlators to be associated with the non-vacuum or non-trivial solutions of the Einstein-Hilbert action in AdS_3.**

7.2 Analysis of the non-perturbative corrections in Virasoro blocks

7.2.1 Analysis of the generic regulating function $S[x, c]$

Recall the regulating function we found in the previous chapter, given by Eq. 6.21. Given our analysis, we found that this function resolves the presence of forbidden singularities. Let us now Borel resum this result and see what it has to say about the non-perturbative corrections. We have

$$\begin{aligned} S[x,c] &= \frac{1}{\Gamma(2h_L)} \int_0^\infty dp\; p^{2h_L-1} e^{-px-\frac{\sigma^2}{2b^2}p^2} \\ &\sim \frac{1}{\Gamma(2h_L)} \sum_{n=0}^{\infty} \frac{1}{n!} \left(-\frac{1}{c}\right)^n \left[\int_0^\infty dp\; p^{2h_L-1} e^{-px} p^{2n}\right] \\ &= \sum_{n=0}^{\infty} \frac{1}{n!} \left(-\frac{1}{c}\right)^n \frac{\Gamma(2h_L+2n)}{\Gamma(2h_L)} x^{-2h_L-2n} \end{aligned} \tag{7.8}$$

which we get by solving the standard integral in p. We have a series in terms of the coupling constant $1/c$, and one can see clearly that it is divergent for finite c. Enter Borel resummation: the Borel transform for a generic y (in place of the coupling constant $1/c$) is given by

$$\begin{aligned} B[S[x,y]] &= \sum_{n=0}^{\infty} \frac{1}{n!n!}(-y)^n \frac{\Gamma(2h_L+2n)}{\Gamma(2h_L)} x^{-2h_L-2n} \\ \implies B[x,y] &= \frac{1}{x^{2h_L}}\, {}_2F_1\left(h, h, h+\frac{1}{2}, -\frac{4y}{x^2}\right) \end{aligned} \tag{7.9}$$

and thus, the Borel integral representation is given by

$$\begin{aligned} S[x,c] &= \int_0^{\infty} d(cy)\; e^{-cy} B[x,y] \\ \implies S[x,c] &= \frac{1}{x^{2h_L}} \int_0^{\infty} ds\; e^{-s}\; {}_2F_1\left(h, h, h+\frac{1}{2}; -\frac{4s}{x^2 c}\right) \end{aligned} \tag{7.10}$$

where we have taken $s = cy$ to simplify the integral. To get signatures of non-perturbative behaviour, we look for singularities and other anomalous behaviour that can cause ambiguities in defining the contours for integration, or the integral as a whole.

While there are no singularities on the real axis, the hypergeometric function ${}_2F_1(a,b,c;z)$ has a branch cut $[1,+\infty)$ on the real axis for z. Thus, the ambiguity in the integral arises due to the branch cut, which in terms of s has the range

$$-\frac{x^2 c}{4} \leq s < \infty \tag{7.11}$$

Now recall that $x = t - 2\pi n/r_+$, and thus, near the forbidden singularities, we have $x \approx 0$ for any finite value of c. This implies that the branch cut is approximately over the range

$$0 \leq s < \infty \tag{7.12}$$

which correspond to the limits of the integral! Around the forbidden singularities, this integral is completely ambiguous and undefined; and that means that the behaviour near the forbidden singularities is dominated completely by non-perturbative corrections that arise from other non-trivial solutions to the Einstein's equations in AdS_3.

Admittedly, this was a roundabout way of stating something that we already "know": **the forbidden singularities in the thermal correlator must be restored by a non-perturbative mechanism**. Of course, that is not completely true, we now have a quantitative way of confirming that this hypothesis is indeed true, and we also know what the restoring function must look like, namely, $S[x,c]$.

7.2.2 Analysis of a known Virasoro block $\tilde{\mathcal{V}}_{2,1}$

The analysis in the previous section was quite general, and thus, also vague regarding the exact details about the origin of the non-perturbative corrections to the blocks. In this section, let us look at the degenerate block $\tilde{\mathcal{V}}_{2,1}$ which we have already looked at before in Sec. 5.1.2 to motivate the derivation of the master equation. We already know how the exact b solution mitigates the singularities that are caused due to the semi-classical $b \to \infty$ solution. Let us see what the resummation techniques have to say about this feature. We have

$$\tilde{\mathcal{V}}_{2,1}(z) = (1-z)\ {}_2F_1(2, b^2+1, 2b^2+2; z) \tag{7.13}$$

It turns out that one can write it in a more suggestive form in terms of the variable

$$w = 2\log\left(\sinh\left(\frac{t}{2}\right)\right) \tag{7.14}$$

where $1 - z = e^{-t}$. In these coordinates, one can write down

$$\tilde{\mathcal{V}}_{2,1}(w) = \sqrt{1+e^{-w}} \sum_{k=0}^{\infty} \left(\frac{1}{b^2}\right)^k G_k(w) \tag{7.15}$$

where the series terms $G_k(w)$ are known due to some analytic properties of the hypergeometric functions. One then finds out the Borel transform, which leads to an integral representation

$$\tilde{\mathcal{V}}_{2,1}(w) = 1 - \sqrt{1+e^{-w}} \int_0^{\infty} dy\ \frac{e^{-y-\frac{3y}{2b^2}-\frac{3w}{2}}}{\left(1+e^{w-\frac{y}{b^2}}\right)^{\frac{3}{2}}} \tag{7.16}$$

which we can immediately verify to be true.

What we are interested in, is whether we can find any singularities, and whether we can find any association between them and the non-trivial solutions of the classical field theory (here, the Einstein equations in AdS_3). Clearly, there are (Borel) singularities at

$$y = b^2(w - i\pi(1+2n)) \ \text{ for } \ n \in \mathbb{Z} \tag{7.17}$$

and these will correspond to the different non-trivial classical field theory solutions.

Recall that our analysis has been about vacuum blocks so far, that is, we know that the physical state exchanged between the light probe and the heavy black hole is the vacuum block. However, we have found the presence of a non-perturbative effect in the series expansion of the vacuum block. What does this correspond to? Due to a curious feature of degenerate Virasoro blocks, we can even identify what causes the non-perturbative effect. It turns out that due to something called the **fusion rules**, the Virasoro block expansion of

a four-point correlation function with degenerate operators can contain only specific Virasoro blocks. In particular, we find that if we consider a four-point function with two heavy degenerate operators $h_{2,1}$, then the only Virasoro blocks that are present in the block decomposition are the vacumm or identity block (corresponding to $h = 0$) and a block with $h \equiv h_{3,1}$. Schematically, we have

$$\langle \dots \mathcal{O}_{2,1}\mathcal{O}_{2,1} \dots \rangle \sim \mathcal{V}_0 + \mathcal{V}_{3,1} \tag{7.18}$$

Note that this is a very informal relation that is only meant to highlight the finiteness of the block decomposition. However, this is very indicative of what is causing the non-perturbative effect: a "heavy" $h_{3,1}$ state is also being exchanged! Thus, what we discover is that the perturbative part of four-point function is controlled by exchange of the vacuum block, while the non-perturbative contribution comes from the exchange of this heavy state, which comes through another classical solution of the field equations. Note that, we have found an entire branch cut's worth of ambiguity here; this might be because the exchange is really $\mathcal{O}_{3,1}$ and **all its descendants**!

With this, we end our discussion on the analysis of degenerate blocks and their relation to the black hole information loss problem, and move onto understanding how these structures arise in the bulk theory.

Part III

Virasoro blocks and Information Loss II: A prescription to construct the holographic dual for the conformal Virasoro block in the bulk

Chapter 8

Why conformal Virasoro blocks and geodesic Witten diagrams

Thus far, we have dealt with Virasoro blocks to understand the information loss problem in AdS_3/CFT_2. This has been very useful in understanding where the differences between the finite c theory and the semi-classical limits lie, and how one can mitigate them (here, we have done it up till order $1/c$ corrections). Nonetheless, we would also like to understand this mechanism via a bulk construction, that is, we would like to see how one can translate the various things we learnt on the boundary CFT into observables associated with the bulk theory of gravity.

But we are getting too ahead of ourselves, we must first start with more basic things. One of the most natural questions that one can ask is what is the holographic dual to a Virasoro block in the bulk? That is, can we figure out what observable or computation in the bulk corresponds to the Virasoro block that we are familiar from the boundary CFT theory? The relation between four-point functions and Witten diagrams (crudely speaking, these are Feynman diagrams in AdS) has been known for a long time [19, 20, 21, 22, 23, 24, 25, 26]. However, an equivalent mapping for the Virasoro block was not known; exactly what corresponds to a "decomposition" of the Witten diagram in the way a Virasoro block is a decomposition of the four-point function was not well understood.

However, an exact equivalence between Virasoro conformal blocks was made with **geodesic Witten diagrams** [27, 28, 29] and that has greatly aided and extended our understanding of the Virasoro block in the bulk in a geometric way. In this part of the thesis, we will use this generalized bulk prescription and present a modified version of it that is particularly well-suited in understanding the bulk version of the Virasoro block for an AdS_3 black hole (that is, a BTZ black hole). The results we get from such a construction will also be useful to gain further insight into how one could construct the finite c version of the Virasoro blocks on the bulk side.

Before we jump into this calculation, we will briefly review the main (qualitative) features of a Witten diagram and its modified geodesic version which is central to all further discussions in this chapter.

8.1 Witten diagrams

Witten diagrams are a diagrammatic procedure used to compute n-point CFT correlation functions using the operator duals in the corresponding AdS space. The reader will be encouraged to recall how the Feynman rules and diagrams are derived for say QED, the cleanest way to do it is to think about them in terms of the path integral. The Witten diagram rules are the analogue of that for an action associated with a theory of gravity in AdS, modulated by a perturbative expansion in terms of the gravitational coupling constant G_N.

The Witten diagram is conventionally represented by a disc, whose interior corresponds to the interior of AdS while the boundary circle corresponds to the boundary of AdS (see Fig 8.1). Given the metric of Euclidean AdS_{d+1} in global coordinates ($l = 1$)

$$ds^2 = \frac{1}{\cos^2\rho}\left(d\tau^2 + d\rho^2 + \sin^2\rho\, d\Omega_{d-1}^2\right) \tag{8.1}$$

the interior is described by the coordinates $y_i = \{\rho, \tau, \Omega_{d-1}\}$ while the boundary coordinates are given by $x_i = \{\tau, \Omega_{d-1}\}$.

The components required to compute a Witten diagram are:

1. **Boundary points** x_i which are the locations of the **source operators** $O_i(x_i)$ with dimesions h_i. They are dual to the bulk (for us, scalar) field ϕ with mass $m^2 = 4h(h-1)$.
2. A **bulk-boundary propagator** $G_{b\partial}(y, x_i)$ which joins an external boundary point to an internal interaction vertex location y in the bulk. This propagator is a scaled version of the bulk-bulk propagator which we cover next.
3. A **bulk-bulk propagator** that covers connects two interaction vertices y, y' in the bulk, usually denoted by $G_{bb}(y, y')$. The bulk-bulk propagator is actually the Green's function for the AdS wave equation; that is, it is the solution to

$$\Box G_{bb}(y, y') = -\delta^{(d+1)}(y - y') \tag{8.2}$$

4. The structure of the interior points or interaction vertices is dictated by the interaction term in the action, that is, whether it is a ϕ^3 theory and so on.

The following illustrations will be useful in understanding how a Witten diagram is calculated. Consider the tree-level contribution to a four-point function of scalar fields ϕ_i

dual to the scalar operators $\mathcal{O}_i$ located at x_i on the boundary for

1. Quartic interaction term:

$$\int_y G_{b\partial}(y,x_1)G_{b\partial}(y,x_2)G_{b\partial}(y,x_3)G_{b\partial}(y,x_4) \tag{8.3}$$

2. Exchange interaction term:

$$\int_y \int_{y'} G_{b\partial}(y,x_1)G_{b\partial}(y,x_2) \times G_{bb}(y,y';\Delta,l) \times G_{b\partial}(y',x_3)G_{b\partial}(y',x_4) \tag{8.4}$$

where

$$\int_y \equiv \int d^{d+1}y\sqrt{g(y)} \tag{8.5}$$

The Witten diagrams for the same are given in Fig. 8.1.

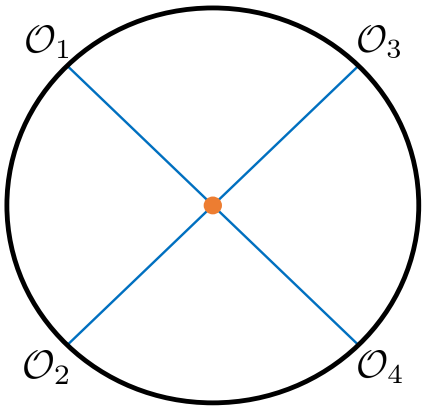

(a) Contact diagram for a quartic interaction term

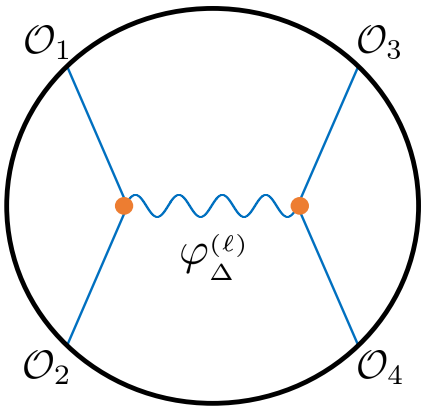

(b) Exchange interaction via a symmetric traceless spin-l tensor field with conformal dimension Δ.

Figure 8.1: Tree-level Witten diagrams (orange dots depict bulk vertices that are to be integrated over all of AdS space). Reproduced from [29].

8.2 Geodesic Witten Diagrams

The punchline of the entire story about finding the holographic dual to a Virasoro block is the following [27, 28, 29]: A Virasoro block of a four-point function for scalar operators $\mathcal{O}_i(x_i)$ with conformal dimensions $(h_i, \bar{h}_i)$ can be computed exactly using a **geodesic Witten diagram**; and the relation between the diagram and the block is

$$W_{\Delta,l} \sim \mathcal{V}_h(c,h_i,h;z)\mathcal{V}_{\bar{h}}(c,h_i,\bar{h};\bar{z}) \tag{8.6}$$

where

$$W_{\Delta,l} = \int_{\gamma_{12}} \int_{\gamma_{34}} G_{b\partial}(y(\lambda), x_1) G_{b\partial}(y(\lambda), x_2) \times G_{bb}(y(\lambda), y(\lambda'); \Delta, l) \times G_{b\partial}(y(\lambda'), x_3) G_{b\partial}(y(\lambda'), x_4) \tag{8.7}$$

Note that the external operator dimensions are finite, that is, they do not scale as c in the large c limit.

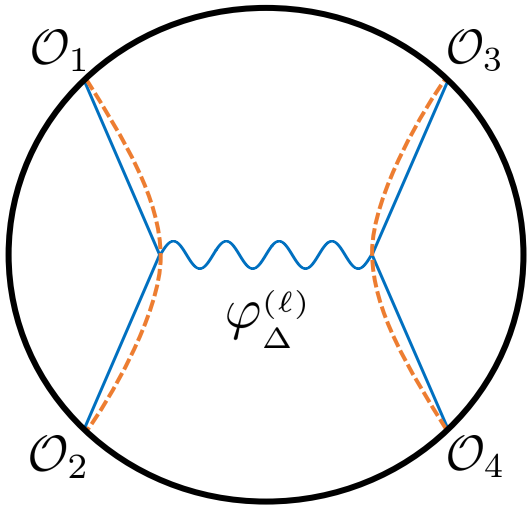

Figure 8.2: A geodesic Witten diagram for the exchange of a field with scaling dimension Δ and spin l. Notice how there are no orange dots here, but rather orange dotted lines that depict the geodesics over which the integration is carried out. Reproduced from [29].

Observe the difference between a Witten diagram and the geodesic version of it; in the former one has to really integrate over the entire AdS space whereas in the latter, one only needs to integrate over the geodesics that connect the various boundary operators. The various pieces in the geodesic Witten diagram are as follows:

1. **Geodesics** γ_{ij}:
   These connect the operators $\mathcal{O}_i$ and $\mathcal{O}_j$ each at the boundary locations x_i and x_j respectively, and traverse through the bulk. λ, λ' parametrize the geodesics. (Depicted in Fig. 8.2 by the orange dotted lines)
2. **Bulk-Bulk Propagator** $G_{bb}(y(\lambda), y(\lambda'); \Delta, l)$:
   This is the propagator that connects the two points $y(\lambda)$ and $y(\lambda')$ in the bulk. Note that these two are part of two different geodesics. (Depicted in Fig. 8.2 by the blue squiggly line in the middle)
3. **Bulk-Boundary Propagator** $G_{b\partial}(y(\lambda), x_i)$:
   This is the propagator that connects the point $y(\lambda)$ or $y(\lambda')$ on the geodesic in the bulk

to a boundary point x_i. (Depicted in Fig. 8.2 by the blue lines connecting the points on the geodesics with points on the boundary)

We also have a nice physical interpretation for the Virasoro block in the bulk: The Virasoro block due to the $|h, \bar{h}\rangle\langle h, \bar{h}|$ is related to the contribution of the exchange of a field of conformal dimensions $\Delta = h + \bar{h}$ and spin $l = h - \bar{h}$ between the the "interacting geodesics". This aligns well with what we discussed in Sec. 4.1.2. Of course, one has to be careful when we say Virasoro block, as here, it really the product of the holomorphic and antiholomorphic blocks that is equivalent to the geodesic Witten diagram.

Now that we have a method of computing the holographic dual, let us try to compute it in the heavy-light semi-classical limit that we have seen in the previous chapters and see how it compares to them. Such a verification will be essential to build confidence in this method of bulk construction for the Virasoro blocks.

Chapter 9

The geodesic Witten diagram in the semi-classical heavy-light limit

To calculate the semi-classical Virasoro block in $\mathrm{AdS}_3/\mathrm{CFT}_2$, we need to calculate the geodesic Witten diagram, which is given by

$$\boxed{\mathcal{W}_{2h,0}(\tau,\phi) \equiv \int d\lambda\, G_{b\partial}(x_1, y(\lambda)) G_{b\partial}(x_2, y(\lambda)) \int d\lambda'\, G_{b\partial}(x_3, y(\lambda')) G_{b\partial}(x_4, y(\lambda')) \times G_{bb}(y(\lambda), y(\lambda'); 2h)} \tag{9.1}$$

In particular we want to calculate this in the heavy-light limit wherein $h_L, h, h_H/c$ are fixed as $c \to \infty$.

The motivation of our prescription is through [28]. A brief discussion of the same is given below.

9.1 Review of the "Kraus" prescription

The metric used is given by

$$ds^2 = \frac{\alpha^2}{\cos^2\rho}\left(\frac{d\rho^2}{\alpha^2} + d\tau^2 + \sin^2\rho\, d\phi^2\right) \tag{9.2}$$

We note that $\alpha = 1$ corresponds to the global (Euclidean) AdS_3 metric as we have seen before in Chapter 3, and there is a reason for writing it in this manner. To make sense of the geometry, we make the coordinate transformation

$$r = \alpha \tan\rho \tag{9.3}$$

which implies

$$\tan^2\rho = \frac{r^2}{\alpha^2}, \qquad \frac{1}{\alpha^2}\frac{dr^2}{\frac{r^2}{\alpha^2}+1} = \sec^2\rho\, d\rho^2 \tag{9.4}$$

and so we get the metric form

$$ds^2 = \frac{dr^2}{r^2+\alpha^2} + (r^2+\alpha^2)d\tau^2 + r^2 d\phi^2 \tag{9.5}$$

which corresponds to a conic defect metric (we know this geometrically for the case $\alpha = 1/N$ for $N \in \mathbb{N}$). Furthermore, we also see that a naive analytic continuation of α reproduces the BTZ black hole metric; in particular defining $\alpha^2 = -r_+^2$ gives us

$$ds^2 = \frac{dr^2}{r^2-r_+^2} + (r^2-r_+^2)d\tau^2 + r^2 d\phi^2 \tag{9.6}$$

The geodesic Witten diagram calculation is done in a slick way in [29] by leveraging the analytic properties of this parameter α. The reader is encouraged to read this prescription, but since we are going to explain the entire procedure via a new prescription that retains the physics of the procedure anyway, we will not do a comprehensive review of the "Kraus" prescription. Instead, we note down some salient features from their technique, namely

1. Recognize that $\alpha = 1$ is the global AdS_3 limit. This is important since we already know what the propogators look like for global AdS.
2. Use the propagators in the global limit and make the substitutions $\tau, \phi \to \alpha\tau, \alpha\phi$ to get the propagators for this new α scaled metric that was created due to the backreaction of the heavy h_H geodesic on the ambient AdS_3.
3. This new α scaled metric corresponds to a conic defect metric for $0 < \alpha < 1$ and a BTZ black hole for $\alpha^2 < 0$. Choose the former for the sake of the calculation, as one can always analytically continue the α later to get the answer for the case of black holes.
4. Do the geodesic Witten diagram calculation in the "simpler" conic defect geometry and then substitute the analytically continued $\alpha = ir_+$ in the final answer.
5. To compare this answer with CFT_2 calculations, one can invert the standard radial quantization map given by

$$z = e^{iw} \;\text{ with }\; w = \phi + it \tag{9.7}$$

to go from the boundary to the complex plane. Compare this with Sec. 2.3.1.

Now, while this is a valid way of doing the calculation, there are a couple of reasons to consider doing the entire calculation directly in a BTZ geometry as opposed to the method

outlined above. Firstly, this way of analytically continuing the parameters causes geodesics in the conic defect geometry to become complex valued in the BTZ geometry, and this has no physical interpretation whatsoever. That is something that we want to fix, and in fact doing an explicit calculation does lead to very suggestive results regarding the actual physical geodesics. The second problem is related to the "source" of the geometry: the natural source of the geometry is at $\rho = 0$ for the conic defect geometry, but when translated for the BTZ case, it implies that the source of the geometry is at $r = 0$. This, however, is not very convincing as the Euclidean BTZ does not have an interior region behind the horizon ($r < r_+$ does not exist).

To make sense of these questions, let us now look at a modified prescription of understanding the geodesic Witten diagram in the explicit case of a BTZ black hole geometry. We also find it to be cleaner in terms of its physical interpretation.

9.2 A new prescription for calculating the geodesic Witten diagram in the heavy-light limit

9.2.1 Interpreting the heavy-light limit in the geodesic Witten diagram

We want to calculate the Virasoro blocks in the heavy-light limit. We already know that when we want to do this calculation in the so-called **global limit** (all h_i and h finite and fixed when $c \to \infty$), we simply calculate the geodesic Witten diagram in AdS_3 space, as in Eq. 9.1.

This motivates a natural generalization for calculating the Virasoro blocks in the heavy-light limit where $h_3 = h_4 = h_L$ are finite and $h_1 = h_2 = h_H \sim c$ when $c \to \infty$. In the context of the dual scalar fields, this has a very natural interpretation that we have repeatedly used before: it is akin to a light probe in the geometry of a (heavy) black hole. In terms of the Witten diagram components, we call the γ_{12} geodesic connecting the two heavy operators a "heavy" geodesic, and the γ_{34} geodesic connecting two light operators the "light" geodesic. Given the bulk interpretation, it is natural to suggest that the **heavy geodesic γ_{12} backreacts on the ambient AdS_3 and sets up a Euclidean black hole-like geometry**, and so, to calculate the heavy-light Virasoro block, one needs to calculate the **geodesic Witten diagram in this new spacetime due to the bakcreaction**.

It is reasonable to conclude that the heavy geodesic acts like the "source" for this new spacetime, and thus, we ought to place it at the natural centre of the new geometry. Here, that corresponds to the horizon $r = r_+$, as that is where the Euclidean BTZ geometry begins (recall our discussion of the tip of the Euclidean BTZ cigar in Chapter 3). The geodesic Witten diagram calculation must now be done using the bulk-bulk and bulk-boundary propagators, as well as geodesics set in the BTZ-like geometry rather than simply global AdS.

Fortunately, the boundary of the BTZ geometry and AdS are indistinguishable from each other, and so, we can still keep the same interpretation for the light geodesic γ_{34}. That is, the light operators are on the boundary ($r \to \infty$), and they probe this geometry created by the backreaction of the heavy operators. We can interpret the intermediate "exchange operator" as a probe interfacing between the heavy and light operators; it can be thought of as a field of conformal dimensions $(h, \bar{h})$ being exchanged between the light and heavy operator geodesics. More precisely, it will be manifested via a bulk-bulk propagator connecting a point on the light operator geodesic to a point on the heavy operator geodesic.

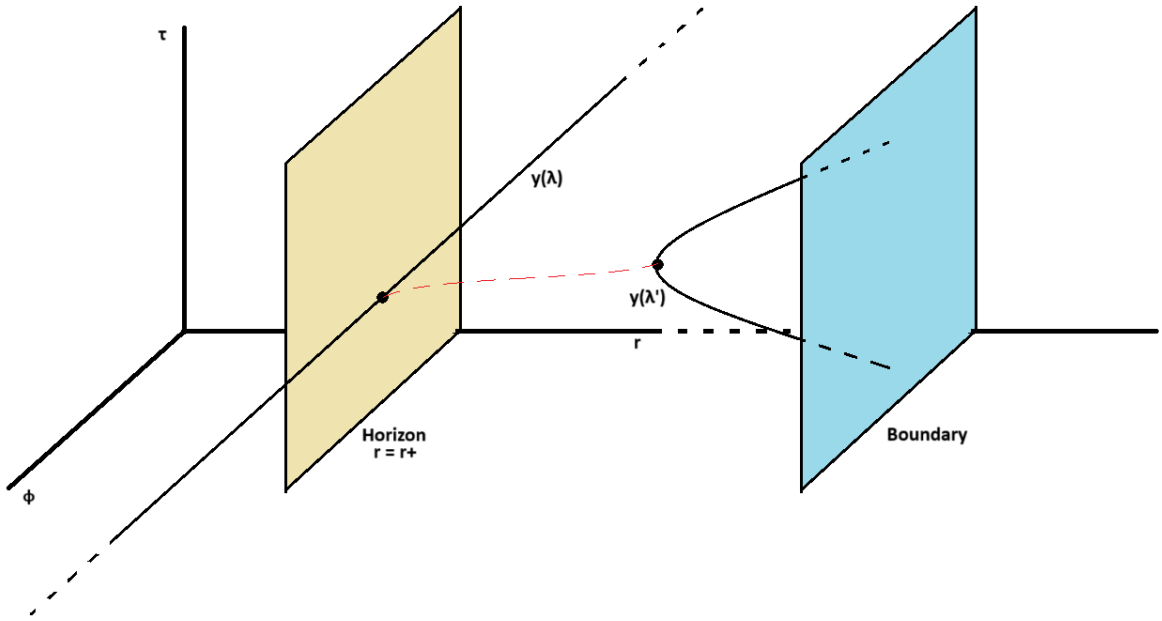

Figure 9.1: New bulk prescription

9.2.2 Setting up the calculation

With this interpretation of the prescription (refer to Fig. 9.1), we can now start with the actual calculation. The metric is given by

$$ds^2 = (r^2 - r_+^2)d\tau^2 + \frac{dr^2}{(r^2 - r_+^2)} + r^2 d\phi^2 \tag{9.8}$$

and so the interior points are given by $y = \{r, \tau, \phi\}$, while the boundary points are given by $x_i = \{\tau, \phi\}$. Furthermore, an important observation here is that the backreaction of the heavy geodesic does not lead to a geometry that has quotiented the AdS_3 space, that is, the span of the coordinates τ, ϕ is $(-\infty, +\infty)$.

We place the heavy operators at the source of the geometry, the most natural point for

that being the horizon, namely

$$\begin{aligned} x_1 &= (r = r_+, \phi = -\infty, \tau = \tau_0) \\ x_2 &= (r = r_+, \phi = +\infty, \tau = \tau_0) \end{aligned} \tag{9.9}$$

This is because, as one can see from Eq. 9.8, when one sets r to some constant value, and if that value is $r = r_+$, then we have $ds^2 = r_+^2 d\phi^2$, and so, only the ϕ coordinate has a natural interpretation as an affine parameter at the horizon $r = r_+$. This is exactly what we saw in Fig. 3.4, the τ vanishes smoothly as $r \to r_+$.

Next, we will put the light operators on the boundary as per

$$\begin{aligned} x_3 &= (r' \to \infty, \tau = \tau_1, \phi = \phi_1) \\ x_4 &= (r' \to \infty, \tau = \tau_2, \phi = \phi_2) \end{aligned} \tag{9.10}$$

To simplify things a bit more, we take $\phi_1 = \phi_2 =$ constant. Note that this is just a prescription, the calculation should work for any appropriately placed operator arrangement, we are just identifying the most natural scheme that both simplifies our calculation and gives us some insight into the physical aspects of the calculation.

9.2.3 Propagators

To calculate the geodesic Witten diagram in explicit BTZ coordinates, we need to use the bulk-bulk and the bulk-boundary propagators in BTZ coordinates. To start with, we first identify that the Kraus et al [29] got the result by considering the global AdS_3 propagator

$$G_{bb}(y, y'; 2h) = G_F^E(\xi) = \xi^{2h}\ {}_2F_1(h, h + \frac{1}{2}; 2h; \xi^2) \tag{9.11}$$

where ξ is given by

$$\xi = \frac{\cos\rho \cos\rho'}{\cosh(\tau - \tau)' - \sin\rho \sin\rho' \cos(\phi - \phi')} \tag{9.12}$$

which was suitably changed by making the substitution $\tau, \phi \to \alpha\tau, \alpha\phi$. Now in general, the BTZ propagator [39] is given as a mirror sum because of the way the method of images works for the quotient of AdS_3. However, as we mentioned before, we are really looking at AdS_3 in terms of BTZ coordinates, as we have not really identified any periodic behaviour of ϕ. Thus, the trick of scaling τ, ϕ by α used in [29] is comparable to picking only the $n = 0$ piece to get the bulk-bulk propagator for our prescription, namely

$$\boxed{G_{bb}(y, y'; 2h) = G_F^E(\xi) = \xi^{2h}\ {}_2F_1(h, h + \frac{1}{2}; 2h; \xi^2)} \tag{9.13}$$

where

$$\xi = \frac{r_+^2}{rr' \cosh(r_+\Delta\phi) - \sqrt{r^2 - r_+^2}\sqrt{r'^2 - r_+^2}\cos(r_+\Delta\tau)} \tag{9.14}$$

has been written in terms of the BTZ coordinates rather than the global AdS coordinates.

Next, we take the bulk-boundary limit to find the bulk-boundary propagator. This is done by taking one of the points, say r' to the boundary (here, $r' \to \infty$). For that, we follow the boundary limit prescription as used in the conventional extrapolate dictionary, wherein the radial coordinate is scaled by the scaling dimension of the operator. In our case, the scaling dimension is twice as the conformal dimension h owing to the spinless nature of the scalar field. Thus, we get that

$$\begin{aligned} G_{b\partial}(x', y) &= \lim_{r'\to\infty} (r')^{2h} G_{bb}(y, y'; 2h) \\ &= \lim_{r'\to\infty} \left(\frac{r_+^2}{r\cosh(r_+\Delta\phi) - \sqrt{r^2 - r_+^2}\sqrt{1 - \frac{r_+^2}{r'^2}}\cos(r_+\Delta\tau)} \right)^{2h} {}_2F_1(h, h + \frac{1}{2}; 2h; 0) \\ &= \left(\frac{r_+^2}{r\cosh(r_+\Delta\phi) - \sqrt{r^2 - r_+^2}\cos(r_+\Delta\tau)} \right)^{2h} \end{aligned} \tag{9.15}$$

To summarize, we have the different propagators in terms of BTZ coordinates

$$\boxed{\begin{aligned} G_{b\partial}(x', y) &= \left(\frac{r_+^2}{r\cosh(r_+\Delta\phi) - \sqrt{r^2 - r_+^2}\cos(r_+\Delta\tau)} \right)^{2h} \\ G_{bb}(y, y'; 2h) &= \left(\frac{r_+^2}{rr'\cosh(r_+\Delta\phi) - \sqrt{r^2 - r_+^2}\sqrt{r'^2 - r_+^2}\cos(r_+\Delta\tau)} \right)^{2h} \\ &\quad {}_2F_1\left(h, h + \frac{1}{2}; 2h; \left[\frac{r_+^2}{rr'\cosh(r_+\Delta\phi) - \sqrt{r^2 - r_+^2}\sqrt{r'^2 - r_+^2}\cos(r_+\Delta\tau)} \right]^2 \right) \end{aligned}} \tag{9.16}$$

9.2.4 Heavy operator geodesic and boundary correlator

Consider the first piece of the double integral in Eq. 9.1, that is, the one over the parameter λ. The heavy geodesic sits at $r = r_+$ and extends from $\phi = -\infty$ to $\phi = \infty$. The τ span of this vanishes, as we have discussed earlier. Consequently, we have

$$\lambda = r_+\phi \tag{9.17}$$

The product of the boundary correlators

$$\boxed{\begin{aligned} G_{b\partial}(x_1, y(\lambda)) G_{b\partial}(x_2, y(\lambda)) &= G_{b\partial}(\phi = -\infty, \phi(\lambda)) G_{b\partial}(\phi = \infty, \phi(\lambda)) \\ &= \left(\frac{r_+}{\cosh(\lambda \to -\infty)}\right)^{2h_H} \left(\frac{r_+}{\cosh(\lambda \to +\infty)}\right)^{2h_H} \\ &= 1 \end{aligned}} \tag{9.18}$$

and thus this piece contributes unity (up to some constant prefactors that we do not worry about).

9.2.5 Light operator geodesic and boundary correlator

To calculate the various bulk-boundary pieces of the light operators, we will first need to find the expression for the light geodesic.

Geodesic equations

We note that the metric we are working in is given by (to be very precise, the variables here are the primed one (r', τ', ϕ') but it is understood that we will use those after the calculations in this section)

$$ds^2 = (r^2 - r_+^2) d\tau^2 + \frac{1}{(r^2 - r_+^2)} dr^2 + r^2 d\phi^2 \tag{9.19}$$

Now, we observe that for the light geodesic, we have considered a constant ϕ slice, and so, using that information and the fact that the affine parameter λ' is related to the invariant distance ds^2, we get

$$\boxed{(r^2 - r_+^2)\dot{\tau}^2 + \frac{1}{(r^2 - r_+^2)}\dot{r}^2 = 1} \tag{9.20}$$

where $\dot{x}$ signifies the derivative of x with respect to λ'. We will use this equation as it relates the first derivatives of both variables, and thus, it saves us from the trouble of using two second order differential equations (the usual geodesic equation for $\ddot{r}, \ddot{\tau}$ as given below).

Next, we can write down the geodesic equation we get for τ by considering the usual second order equation

$$\frac{\partial^2 x^\sigma}{\partial \lambda^2} + \Gamma^\sigma_{\mu\nu} \frac{\partial x^\mu}{\partial \lambda} \frac{\partial x^\nu}{\partial \lambda} = 0 \tag{9.21}$$

which leads to

$$\boxed{\ddot{\tau} + \left(\frac{2r}{r^2 - r_+^2}\right) \dot{r}\dot{\tau} = 0} \tag{9.22}$$

Solving for $r(\lambda'), \tau(\lambda')$

With Eqs 9.20 and 9.22, we can solve for $r(\lambda'), \tau(\lambda')$. We start with

$$\begin{aligned} \ddot{\tau} + \left(\frac{2r}{r^2 - r_+^2}\right)\dot{r}\dot{\tau} &= 0 \\ \implies \int \frac{d\dot{\tau}}{\dot{\tau}} &= -\int \frac{2rdr}{r^2 - r_+^2} \\ \implies \ln \dot{\tau} &= -\ln\left(r^2 - r_+^2\right) + c \end{aligned} \tag{9.23}$$

and so we get that

$$\boxed{\dot{\tau} = \frac{c_1}{r^2 - r_+^2}} \tag{9.24}$$

where c_1 is some constant of integration that we will set according to the boundary conditions. Plugging Eq. 9.24 in Eq. 9.20. we get

$$\begin{aligned} (r^2 - r_+^2)\left(\frac{c_1}{r^2 - r_+^2}\right)^2 + \frac{1}{(r^2 - r_+^2)}\dot{r}^2 &= 1 \\ \implies \dot{r}^2 = r^2 - (r_+^2 + c_1^2) &= r^2 - k^2 \\ \implies \int \frac{dr}{\sqrt{r^2 - k^2}} &= \int \pm d\lambda' \end{aligned} \tag{9.25}$$

Using the substitution $r = k\cosh t$, we get that

$$\cosh^{-1}\frac{r}{k} = \pm\lambda' + c \tag{9.26}$$

Now, since λ' is an affine parameter, we can always absorb a multiplicative factor and an additive constant, that is, $\lambda' \to a\lambda' + b$. Here, this amounts to saying that we are choosing that $\lambda' \to -\infty$ corresponds to x_3 and $\lambda' \to \infty$ corresponds to x_4. We now have

$$\boxed{r = \sqrt{r_+^2 + c_1^2}\cosh\lambda'} \tag{9.27}$$

We can immediately check if it is consistent with the boundary conditions, which it is, as $\lambda' \to \pm\infty$ gives us $r \to \infty$ which is precisely the boundary limit that we want. Next, plugging Eq.9.27 into Eq. 9.24, we have

$$\begin{aligned} \dot{\tau} &= \frac{c_1}{(r_+^2 + c_1^2)\cosh^2\lambda' - r_+^2} \\ \implies \int dw &= c_1 \int \frac{2d\lambda'}{k^2\cosh 2\lambda' + (c_1^2 - r_+^2)} \end{aligned} \tag{9.28}$$

which gives us

$$\boxed{\tau + c_2 = \frac{1}{r_+} \tan^{-1}\left(\frac{r_+}{c_1} \tanh \lambda'\right)} \tag{9.29}$$

Solutions

All that is left to be done now, is to impose the boundary conditions for τ at $\lambda' = \pm\infty$, these are τ_1, τ_2 respectively. Plugging this into Eq. 9.29, we can solve for c_1, c_2

$$\begin{aligned} c_1 &= r_+ \cot\left[\frac{r_+}{2}(\tau_2 - \tau_1)\right] \\ c_2 &= -\frac{(\tau_1 + \tau_2)}{2} \end{aligned} \tag{9.30}$$

which we can plug back into Eqs. 9.27 and 9.29 to get

$$\boxed{\begin{aligned} r(\lambda') &= r_+ \csc\left[\frac{r_+}{2}(\tau_2 - \tau_1)\right] \cosh \lambda' \\ \tau(\lambda') &= \frac{(\tau_1 + \tau_2)}{2} + \frac{1}{r_+} \tan^{-1}\left(\tan\left[\frac{r_+}{2}(\tau_2 - \tau_1)\right] \tanh \lambda'\right) \\ \phi(\lambda') &= \text{const.} \end{aligned}} \tag{9.31}$$

To simplify the expressions, we introduce two new placeholder angular variables defined as

$$\begin{aligned} \theta(\lambda') &= r_+ \left[\tau(\lambda') - \left(\frac{\tau_1 + \tau_2}{2}\right)\right] \\ \psi &= \frac{r_+}{2}(\tau_2 - \tau_1) = \frac{r_+ \tau}{2} \end{aligned} \tag{9.32}$$

Here, we are renaming the difference in initial and final times as τ since we are really only interested in the time difference. The geodesic equations can be written in a condensed form after these re-definitions, namely

$$\boxed{\begin{aligned} r &= r_+ \csc\psi \cosh \lambda' \\ \tan\theta &= \tan\psi \tanh \lambda' \end{aligned}} \tag{9.33}$$

Note that it should be $|\csc\psi|$ for the r geodesic equation, but we have not retained the absolute value sign as all computations thereafter remain the same under $|\csc\psi| \to \csc\psi$, and the final expressions we have are all in terms of $\csc^2\psi$.

Boundary correlators for the light operators

Now that we have the geodesic equations in place, we can try to simplify the boundary correlators for the light operators. We have that

$$G_{b\partial}(x', y) = \left(\frac{r_+^2}{r \cosh(r_+ \Delta\phi) - \sqrt{r^2 - r_+^2} \cos(r_+ \Delta\tau)} \right)^{2h} \tag{9.34}$$

Plugging in the various geodesic equations given by Eq. 9.31, we have

$$\begin{aligned} G_{b\partial}(\tau_1, y(\lambda')) &= \left(\frac{r_+^2}{r(\lambda') - \sqrt{(r^2(\lambda') - r_+^2)} \cos[r_+(\tau(\lambda') - \tau_1)]} \right)^{2h_L} \\ &= \left(\frac{r_+^2}{r_+ \csc\psi \cosh\lambda' - r_+ \sqrt{(\csc^2\psi \cosh^2\lambda' - 1)} \cos(\theta + \psi)} \right)^{2h_L} \\ &= \left(\frac{r_+}{\csc\psi \cosh\lambda' - \sqrt{(\csc^2\psi \cosh^2\lambda' - 1)}(\cos\theta \cos\psi - \sin\theta \sin\psi)} \right)^{2h_L} \end{aligned} \tag{9.35}$$

which we have to simplify using various trigonometric and hyperbolic function identities to get

$$\boxed{G_{b\partial}(\tau_1, y(\lambda')) = \left(r_+ \frac{e^{-\lambda'}}{\sin\psi} \right)^{2h_L}} \tag{9.36}$$

We can do the same for the other boundary point and we observe that since we have $\cos(\theta - \psi)$, we get $e^{+\lambda'}$ in the numerator

$$\boxed{G_{b\partial}(\tau_2, y(\lambda')) = \left(r_+ \frac{e^{+\lambda'}}{\sin\psi} \right)^{2h_L}} \tag{9.37}$$

and thus, we have

$$\boxed{\begin{aligned} G_{b\partial}(x_3, y(\lambda')) G_{b\partial}(x_4, y(\lambda')) &= G_{b\partial}(\tau_1, y(\lambda')) G_{b\partial}(\tau_2, y(\lambda')) \\ &= \left(\frac{1}{\sin^2\psi} \right)^{2h_L} \end{aligned}} \tag{9.38}$$

Again, this is up to some constant prefactors.

9.2.6 Bulk-bulk propagator

The last piece of the geodesic Witten diagram is the bulk-bulk propagator, which is the field exchanged between the light and heavy operator geodesics. We have

$$G_{bb}(y,y';2h) = \left(\frac{r_+^2}{rr'\cosh\left(r_+(\phi-\phi')\right) - \sqrt{r^2-r_+^2}\sqrt{r'^2-r_+^2}\cos\left(r_+(\tau-\tau')\right)}\right)^{2h} \\ {}_2F_1\left(h, h+\frac{1}{2}; 2h; \left[\frac{r_+^2}{rr'\cosh\left(r_+(\phi-\phi)\right) - \sqrt{r^2-r_+^2}\sqrt{r'^2-r_+^2}\cos\left(r_+(\tau-\tau')\right)}\right]^2\right) \tag{9.39}$$

where the primed coordinates belong to the light operator geodesic, while the unprimed ones are on the heavy operator geodesic. We can make use of special properties of the individual geodesics to simplify the expression considerably.

We note that since $r = r_+$ for the hevay geodesic, the factor in front of the $\cos(r_+\Delta\tau)$ vanishes, and so, this function is only dependent on r, r', ϕ, ϕ'. We can simplify things even more if we take $\phi' = 0$; as it stands, the light operator geodesic is on a constant ϕ' surface, so choosing a constant value amounts to fixing that surface. Furthermore, since $\lambda = r_+\phi$ for the heavy geodesic, we can think of this constant ϕ' of the light operator geodesic as a constant added to the affine parameter λ of the heavy geodesic. In either case, what remains inside the hyperbolic cosine is simply λ. Using this, we get that

$$G_{bb}(y,y';2h) = \left(\frac{r_+}{r'(\lambda')\cosh\lambda}\right)^{2h} {}_2F_1\left(h, h+\frac{1}{2}; 2h; \left[\frac{r_+}{r'(\lambda')\cosh\lambda}\right]^2\right) \tag{9.40}$$

To this, we add the information we obtain from the light geodesic equation Eq. 9.31 to get

$$\boxed{G_{bb}(y,y';2h) = \left(\frac{\sin\psi}{\cosh\lambda'\cosh\lambda}\right)^{2h} {}_2F_1\left(h, h+\frac{1}{2}; 2h; \left[\frac{\sin\psi}{\cosh\lambda'\cosh\lambda}\right]^2\right)} \tag{9.41}$$

9.2.7 Calculating the geodesic Witten diagram

With all the pieces assembled, we can now calculate the geodesic Witten diagram (note that some constant prefactors have been dropped).

$$\begin{aligned}\mathcal{W}_{2h,0}(\tau,\phi) &\equiv \int d\lambda\, G_{b\partial}(x_1,y(\lambda))G_{b\partial}(x_2,y(\lambda)) \int d\lambda'\, G_{b\partial}(x_3,y(\lambda))G_{b\partial}(x_4,y(\lambda)) \times G_{bb}(y(\lambda),y(\lambda');2h) \\ &\sim \int_{-\infty}^{+\infty} d\lambda \int_{-\infty}^{+\infty} d\lambda' \left(\frac{1}{\sin^2\psi}\right)^{2h_L} \left(\frac{\sin\psi}{\cosh\lambda'\cosh\lambda}\right)^{2h} \\ &\qquad \times\ {}_2F_1\left(h, h+\frac{1}{2}; 2h; \left[\frac{\sin\psi}{\cosh\lambda'\cosh\lambda}\right]^2\right)\end{aligned} \tag{9.42}$$

Our choice of prescription has led to the ϕ dependence to drop out, and since we are interested in the τ dependence of the Virasoro blocks anyway, we will denote it as $\mathcal{W}_{2h,0}(\tau)$ henceforth to make the time dependence explicit.

To calculate this, we first expand out the hypergeometric function in terms of its defining power series, namely

$$\begin{aligned}&{}_2F_1(a,b;c;z) = \sum_{n=0}^{\infty} \frac{(a)_n(b)_n}{(c)_n}\frac{z^n}{n!} \\ \implies &{}_2F_1\left(h, h+\frac{1}{2}; 2h; \left[\frac{\sin\psi}{\cosh\lambda'\cosh\lambda}\right]^2\right) = \sum_{n=0}^{\infty} \frac{(h)_n(h+\frac{1}{2})_n}{(2h)_n}\frac{x^n}{n!}(\cosh\lambda\cosh\lambda')^{-2n}\end{aligned} \tag{9.43}$$

where $(a)_n$ is the Pochhammer symbol; and $x = \sin^2\psi$. Thus, we have

$$\boxed{\mathcal{W}_{2h,0}(\tau) \sim x^{-2h_L+h} \sum_{n=0}^{\infty} \frac{(h)_n(h+\frac{1}{2})_n}{(2h)_n}\frac{x^n}{n!} \int_{-\infty}^{+\infty} d\lambda\, (\cosh\lambda)^{-2n-2h} \int_{-\infty}^{+\infty} d\lambda'\, (\cosh\lambda')^{-2n-2h}} \tag{9.44}$$

We can easily evaluate the integral as

$$\int_{-\infty}^{+\infty} d\lambda\, (\cosh\lambda)^{-2n-2h} = \frac{\Gamma(\frac{1}{2})\Gamma(h+n)}{\Gamma(h+n+\frac{1}{2})} \sim \frac{(h)_n}{(h+\frac{1}{2})_n} \tag{9.45}$$

and plugging this into Eq. 9.44, we get

$$\begin{aligned}\mathcal{W}_{2h,0}(\tau) &\sim x^{-2h_L+h} \sum_{n=0}^{\infty} \frac{(h)_n(h)_n(h)_n}{(h+\frac{1}{2})_n(2h)_n}\frac{x^n}{n!} \\ &= (\sin^2\psi)^{-4h_L+2h}\ {}_4F_3\left(\begin{matrix} h, h, h, h \\ h, h+\frac{1}{2}, 2h \end{matrix}; x\sin^2\psi\right)\end{aligned} \tag{9.46}$$

Next, we use an identity used in [28], namely

$$ {}_4F_3\left(\begin{matrix} a, b-a, a', b-a' \\ \frac{b}{2}, \frac{b+1}{2}, b \end{matrix} ; \frac{z^2}{4(z-1)}\right) = {}_2F_1\left(a, a'; b; z\right) \cdot {}_2F_1\left(a, a'; b; \frac{z}{z-1}\right) \tag{9.47} $$

and it is clear that for

$$ z = 1 - e^{2i\psi}, \qquad a = a' = h, \qquad b = 2h \tag{9.48} $$

we can reconstruct the ${}_4F_3$ in Eq. 9.47.

Plugging in these values in the product of the ${}_2F_1$'s on the R.H.S, and substituting the ψ according to Eq. 9.32, we finally have an expression for the Virasoro blocks using the bulk prescription, namely

$$ \boxed{\mathcal{W}_{2h,0}(\tau) \sim \left[\sin\left(\frac{r_+\tau}{2}\right)\right]^{2h-4h_L} {}_2F_1\left(h, h; 2h; 1-e^{ir_+\tau}\right) \cdot {}_2F_1\left(h, h; 2h; 1-e^{-ir_+\tau}\right)} \tag{9.49} $$

9.3 Geodesic Witten diagram using an explicit wave equation solution

We can leverage some of our knowledge of Green's functions to calculate the geodesic Witten diagram in a way that is more suggestive of the role the bulk-bulk propagator plays. Observe that the diagram can be written as

$$ \begin{aligned} \mathcal{W}_{2h,0}(\tau, \phi) &\equiv \int d\lambda\, G_{b\partial}(x_1, y(\lambda)) G_{b\partial}(x_2, y(\lambda)) \int d\lambda'\, G_{b\partial}(x_3, y(\lambda)) G_{b\partial}(x_4, y(\lambda)) \times G_{bb}(y(\lambda), y(\lambda'); 2h) \\ &= \int d\lambda'\, G_{b\partial}(x_3, y(\lambda')) G_{b\partial}(x_4, y(\lambda')) \Psi(y(\lambda')) \end{aligned} \tag{9.50} $$

where $\Psi(y')$ is given by the inner integral

$$ \begin{aligned} \Psi(y') &= \int d\lambda\, G_{b\partial}(x_1, y(\lambda)) G_{b\partial}(x_2, y(\lambda)) \times G_{bb}(y(\lambda), y'; 2h) \\ &= \int d\lambda\, G_{bb}(y(\lambda), y'; 2h) \\ &= r_+ \int d\phi\, G_{bb}(y(r_+\phi), y'; 2h) \end{aligned} \tag{9.51} $$

Notice that we have kept the second bulk point y' (parametrized by (r', θ', τ')) arbitrary for now, but when we get the final form of $\Psi(y')$ we will pull back $y' \to y(\lambda')$ onto the geodesics that we calculated before.

Observe that the presence of the G_{bb} function inside the integral indicates that the overall function satisfies the scalar wave equation for a field of mass $m^2 = 4h(h-1)$. This means that it represents a scalar field associated with the probe interacting between the light and the heavy geodesics away from a delta source at $r' = r_+$. Such a scalar field will satisfy the wave equation given by

$$\Box' \Psi(y') = 4h(h-1)\Psi(y') \tag{9.52}$$

where

$$\Box \equiv \frac{1}{\sqrt{g}} \partial_\mu (\sqrt{g} g^{\mu\nu} \partial_\nu) \tag{9.53}$$

Given the metric

$$ds^2 = \frac{1}{(r^2 - r_+^2)} dr^2 + (r^2 - r_+^2) d\tau^2 + r^2 d\phi^2 \tag{9.54}$$

we can easily read of the metric components. Furthermore, we note that the overall function does not have a τ, ϕ dependence, and also that it should have a normalizable fall off at the AdS boundary ($r' \to \infty$). Using these constraints and boundary conditions, we can solve the wave equation to get an expression for $\Psi(y')$. The differential equation is

$$\begin{aligned} &\Box' \Psi(y) = 4h(h-1)\Psi(y) \\ \implies &\frac{1}{r'} \frac{d}{dr'} \left(r'(r'^2 - r_+^2) \frac{d}{dr'} \right) \Psi(r') = 4h(h-1)\Psi(r') \end{aligned} \tag{9.55}$$

which gives us the solutions

$$\boxed{\Psi(r') = \left\{ \begin{array}{l} {}_2F_1 \left(1-h, h, 1, \frac{r'^2}{r_+^2} \right) \\ \\ G^{2,0}_{2,2} \left(\begin{array}{c|c} 1-h, h & \\ 0, 0 & \frac{r'^2}{r_+^2} \end{array} \right) \end{array} \right\}} \tag{9.56}$$

Here,

$$G^{m,n}_{p,q} \left(\begin{array}{c|c} a_1, \ldots, a_p & \\ b_1, \ldots, b_q & z \end{array} \right) = \frac{1}{2\pi i} \int_L \frac{\prod_{j=1}^m \Gamma(b_j - s)}{\prod_{j=m+1}^q \Gamma(1 - b_j + s)} \frac{\prod_{j=1}^n \Gamma(1 - a_j + s)}{\prod_{j=n+1}^p \Gamma(a_j - s)} z^s \, ds \tag{9.57}$$

is the Meijer G-function; it can be thought of as a generalization of the hypergeometric variety of special functions. This form of the solution is not very useful, as it not transparent how the boundary fall off condition is going to be obeyed; and one will have to resort to various hypergeometric connection formulae to bring it into a form that is obviously normalizable at $r \to \infty$.

However, we can be a little slick about solving the differential equation itself by working

in a variable that takes care of this issue. We define

$$x = \frac{r_+^2}{r'^2} \tag{9.58}$$

Notice how the resulting solution can now be written as an expansion around the usual $x = 0$. With this, our differential equation becomes much more clean, namely,

$$x^2(1-x)\Psi''(x) - x^2\Psi'(x) - h(h-1)\Psi(x) = 0 \tag{9.59}$$

which can be immediately identified as a type of hypergeometric differential equation; the solutions are

$$\boxed{\Psi(x) = \begin{Bmatrix} (-x)^{1-h}\ {}_2F_1\left(1-h, 1-h, 2-2h, x\right) \\ \\ (-x)^{h}\ {}_2F_1\left(h, h, 2h, x\right) \end{Bmatrix}} \tag{9.60}$$

and we can see that only the latter is normalizable at $x \to 0 \iff r \to \infty$. Thus, we have

$$\boxed{\Psi(y') = \left(\frac{r_+^2}{r'^2}\right)^h\ {}_2F_1\left(h, h, 2h, \frac{r_+^2}{r'^2}\right)} \tag{9.61}$$

Pulling this back onto the light geodesic means letting $y' \equiv y'(\lambda')$, and so substituting Eqs. 9.31 and plugging it back into the geodesic Witten diagram and expanding out the hypergeometric series, we have

$$\begin{aligned}
\mathcal{W}_{2h,0}(\tau,\phi) &= \int d\lambda'\ \left(\frac{1}{\sin^2\psi}\right)^{2h_L}\left(\frac{\sin^2\psi}{\cosh^2\lambda'}\right)^h\ {}_2F_1\left(h,h,2h,\frac{\sin^2\psi}{\cosh^2\lambda'}\right) \\
&= \left(\frac{1}{\sin\psi}\right)^{2h-4h_L}\int d\lambda'\ \left(\frac{1}{\cosh^2\lambda'}\right)^h\ {}_2F_1\left(h,h,2h,\frac{\sin^2\psi}{\cosh^2\lambda'}\right) \\
&= \sum_{n=0}^{\infty}\frac{(h)_n(h)_n}{(2h)_n}\frac{1}{n!}\left(\frac{1}{\sin\psi}\right)^{2n+2h-4h_L}\int d\lambda'\ (\cosh\lambda')^{-2n-2h} \\
&\sim \sum_{n=0}^{\infty}\frac{(h)_n(h)_n(h)_n}{(2h)_n(h+\frac{1}{2})_n}\frac{1}{n!}\left(\frac{1}{\sin\psi}\right)^{2n+2h-4h_L} \\
&= (\sin\psi)^{-4h_L+2h}\ {}_4F_3\left(\begin{matrix} h,h,h,h \\ h,h+\frac{1}{2},2h \end{matrix}\ ;\ \sin^2\psi\right)
\end{aligned} \tag{9.62}$$

and using the identity Eq. 9.47 as before, we get the same answer as before

$$\boxed{\mathcal{W}_{2h,0}(\tau) \sim \left[\sin\left(\frac{r_+\tau}{2}\right)\right]^{2h-4h_L}\ {}_2F_1\left(h,h;2h;1-e^{ir_+\tau}\right)\cdot\ {}_2F_1\left(h,h;2h;1-e^{-ir_+\tau}\right)} \tag{9.63}$$

We have thus reproduced the geodesic Witten diagram, albeit, in a more direct way involving the wave equation.

What we have found is a robust semi-classical heavy-light limit interpretation and prescription of Virasoro blocks as being equivalent to a geodesic Witten diagram that calculates the interaction between a light probe and a heavy state that has backreacted on the ambient AdS_3 geometry to give rise to a BTZ black hole. Our computation given by Eq. 9.63 is also in exact agreement with the results presented in [15, 16, 17] through a CFT calculation in the semi-classical heavy-light limit, which is very encouraging. In fact, one can immediately find out that the vacuum block product ($h = 0$) is

$$\mathcal{W}_{2h,0}(\tau) \sim \frac{1}{\left[\sin\left(\frac{r_+\tau}{2}\right)\right]^{4h_L}} \tag{9.64}$$

which we can compare with Eqs. 6.9 and 6.12 to see the agreement.

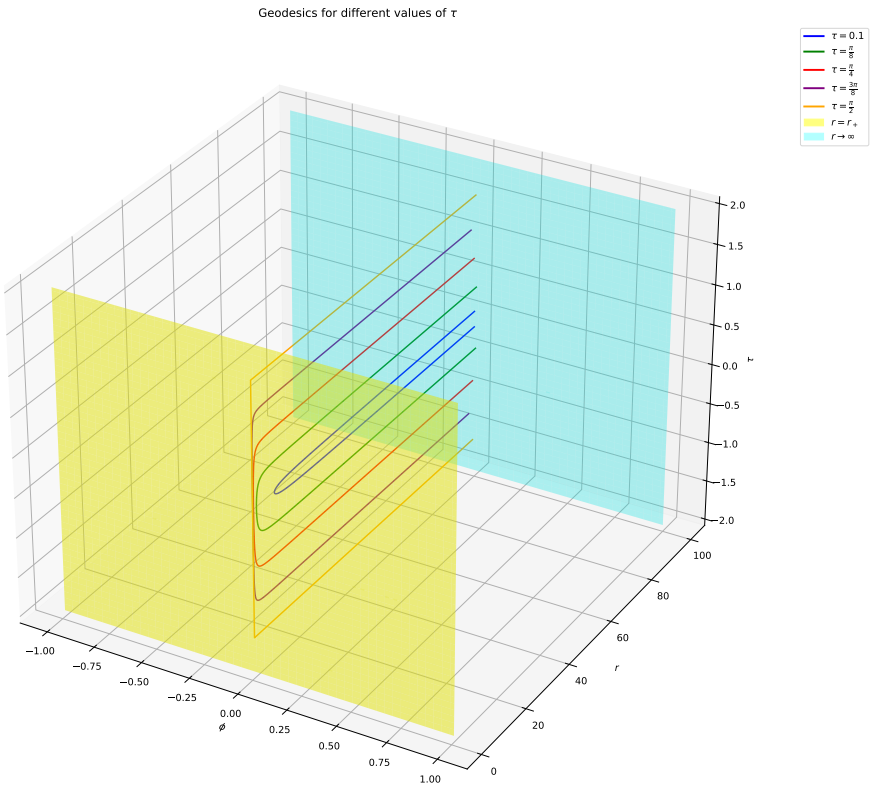

Figure 9.2: Geodesic plots for different τ values. The boundary is given in blue, while the horizon is given in yellow. Observe how as $\tau \to \pi/2$, the geodesics go closer to the horizon and also get a more rectangular profile

9.4 Geodesics in the bulk prescription

Recall our discussion from Sec. 6.2.2 regarding deviations of the semi-classical Virasoro blocks from the exact blocks (computed numerically). The reader is encouraged to refresh the points mentioned there to appreciate the following discussion.

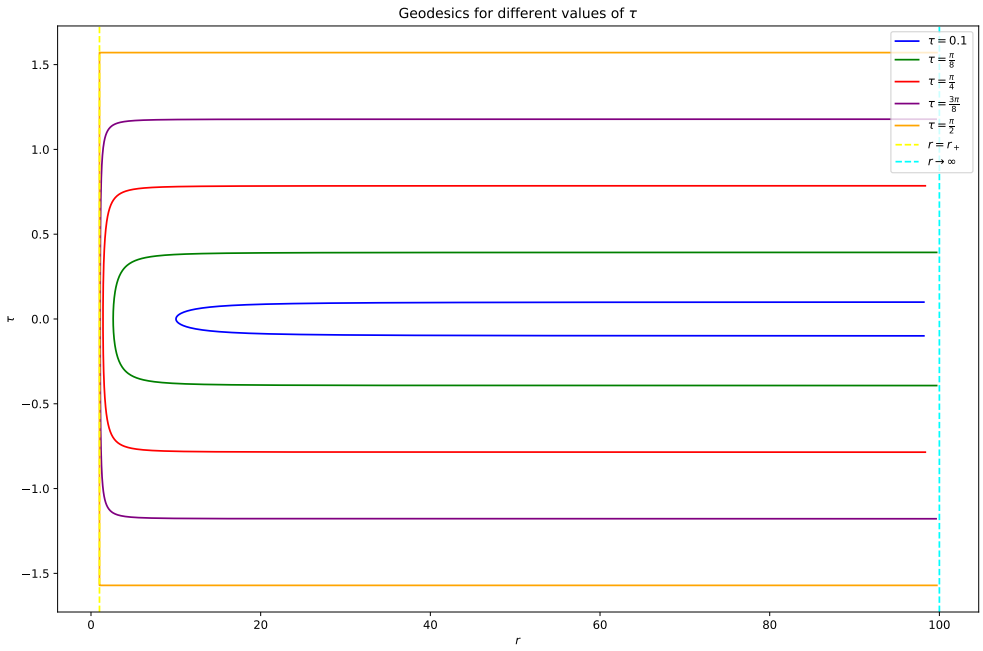

Figure 9.3: Geodesic plots for different τ values. The boundary is given in blue, while the horizon is given in yellow. Observe how as $\tau \to \pi/2$, the geodesics go closer to the horizon and also get a more rectangular profile

We find an interesting connection to this with what we know through the bulk prescription introduced in this chapter. We know the relation between β, T_H and r_+; indeed $\beta/2 = \pi/r_+$. If we look for what happens around $\tau = \pi/r_+$ for our geodesics, we observe that around this time, the geodesics start straddling the horizon (refer to Figs. 9.2 and 9.3). If our prescription is to be believed (clearly, it passes the non-trivial check of reconstructing the Virasoro blocks) then what we infer, is that the deviation of the exact blocks from the semi-classical Virasoro blocks has something to with near-horizon effects. Something changes when the goedesic starts probing the horizon at close distances; maybe it is a change in the bulk-bulk propagator, or something else.

While it is not clear what is causing this phenomenon, we know that near-horizon quantum effects play a significant role in the behaviour and structure of the Virasoro blocks when calculated in the bulk. Our prescription is giving us a **clear indication that probing near-horizon phenomenon could explain the discrepancy between the semi-classical limit and the exact calculation**, and gives us a clear direction for future research.

Part IV

Conclusion

Chapter 10

Concluding remarks and future directions of research

10.1 Summary and conclusion

Here, we summarize the key takeaways from this thesis.

1. The basic theory of CFTs was introduced. A detailed review of CFT_2 was presented and the radial quantization formalism was understood.
2. A primer for understanding AdS_3 was provided. The BTZ black hole solution in AdS_3 was introduced and various geometric features of the relation between global AdS and BTZ black holes were studied.
3. The formalism of degenerate operators, Virasoro blocks and the BPZ equation was introduced. The relation between degenerate blocks and their analytically continued versions was understood and connected with semi-classical heavy-light Virasoro blocks.
4. A perturbative master equation governing non-perturbative effects in c was derived and the blocks obtained from them were understood analytically and numerically. A match between blocks computed in the degenerate operator formalism presented here and previous results from CFT calculations was verified.
5. The non-perturbative features of the master equation solutions were studied under the paradigm of Borel resummation and the results were understood in terms of non-perturbative gravitational solutions.
6. The formalism of Witten diagrams was introduced. The connection between the geodesic version of the Witten diagrams and Virasoro blocks was motivated. The geodesic Witten diagram formalism was used to create a novel bulk prescription for

computing semi-classical heavy-light Virasoro blocks catering specifically to the case of Euclidean BTZ black holes.

7. The geodesic picture arising from this prescription was found to give a convincing bulk interpretation to departures between the exact and semi-classical Virasoro blocks, namely, near-horizon quantum effects.

10.2 Directions for future research

Further work that needs to be done

1. The geodesic diagrams suggest that modifications to the bulk prescription possibly arise from near-horizon effects, and the most likely candidate for said modifications is the bulk-bulk propagator. While attempts were made to figure out what modifications should be made to explain the non-perturbative effects, they were largely unsuccessful and open ended at the time of writing.
2. The second way of calculating the geodesic Witten diagram (using the scalar wave equation) is suggestive of an intimate relation between the form of the differential equation for the propagator (the BTZ wave function) and the semi-classical limit of the master equation, or more precisely, the semi-classical limit of the BPZ equation. Both are second order differential equations that give a solution with the very important ${}_2F_1(h, h, 2h; z)$ structure. This suggests that the finite c version of the BPZ equation should give us an extension of the usual BTZ wave equation that involves finite c effects. This could also motivate a finite c version of the usual BTZ wave equation; while attempts so far have not resulted in any fruitful results, there are many open possibilities that are being investigated at the time of writing.

Part V

Appendix

Appendix A

Miscellaneous calculations

A.1 Action of the differential operators on correlation functions

We have the following equations:

$$\begin{aligned}
[L_r, \mathcal{O}(z)] &= \left[z^{r+1}\frac{d}{dz} + h(r+1)z^r \right] \mathcal{O}(z) = \mathcal{D}_{r,z}\mathcal{O}(z) \\
\langle h_{r,1}|\mathcal{O}_{r,1}(0)\mathcal{O}_L(x)\mathcal{O}_L(y)\rangle &= \frac{1}{(x-y)^{2h_L}}\tilde{\mathcal{V}}\left(1-\frac{x}{y}\right)
\end{aligned} \tag{A.1}$$

A.1.1 $\langle h_{2,1}|\mathcal{O}_{2,1}(0)L_r\mathcal{O}_L(x)\mathcal{O}_L(y)\rangle$

$$\begin{aligned}
\langle h_{r,1}|\mathcal{O}_{r,1}(0)L_r\mathcal{O}_L(x)\mathcal{O}_L(y)\rangle &= \langle h_{r,1}|\mathcal{O}_{r,1}(0)[L_r,\mathcal{O}_L(x)]\mathcal{O}_L(y)\rangle + \langle h_{r,1}|\mathcal{O}_{r,1}(0)\mathcal{O}_L(x)L_r\mathcal{O}_L(y)\rangle \\
&= \langle h_{r,1}|\mathcal{O}_{r,1}(0)\mathcal{D}_{r,x}\mathcal{O}_L(x)\mathcal{O}_L(y)\rangle + \langle h_{r,1}|\mathcal{O}_{r,1}(0)\mathcal{O}_L(x)L_r\mathcal{O}_L(y)\rangle \\
&= \langle h_{r,1}|\mathcal{O}_{r,1}(0)\mathcal{D}_{r,x}\mathcal{O}_L(x)\mathcal{O}_L(y)\rangle + \langle h_{r,1}|\mathcal{O}_{r,1}(0)\mathcal{O}_L(x)[L_r,\mathcal{O}_L(y)]\rangle \\
&= \langle h_{r,1}|\mathcal{O}_{r,1}(0)\mathcal{D}_{r,x}\mathcal{O}_L(x)\mathcal{O}_L(y)\rangle + \langle h_{r,1}|\mathcal{O}_{r,1}(0)\mathcal{O}_L(x)\mathcal{D}_{r,y}\mathcal{O}_L(y)\rangle \\
&= [\mathcal{D}_{r,x}+\mathcal{D}_{r,y}]\langle h_{r,1}|\mathcal{O}_{r,1}(0)\mathcal{O}_L(x)\mathcal{O}_L(y)\rangle
\end{aligned} \tag{A.2}$$

where we have used the fact that the operators are differential operators whose action is on the entire correlator, and also that $L_r|0\rangle = 0$. Since we know the form of the differential

operators as well as the four-point correlator from Eq. A.1, we have

$$\langle h_{r,1}|\mathcal{O}_{r,1}(0)L_r\mathcal{O}_L(x)\mathcal{O}_L(y)\rangle = \left[x^{r+1}\frac{d}{dx} + (r+1)h_L x^r + y^{r+1}\frac{d}{dy} + (r+1)h_L y^r\right]\frac{1}{(x-y)^{2h_L}}\tilde{\mathcal{V}}\left(1-\frac{x}{y}\right) \tag{A.3}$$

Solving this, and expanding it out, we have

$$\boxed{\begin{aligned}\langle h_{r,1}|\mathcal{O}_{r,1}(0)L_r\mathcal{O}_L(x)\mathcal{O}_L(y)\rangle = \\ \frac{1}{(x-y)^{2h_L}}\frac{h_L}{(x-y)}\tilde{\mathcal{V}}\left(1-\frac{x}{y}\right)\left[y^r(rx-ry+x+y)-x^r(-rx+ry+x+y)\right] \\ -\frac{1}{(x-y)^{2h_L}}\frac{x(x^r-y^r)}{y}\tilde{\mathcal{V}}'\left(1-\frac{x}{y}\right)\end{aligned}} \tag{A.4}$$

A.1.2 $\langle h_{r,1}|\mathcal{O}_{r,1}(0)L_jL_{r-j}\mathcal{O}_L(x)\mathcal{O}_L(y)\rangle$

We follow the same algorithm here

$$\begin{aligned}\langle h_{r,1}|\mathcal{O}_{r,1}(0)L_jL_{r-j}\mathcal{O}_L(x)\mathcal{O}_L(y)\rangle &= \langle h_{r,1}|\mathcal{O}_{r,1}(0)L_j[L_{r-j},\mathcal{O}_L(x)]\mathcal{O}_L(y)\rangle + \langle h_{r,1}|\mathcal{O}_{r,1}(0)L_j\mathcal{O}_L(x)L_{r-j}\mathcal{O}_L(y)\rangle \\ &= \langle h_{r,1}|\mathcal{O}_{r,1}(0)L_j\mathcal{D}_{r-j,x}\mathcal{O}_L(x)\mathcal{O}_L(y)\rangle + \langle h_{r,1}|\mathcal{O}_{r,1}(0)L_j\mathcal{O}_L(x)L_{r-j}\mathcal{O}_L(y)\rangle \\ &= \langle h_{r,1}|\mathcal{O}_{r,1}(0)L_j\mathcal{D}_{r-j,x}\mathcal{O}_L(x)\mathcal{O}_L(y)\rangle + \langle h_{r,1}|\mathcal{O}_{r,1}(0)L_j\mathcal{O}_L(x)\mathcal{D}_{r-j,y}\mathcal{O}_L(y)\rangle \\ &= [\mathcal{D}_{r-j,x}+\mathcal{D}_{r-j,y}]\langle h_{r,1}|\mathcal{O}_{r,1}(0)L_j\mathcal{O}_L(x)\mathcal{O}_L(y)\rangle \\ &= [\mathcal{D}_{r-j,x}+\mathcal{D}_{r-j,y}][\mathcal{D}_{j,x}+\mathcal{D}_{j,y}]\langle h_{r,1}|\mathcal{O}_{r,1}(0)\mathcal{O}_L(x)\mathcal{O}_L(y)\rangle\end{aligned} \tag{A.5}$$

Using Eq. A.1, we have

$$\begin{aligned}&\langle h_{r,1}|\mathcal{O}_{r,1}(0)L_jL_{r-j}\mathcal{O}_L(x)\mathcal{O}_L(y)\rangle \\ &= \left[x^{r-j+1}\frac{d}{dx} + (r-j+1)h_L x^{r-j} + y^{r-j+1}\frac{d}{dy} + (r-j+1)h_L y^{r-j}\right] \\ &\quad\left[x^{j+1}\frac{d}{dx} + (j+1)h_L x^j + y^{j+1}\frac{d}{dy} + (j+1)h_L y^j\right]\frac{1}{(x-y)^{2h_L}}\tilde{\mathcal{V}}\left(1-\frac{x}{y}\right)\end{aligned} \tag{A.6}$$

Solving this and expanding it out while keeping only the second derivative, we get

$$\boxed{\langle h_{r,1}|\mathcal{O}_{r,1}(0)L_jL_{r-j}\mathcal{O}_L(x)\mathcal{O}_L(y)\rangle = \frac{1}{(x-y)^{2h_L}}\frac{1}{(xy)^j}\frac{x^2}{y^2}(x^j-y^j)(x^ry^j-y^rx^j)\tilde{\mathcal{V}}''\left(1-\frac{x}{y}\right)} \tag{A.7}$$

A.2 Coefficients of $\tilde{\mathcal{V}}$ and $\tilde{\mathcal{V}}''$ in the Master Equation

A.2.1 Coefficients of $\tilde{\mathcal{V}}(t)$ and $\tilde{\mathcal{V}}(t)''$ in the Master Equation

The coefficient $g_r(t)$

The factor sitting in front of $\tilde{\mathcal{V}}(t)$ is given by

$$\begin{aligned}\frac{(1+e^{-t})}{(1-e^{-t})} - r\frac{(1+e^{-rt})}{(1-e^{-rt})} &= \frac{(e^{\frac{t}{2}}+e^{-\frac{t}{2}})}{(e^{\frac{t}{2}}-e^{-\frac{t}{2}})} - r\frac{(e^{\frac{rt}{2}}+e^{-\frac{rt}{2}})}{(e^{\frac{rt}{2}}-e^{-\frac{rt}{2}})} \\ &= \coth\frac{t}{2} - r\coth\frac{rt}{2}\end{aligned} \tag{A.8}$$

and thus we get

$$\boxed{g_r(t) = \coth\frac{t}{2} - r\coth\frac{rt}{2}} \tag{A.9}$$

The coefficient $\Sigma_r(t)$

The factor sitting in front of $\tilde{\mathcal{V}}(t)$ is given by

$$\begin{aligned}\sum_{j=1}^{r-1}\frac{1}{j(r-j)}\left[\frac{(1-e^{jt})(e^{-rt}-e^{-jt})}{(1-e^{-rt})}\right] &= \frac{1}{(1-e^{-rt})}\sum_{j=1}^{r-1}\frac{1}{j(r-j)}(1+e^{-rt}-e^{-jt}-e^{-(r-j)t}) \\ &= \frac{1}{r(1-e^{-rt})}\sum_{j=1}^{r-1}\left[\frac{1}{j}+\frac{1}{(r-j)}\right](1+e^{-rt}-e^{-jt}-e^{-(r-j)t}) \\ &= \frac{2}{r(1-e^{-rt})}\sum_{j=1}^{r-1}\frac{1}{j}(1+e^{-rt}-e^{-jt}-e^{-(r-j)t}) \\ &= \frac{1}{r\sinh\frac{rt}{2}}\sum_{j=1}^{r-1}\frac{1}{j}(e^{\frac{rt}{2}}+e^{\frac{-rt}{2}}-e^{\frac{rt}{2}-jt}-e^{-\frac{rt}{2}+jt})\end{aligned} \tag{A.10}$$

and now we can define

$$\tilde{B}_r(t) = \sum_{j=1}^{r-1}\frac{e^{jt}}{j} \tag{A.11}$$

to get

$$\boxed{\Sigma_r(t) = -\frac{1}{r\sinh\frac{rt}{2}}\left[e^{-\frac{rt}{2}}\tilde{B}_r(t) + e^{\frac{rt}{2}}\tilde{B}_r(-t) - 2\cosh\left(\frac{rt}{2}\right)\tilde{B}_r(0)\right]} \tag{A.12}$$

A.2.2 Coefficients of $\mathcal{V}(x)$ and $\mathcal{V}''(x)$ in the scaling limit

We have the substitution

$$t = ik + \frac{x}{b} \tag{A.13}$$

with

$$k = \frac{2\pi n}{r} \Leftrightarrow \frac{ikr}{2} = in\pi \tag{A.14}$$

A.2.3 $\tilde{g}_r(x)$

We have

$$\begin{aligned} \tilde{g}_r(x) &= 1 - r\coth\left(\frac{ikr}{2} + \frac{rx}{2b}\right) \\ &= \frac{\sinh\left(in\pi + \frac{rx}{2b}\right) - r\cosh\left(in\pi + \frac{rx}{2b}\right)}{\sinh\left(in\pi + \frac{rx}{2b}\right)} \end{aligned} \tag{A.15}$$

Since

$$\begin{aligned} \sinh\left(\frac{rt}{2}\right) &= \sinh\left(in\pi + \frac{rx}{2b}\right) = (-1)^n \sinh\frac{rx}{2b} \\ \cosh\left(\frac{rt}{2}\right) &= \cosh\left(in\pi + \frac{rx}{2b}\right) = (-1)^n \cosh\frac{rx}{2b} \end{aligned} \tag{A.16}$$

Plugging in these two expressions, we have

$$\boxed{\tilde{g}_r(x) = \frac{1}{\sinh\left(\frac{rx}{2b}\right)}\left[\sinh\left(\frac{rx}{2b}\right) - r\cosh\left(\frac{rx}{2b}\right)\right]} \tag{A.17}$$

A.2.4 $\Sigma_r(x)$

We have

$$\begin{aligned} \Sigma_r(t) &= \frac{1}{(1-e^{-rt})}\sum_{j=1}^{r-1}\frac{1}{j(r-j)}(1 + e^{-rt} - e^{-jt} - e^{-(r-j)t}) \\ &= \frac{1}{\sinh\left(\frac{rt}{2}\right)}\sum_{j=1}^{r-1}\frac{1}{j(r-j)}\left(\cosh\left(\frac{rt}{2}\right) - \cosh\left(\frac{rt}{2} - jt\right)\right) \\ &= \frac{2}{\sinh\left(\frac{rt}{2}\right)}\sum_{j=1}^{r-1}\frac{\sinh\left(\frac{(r-j)t}{2}\right)\sinh\left(\frac{jt}{2}\right)}{j(r-j)} \end{aligned} \tag{A.18}$$

Now, using

$$\sinh\left(\frac{(r-j)t}{2}\right) = \sinh\left(\frac{rt}{2}\right)\cosh\left(\frac{jt}{2}\right) - \sinh\left(\frac{jt}{2}\right)\cosh\left(\frac{rt}{2}\right) \tag{A.19}$$

we have

$$\Sigma_r(t) = \frac{2}{\sinh\left(\frac{rt}{2}\right)}\sum_{j=1}^{r-1}\frac{\sinh\left(\frac{jt}{2}\right)}{j(r-j)}\left[\sinh\left(\frac{rt}{2}\right)\cosh\left(\frac{jt}{2}\right) - \sinh\left(\frac{jt}{2}\right)\cosh\left(\frac{rt}{2}\right)\right] \tag{A.20}$$

Next, we can substitute the scaling relation and using the expressions for $\sinh\left(\frac{rt}{2}\right), \cosh\left(\frac{rt}{2}\right)$; we get

$$\boxed{\Sigma_r(x) = \frac{2}{\sinh\left(\frac{rx}{2b}\right)}\sum_{j=1}^{r-1}\frac{1}{j(r-j)}\left[\sinh\left(\frac{rx}{2b}\right)\sinh\left(\frac{jt}{2}\right)\cosh\left(\frac{jt}{2}\right) - \sinh^2\left(\frac{jt}{2}\right)\cosh\left(\frac{rx}{2b}\right)\right]} \tag{A.21}$$

A.2.5 Coefficients of $\mathcal{V}(x)$ and $\mathcal{V}''(x)$ in the generalized fixed point limit

We have

$$t = t_* + x \tag{A.22}$$

Near the n^{th} singularity $t_* = \frac{2\pi i n}{r}$

We have

$$\begin{aligned}\tilde{g}_{r_+}(x) &= 1 - r_+\cot\left(\pi n + \frac{r_+ x}{2}\right)\\ &= \frac{\sin\left(n\pi + \frac{r_+x}{2}\right) - r_+\cos\left(n\pi + \frac{r_+x}{2}\right)}{\sin\left(n\pi + \frac{r_+x}{2}\right)}\end{aligned} \tag{A.23}$$

Since

$$\begin{aligned}\sinh\left(\frac{rt}{2}\right) &= \sinh\left(in\pi + \frac{rx}{2b}\right) = (-1)^n\sinh\frac{rx}{2b}\\ \cosh\left(\frac{rt}{2}\right) &= \cosh\left(in\pi + \frac{rx}{2b}\right) = (-1)^n\cosh\frac{rx}{2b}\end{aligned} \tag{A.24}$$

Plugging in these two expressions and noting that we have to consider the $x \to 0$ limit, we have

$$\boxed{\tilde{g}_r(x) = \frac{1}{\sinh\left(\frac{rx}{2}\right)}\left[\sinh\left(\frac{rx}{2}\right) - r\cosh\left(\frac{rx}{2}\right)\right] \approx -\frac{2}{x}} \tag{A.25}$$

Next, we have

$$\begin{aligned}\Sigma_r(t) &= -\frac{1}{r\sinh\frac{rt}{2}}\left[e^{-\frac{rt}{2}}\tilde{B}_r(t) + e^{\frac{rt}{2}}\tilde{B}_r(-t) - 2\cosh\left(\frac{rt}{2}\right)\tilde{B}_r(0)\right] \\ &\approx -\frac{(-1)^n}{r\sinh\frac{rx}{2}}\left[e^{-i\pi n}\tilde{B}_r(x) + e^{i\pi n}\tilde{B}_r(-x) - 2(-1)^n\cosh\left(\frac{rx}{2}\right)\tilde{B}_r(0)\right] \\ &\approx -\frac{2}{r^2x}\left[\tilde{B}_r(x) + \tilde{B}_r(-x) - 2\tilde{B}_r(0)\right]\end{aligned} \tag{A.26}$$

where we have always dropped terms sub-leading in x. Next, using the definition of

$$\tilde{B}_r(t) = -\log\left(1-e^t\right) - B(e^t; r, 0) \tag{A.27}$$

we have

$$\boxed{\begin{aligned}\Sigma_r(x) &\approx \frac{2}{r^2x}\left[\log\left(1-e^{\frac{2\pi in}{r}}\right) + B(e^{\frac{2\pi in}{r}}; r, 0) + \log\left(1-e^{-\frac{2\pi in}{r}}\right) + B(e^{-\frac{2\pi in}{r}}; r, 0) + 2H_{r-1}\right] \\ &= \frac{2}{r^2x}\left[2\log\left(2\sinh\left(\frac{\pi in}{r}\right)\right) + B(e^{\frac{2\pi in}{r}}; r, 0) + B(e^{-\frac{2\pi in}{r}}; r, 0) + 2H_{r-1}\right]\end{aligned}} \tag{A.28}$$

Near the halfway point to the first singularity $t_* = \frac{\pi i}{r}$

We have

$$\begin{aligned}\tilde{g}_r(x) &= 1 - r\coth\left(\frac{i\pi}{2} + \frac{rx}{2}\right) \\ &= \frac{\sinh\left(\frac{i\pi}{2} + \frac{rx}{2}\right) - r\cosh\left(\frac{i\pi}{2} + \frac{rx}{2}\right)}{\sinh\left(\frac{i\pi}{2} + \frac{rx}{2}\right)}\end{aligned} \tag{A.29}$$

Since

$$\begin{aligned}\sinh\left(\frac{i\pi}{2} + \frac{rx}{2}\right) &= i\cosh\frac{rx}{2} \\ \cosh\left(\frac{i\pi}{2} + \frac{rx}{2}\right) &= i\sinh\frac{rx}{2}\end{aligned} \tag{A.30}$$

Plugging in these two expressions and noting that we have to consider the $x \to 0$ limit, we have

$$\boxed{\tilde{g}_r(x) = \frac{1}{\cosh\left(\frac{rx}{2}\right)}\left[\cosh\left(\frac{rx}{2}\right) - r\sinh\left(\frac{rx}{2}\right)\right] \approx 1} \tag{A.31}$$

Next, we have

$$\begin{aligned}\Sigma_r(t) &= -\frac{1}{r\sinh\frac{rt}{2}}\left[e^{-\frac{rt}{2}}\tilde{B}_r(t) + e^{\frac{rt}{2}}\tilde{B}_r(-t) - 2\cosh\left(\frac{rt}{2}\right)\tilde{B}_r(0)\right] \\ &\approx -\frac{1}{ir\cosh\frac{rx}{2}}\left[e^{-\frac{i\pi}{2}}\tilde{B}_r(x) + e^{\frac{i\pi}{2}}\tilde{B}_r(-x) + 2i\sinh\left(\frac{rx}{2}\right)\tilde{B}_r(0)\right] \\ &\approx \frac{1}{r}\left[\tilde{B}_r(x) - \tilde{B}_r(-x)\right]\end{aligned} \tag{A.32}$$

where we have always dropped terms sub-leading in x. Using the definition of $\tilde{B}_r(t)$, we have

$$\boxed{\begin{aligned}\Sigma_r(x) &\approx \frac{1}{r}\left[\log\left(1-e^{-\frac{i\pi}{r}}\right) + B(e^{-\frac{i\pi}{r}};r,0) - \log\left(1-e^{\frac{i\pi}{r}}\right) - B(e^{\frac{i\pi}{r}};r,0)\right] \\ &= \frac{1}{r}\left[\log\left(-e^{-\frac{i\pi}{r}}\right) + B(e^{-\frac{i\pi}{r}};r,0) - B(e^{\frac{i\pi}{r}};r,0)\right] \\ &= \frac{1}{r}\left[i\pi - \frac{i\pi}{r} + B(e^{-\frac{i\pi}{r}};r,0) - B(e^{\frac{i\pi}{r}};r,0)\right]\end{aligned}} \tag{A.33}$$

where we have taken the principal value of the logarithm.

A.3 Calculations of the analytically continued Master Equation

We can use the entirety of A.2.5, because all we have to do is replace r with ir_+ and take the appropriate limits.

A.3.1 $t_* = \frac{2\pi n}{r_+}$

The coeffcient $\tilde{g}_r(x)$

We have

$$\begin{aligned}\tilde{g}_r(x) &= 1 - r_+\cot\left(\pi n + \frac{r_+x}{2}\right) \\ &= \frac{\sin\left(n\pi + \frac{rx}{2}\right) - r_+\cos\left(n\pi + \frac{r_+x}{2}\right)}{\sin\left(n\pi + \frac{r_+x}{2}\right)}\end{aligned} \tag{A.34}$$

Since

$$\begin{aligned}\sin\left(\frac{r_+t}{2}\right) &= \sin\left(n\pi + \frac{r_+x}{2}\right) = (-1)^n\sin\frac{r_+x}{2} \\ \cos\left(\frac{r_+t}{2}\right) &= \cos\left(n\pi + \frac{r_+x}{2}\right) = (-1)^n\cos\frac{r_+x}{2}\end{aligned} \tag{A.35}$$

Plugging in these two expressions and noting that we have to consider the $x \to 0$ limit, we have

$$\boxed{\tilde{g}_r(x) = \frac{1}{\sin\left(\frac{r_+ x}{2}\right)}\left[\sin\left(\frac{r_+ x}{2}\right) - r_+ \cos\left(\frac{r_+ x}{2}\right)\right] \approx -\frac{2}{x}} \tag{A.36}$$

The coefficient $\Sigma_{r_+}(x) + \Sigma_{-r_+}(x)$

We have

$$\begin{aligned}
\Sigma_{r_+}(t) &= \frac{1}{r_+ \sin\frac{r_+ t}{2}}\left[e^{-\frac{ir_+ t}{2}}\tilde{B}_{r_+}(t) + e^{\frac{ir_+ t}{2}}\tilde{B}_{r_+}(-t) - 2\cos\left(\frac{r_+ t}{2}\right)\tilde{B}_{r_+}(0)\right] \\
&\approx \frac{(-1)^n}{r_+ \sin\frac{r_+ x}{2}}\left[e^{-i\pi n}\tilde{B}_{r_+}(x) + e^{i\pi n}\tilde{B}_{r_+}(-x) - 2(-1)^n\cos\left(\frac{r_+ x}{2}\right)\tilde{B}_{r_+}(0)\right] \\
&\approx \frac{2}{r_+^2 x}\left[\tilde{B}_{r_+}(x) + \tilde{B}_{r_+}(-x) - 2\tilde{B}_{r_+}(0)\right]
\end{aligned} \tag{A.37}$$

where we have always dropped terms sub-leading in x. Next, using the definition of $\tilde{B}_{r_+}(t)$, we have

$$\begin{aligned}
\Sigma_{r_+}(x) &\approx -\frac{2}{r_+^2 x}\left[\log\left(1 - e^{\frac{2\pi n}{r_+}}\right) + B(e^{\frac{2\pi n}{r_+}}; ir_+, 0) + \log\left(1 - e^{-\frac{2\pi n}{r_+}}\right) + B(e^{-\frac{2\pi n}{r_+}}; ir_+, 0) + 2H_{ir_+ - 1}\right] \\
&= -\frac{2}{r_+^2 x}\left[2\log\left(2\sinh\left(\frac{\pi n}{r_+}\right)\right) + B(e^{\frac{2\pi n}{r_+}}; ir_+, 0) + B(e^{-\frac{2\pi n}{r_+}}; ir_+, 0) + 2H_{ir_+ - 1}\right]
\end{aligned} \tag{A.38}$$

Finally, adding the $-r_+$ part, and using the identity $H_{ir_+ - 1} = H_{ir_+} - \frac{1}{ir_+}$, we have

$$\boxed{\begin{aligned}
\Sigma_{r_+}(x) + \Sigma_{-r_+}(x) = -\frac{2}{r_+^2 x}\Big[&B(e^{\frac{2\pi n}{r_+}}; ir_+, 0) + B(e^{-\frac{2\pi n}{r_+}}; ir_+, 0) + B(e^{-\frac{2\pi n}{r_+}}; -ir_+, 0) + B(e^{\frac{2\pi n}{r_+}}; -ir_+, 0) \\
&+2H_{ir_+} + 2H_{-ir_+} + 4\log\left(2\sinh\left(\frac{\pi n}{r_+}\right)\right) + 2\pi i\Big]
\end{aligned}} \tag{A.39}$$

A.3.2 $t_* = \frac{\pi}{r_+}$

The coefficient $\tilde{g}_{r_+}(x)$

We have

$$\begin{aligned}
\tilde{g}_{r_+}(x) &= 1 - r\cot\left(\frac{\pi}{2} + \frac{r_+ x}{2}\right) \\
&= \frac{\sin\left(\frac{\pi}{2} + \frac{r_+ x}{2}\right) - r_+\cos\left(\frac{\pi}{2} + \frac{r_+ x}{2}\right)}{\sin\left(\frac{\pi}{2} + \frac{r_+ x}{2}\right)}
\end{aligned} \tag{A.40}$$

Since

$$\begin{aligned}\sin\left(\frac{\pi}{2}+\frac{r_+x}{2}\right)&=\cos\frac{r_+x}{2}\\ \cos\left(\frac{\pi}{2}+\frac{r_+x}{2}\right)&=-\sin\frac{r_+x}{2}\end{aligned}\tag{A.41}$$

Plugging in these two expressions and noting that we have to consider the $x\to 0$ limit, we have

$$\boxed{\tilde{g}_r(x)=\frac{1}{\cos\left(\frac{r_+x}{2}\right)}\left[\cos\left(\frac{r_+x}{2}\right)+r_+\sin\left(\frac{r_+x}{2}\right)\right]\approx 1}\tag{A.42}$$

The coefficient $\Sigma_r(x)$

We have

$$\begin{aligned}\Sigma_{r_+}(t)&=\frac{1}{r_+\sinh\frac{r_+t}{2}}\left[e^{-\frac{ir_+t}{2}}\tilde{B}_{r_+}(t)+e^{\frac{ir_+t}{2}}\tilde{B}_{r_+}(-t)-2\cos\left(\frac{r_+t}{2}\right)\tilde{B}_{r_+}(0)\right]\\ &\approx\frac{1}{r_+\cos\frac{r_+x}{2}}\left[e^{-\frac{i\pi}{2}}\tilde{B}_{r_+}(x)+e^{\frac{i\pi}{2}}\tilde{B}_{r_+}(-x)+2\sin\left(\frac{r_+x}{2}\right)\tilde{B}_{r_+}(0)\right]\\ &\approx\frac{i}{r_+}\left[\tilde{B}_{r_+}(-x)-\tilde{B}_{r_+}(x)\right]\end{aligned}\tag{A.43}$$

where we have always dropped terms sub-leading in x. Next, using the definition of $\tilde{B}_r(t)$, we have

$$\begin{aligned}\Sigma_r(x)&\approx\frac{i}{r_+}\left[\log\left(1-e^{\frac{\pi}{r_+}}\right)+B(e^{\frac{\pi}{r_+}};ir_+,0)-\log\left(1-e^{\frac{-\pi}{r_+}}\right)-B(e^{\frac{-\pi}{r_+}};ir_+,0)\right]\\ &=\frac{i}{r_+}\left[\log\left(-e^{-\frac{\pi}{r_+}}\right)+B(e^{\frac{\pi}{r_+}};ir_+,0)-B(e^{\frac{-\pi}{r_+}};ir_+,0)\right]\end{aligned}\tag{A.44}$$

Finally, adding the $-r_+$ part, we have

$$\boxed{\Sigma_{r_+}(x)+\Sigma_{-r_+}(x)=\frac{i}{r_+}\left[-\frac{2\pi}{r_+}+B(e^{\frac{\pi}{r_+}};ir_+,0)+B(e^{\frac{\pi}{r_+}};-ir_+,0)-B(e^{\frac{-\pi}{r_+}};ir_+,0)-B(e^{\frac{-\pi}{r_+}};-ir_+,0)\right]}\tag{A.45}$$

Let us denote this by ϵ when we substitute in our differential equation.

Bibliography

[1] S. W. Hawking. "Particle Creation by Black Holes". In: *Commun. Math. Phys.* 43 (1975). Ed. by G. W. Gibbons and S. W. Hawking. [Erratum: Commun.Math.Phys. 46, 206 (1976)], pp. 199–220. DOI: 10.1007/BF02345020.

[2] S. W. Hawking. "Breakdown of Predictability in Gravitational Collapse". In: *Phys. Rev. D* 14 (1976), pp. 2460–2473. DOI: 10.1103/PhysRevD.14.2460.

[3] Juan Martin Maldacena. "The Large N limit of superconformal field theories and supergravity". In: *Adv. Theor. Math. Phys.* 2 (1998), pp. 231–252. DOI: 10.4310/ATMP.1998.v2.n2.a1. arXiv: hep-th/9711200.

[4] Edward Witten. "Anti-de Sitter space and holography". In: *Adv. Theor. Math. Phys.* 2 (1998), pp. 253–291. DOI: 10.4310/ATMP.1998.v2.n2.a2. arXiv: hep-th/9802150.

[5] S. S. Gubser, Igor R. Klebanov, and Alexander M. Polyakov. "Gauge theory correlators from noncritical string theory". In: *Phys. Lett. B* 428 (1998), pp. 105–114. DOI: 10.1016/S0370-2693(98)00377-3. arXiv: hep-th/9802109.

[6] Juan Martin Maldacena. "Eternal black holes in anti-de Sitter". In: *JHEP* 04 (2003), p. 021. DOI: 10.1088/1126-6708/2003/04/021. arXiv: hep-th/0106112.

[7] Gerard 't Hooft. "On the Quantum Structure of a Black Hole". In: *Nucl. Phys. B* 256 (1985), pp. 727–745. DOI: 10.1016/0550-3213(85)90418-3.

[8] Leonard Susskind, Larus Thorlacius, and John Uglum. "The Stretched horizon and black hole complementarity". In: *Phys. Rev. D* 48 (1993), pp. 3743–3761. DOI: 10.1103/PhysRevD.48.3743. arXiv: hep-th/9306069.

[9] Samir D. Mathur. "The Information paradox: A Pedagogical introduction". In: *Class. Quant. Grav.* 26 (2009). Ed. by A. M. Uranga, p. 224001. DOI: 10.1088/0264-9381/26/22/224001. arXiv: 0909.1038 [hep-th].

[10] Ahmed Almheiri et al. "Black Holes: Complementarity or Firewalls?" In: *JHEP* 02 (2013), p. 062. DOI: 10.1007/JHEP02(2013)062. arXiv: 1207.3123 [hep-th].

[11] Iosif Bena et al. "Fuzzballs and Microstate Geometries: Black-Hole Structure in String Theory". In: (Apr. 2022). arXiv: 2204.13113 [hep-th].

[12] Chethan Krishnan and Pradipta S. Pathak. "Normal modes of the stretched horizon: a bulk mechanism for black hole microstate level spacing". In: *JHEP* 03 (2024), p. 162. DOI: 10.1007/JHEP03(2024)162. arXiv: 2312.14109 [hep-th].

[13] Vaibhav Burman, Suchetan Das, and Chethan Krishnan. "A smooth horizon without a smooth horizon". In: *JHEP* 2024 (2024), p. 014. DOI: 10.1007/JHEP03(2024)014. arXiv: 2312.14108 [hep-th].

[14] Vaibhav Burman and Chethan Krishnan. "A Bottom-Up Approach to Black Hole Microstates". In: (Sept. 2024). arXiv: 2409.05850 [hep-th].

[15] A. Liam Fitzpatrick, Jared Kaplan, and Matthew T. Walters. "Virasoro Conformal Blocks and Thermality from Classical Background Fields". In: *JHEP* 11 (2015), p. 200. DOI: 10.1007/JHEP11(2015)200. arXiv: 1501.05315 [hep-th].

[16] A. Liam Fitzpatrick and Jared Kaplan. "Conformal Blocks Beyond the Semi-Classical Limit". In: *JHEP* 05 (2016), p. 075. DOI: 10.1007/JHEP05(2016)075. arXiv: 1512.03052 [hep-th].

[17] A. Liam Fitzpatrick et al. "Hawking from Catalan". In: *JHEP* 05 (2016), p. 069. DOI: 10.1007/JHEP05(2016)069. arXiv: 1510.00014 [hep-th].

[18] A. Liam Fitzpatrick et al. "On information loss in AdS3/CFT2". In: *Journal of High Energy Physics* 2016.5 (May 2016), p. 109. ISSN: 1029-8479. DOI: 10.1007/JHEP05(2016)109. URL: https://doi.org/10.1007/JHEP05(2016)109.

[19] Hong Liu. "Scattering in anti-de Sitter space and operator product expansion". In: *Phys. Rev. D* 60 (1999), p. 106005. DOI: 10.1103/PhysRevD.60.106005. arXiv: hep-th/9811152.

[20] Hong Liu and Arkady A. Tseytlin. "On four point functions in the CFT / AdS correspondence". In: *Phys. Rev. D* 59 (1999), p. 086002. DOI: 10.1103/PhysRevD.59.086002. arXiv: hep-th/9807097.

[21] Eric D'Hoker and Daniel Z. Freedman. "General scalar exchange in AdS(d+1)". In: *Nucl. Phys. B* 550 (1999), pp. 261–288. DOI: 10.1016/S0550-3213(99)00169-8. arXiv: hep-th/9811257.

[22] Eric D'Hoker et al. "Graviton exchange and complete four point functions in the AdS / CFT correspondence". In: *Nucl. Phys. B* 562 (1999), pp. 353–394. DOI: 10.1016/S0550-3213(99)00525-8. arXiv: hep-th/9903196.

[23] Eric D'Hoker et al. "The Operator product expansion of N=4 SYM and the 4 point functions of supergravity". In: *Nucl. Phys. B* 589 (2000), pp. 38–74. DOI: 10.1016/S0550-3213(00)00523-X. arXiv: hep-th/9911222.

[24] Daniel Z. Freedman et al. "Comments on 4 point functions in the CFT / AdS correspondence". In: *Phys. Lett. B* 452 (1999), pp. 61–68. DOI: 10.1016/S0370-2693(99)00229-4. arXiv: hep-th/9808006.

[25] Laurent Hoffmann, Anastasios C. Petkou, and Werner Ruhl. "Aspects of the conformal operator product expansion in AdS / CFT correspondence". In: *Adv. Theor. Math. Phys.* 4 (2002), pp. 571–615. DOI: 10.4310/ATMP.2000.v4.n3.a3. arXiv: hep-th/0002154.

[26] Laurent Hoffmann, Anastasios C. Petkou, and Werner Ruhl. "A Note on the analyticity of AdS scalar exchange graphs in the crossed channel". In: *Phys. Lett. B* 478 (2000), pp. 320–326. DOI: 10.1016/S0370-2693(00)00283-5. arXiv: hep-th/0002025.

[27] Eliot Hijano, Per Kraus, and River Snively. "Worldline approach to semi-classical conformal blocks". In: *JHEP* 07 (2015), p. 131. DOI: 10.1007/JHEP07(2015)131. arXiv: 1501.02260 [hep-th].

[28] Eliot Hijano et al. "Semiclassical Virasoro blocks from AdS3 gravity". In: *Journal of High Energy Physics* 2015.12 (Dec. 2015), pp. 1–31. ISSN: 1029-8479. DOI: 10.1007/JHEP12(2015)077. URL: https://doi.org/10.1007/JHEP12(2015)077.

[29] Eliot Hijano et al. "Witten diagrams revisited: the AdS geometry of conformal blocks". In: *Journal of High Energy Physics* 2016.1 (Jan. 2016), p. 146. ISSN: 1029-8479. DOI: 10.1007/JHEP01(2016)146. URL: https://doi.org/10.1007/JHEP01(2016)146.

[30] A. A. Belavin, Alexander M. Polyakov, and A. B. Zamolodchikov. "Infinite Conformal Symmetry in Two-Dimensional Quantum Field Theory". In: *Nucl. Phys. B* 241 (1984). Ed. by I. M. Khalatnikov and V. P. Mineev, pp. 333–380. DOI: 10.1016/0550-3213(84)90052-X.

[31] Maximo Banados, Claudio Teitelboim, and Jorge Zanelli. "The Black hole in three-dimensional space-time". In: *Phys. Rev. Lett.* 69 (1992), pp. 1849–1851. DOI: 10.1103/PhysRevLett.69.1849. arXiv: hep-th/9204099.

[32] P. Francesco, P. Mathieu, and D. Senechal. *Conformal Field Theory*. Graduate Texts in Contemporary Physics. Springer New York, 2012. ISBN: 9781461222569. URL: https://books.google.co.in/books?id=5u7jBwAAQBAJ.

[33] David Tong. "String Theory". In: (Jan. 2009). arXiv: 0908.0333 [hep-th].

[34] Paul H. Ginsparg. "APPLIED CONFORMAL FIELD THEORY". In: *Les Houches Summer School in Theoretical Physics: Fields, Strings, Critical Phenomena*. Sept. 1988. arXiv: hep-th/9108028.

[35] Ingemar Bengtsson. *Anti-de Sitter Space*. Lecture notes. 1998. URL: https://3dhouse.se/ingemar/relteori/Kurs.pdf.

[36] Steven Carlip. "The (2+1)-Dimensional black hole". In: *Class. Quant. Grav.* 12 (1995), pp. 2853–2880. DOI: 10.1088/0264-9381/12/12/005. arXiv: gr-qc/9506079.

[37] Yuji Satoh. "Study of three-dimensional quantum black holes". Other thesis. Mar. 1997. DOI: 10.11501/3139896. arXiv: hep-th/9705209.

[38] Ikuo Ichinose and Yuji Satoh. "Entropies of scalar fields on three dimensional black holes". In: *Nuclear Physics B* 447.2 (1995), pp. 340–370. ISSN: 0550-3213. DOI: https://doi.org/10.1016/0550-3213(95)00197-Z. URL: https://www.sciencedirect.com/science/article/pii/055032139500197Z.

[39] Esko Keski-Vakkuri. "Bulk and boundary dynamics in BTZ black holes". In: *Phys. Rev. D* 59 (1999), p. 104001. DOI: 10.1103/PhysRevD.59.104001. arXiv: hep-th/9808037.

[40] Louis Benoit and Yvan Saint-Aubin. "Degenerate conformal field theories and explicit expressions for some null vectors". In: *Physics Letters B* 215.3 (1988), pp. 517–522. ISSN: 0370-2693. DOI: https://doi.org/10.1016/0370-2693(88)91352-4. URL: https://www.sciencedirect.com/science/article/pii/0370269388913524.

[41] Daniel Harlow, Jonathan Maltz, and Edward Witten. "Analytic Continuation of Liouville Theory". In: *JHEP* 12 (2011), p. 071. DOI: 10.1007/JHEP12(2011)071. arXiv: 1108.4417 [hep-th].

[42] Matteo Beccaria, Alberto Fachechi, and Guido Macorini. "Virasoro vacuum block at next-to-leading order in the heavy-light limit". In: *JHEP* 02 (2016), p. 072. DOI: 10.1007/JHEP02(2016)072. arXiv: 1511.05452 [hep-th].

[43] Hongbin Chen et al. "A Numerical Approach to Virasoro Blocks and the Information Paradox". In: *JHEP* 09 (2017), p. 102. DOI: 10.1007/JHEP09(2017)102. arXiv: 1703.09727 [hep-th].

[44] Gerard 't Hooft. "Can We Make Sense Out of Quantum Chromodynamics?" In: *Subnucl. Ser.* 15 (1979). Ed. by Antonino Zichichi, p. 943.